ARIZONA GEOL. SOC. DIGEST VOL. XIV 1981 30 MAR 87

IN RELATIONS OF TECTONICS TO ORE DEPOSITS IN THE SOUTHERN CORDILLERA

DAVID BLOOM

PLATE TECTONIC EVOLUTION OF THE SOUTHERN CORDILLERA

William R. Dickinson
Laboratory of Geotectonics, Department of Geosciences, University of Arizona Tucson, Arizona 85721, USA

ABSTRACT

Plate interactions along both the Cordilleran and Ouachitan margins of the craton have affected the southern Cordillera at the southwest corner of the continent. Proterozoic orogenic terranes of the transcontinental arch form a prong of Precambrian basement that extends across the region into the circum-Pacific orogenic belt. Rifts that delineated latest Precambrian to early Paleozoic passive continental margins along both flanks of the continent connected somehow around or across this Precambrian prong.

Probable arc-continent collisions along the Cordilleran belt during the Devono-Mississippian Antler orogeny and the Permo-Triassic Sonoma orogeny apparently affected the Mojave region and perhaps Sonora as well as Nevada. In Nevada, a continuous Antler foreland basin developed parallel to the Roberts Mountains allochthon, but the Sonoma foreland region was more fragmented adjacent to the Golconda allochthon. Cordilleran subduction beneath the continent as part of the circum-Pacific orogenic belt was initiated in Jura-Triassic time by arc reversal following the Sonoma event.

Probable continent-continent collision during the Permo-Carboniferous Ouachita orogeny sutured parts of Gondwana including Yucatan to the southern edge of the continent. Coordinate intracontinental deformation induced by the collision orogeny formed the Ancestral Rockies uplifts and basins. Foreland basins of the late Paleozoic Ouachita belt included reactivated early Paleozoic aulacogens affected by wrench tectonics during the Ouachita orogeny.

Jurassic rifting and opening of the Gulf of Mexico probably was associated with thermotectonic uplift of the Mogollon highlands in Arizona and eastward, and was succeeded by the subsidence of Jura-Cretaceous rift troughs extending northwest as far as Arizona. Coordinate sinistral displacement of older terranes probably occurred along the Mojave-Sonora megashear.

Migratory late Mesozoic and early Cenozoic pulses of circum-Pacific magmatism and deformation were controlled by subduction of oceanic plates at varying angles of descent beneath the continent, and by accretion of exotic crustal blocks to the Cordilleran margin. An eastward sweep of arc magmatism and associated retroarc tectonism during Laramide time was followed by a westward sweep accompanied by complex extensional tectonics during mid-Cenozoic time. Late Cenozoic growth of the San Andreas transform system along the coast progressively extinguished arc magmatism, opened the Gulf of California, and triggered a complex regime of block faulting and basaltic volcanism farther inland.

INTRODUCTION

The geologic evolution of the southern Cordillera has been influenced throughout the Phanerozoic by plate interactions along both the Cordilleran and Ouachitan margins of the North American craton. Evolving tectonic elements have thus belonged partly to the circum-Pacific orogenic belt, or to preceding paleo-Pacific tectonic systems, and partly to the Caribbean region of the Atlantic realm, or to preceding Hercynian tectonics. In this respect, tectonic analysis of the southern Cordillera is inherently more complex than comparable analysis of the northern Cordillera or the Appalachian region. In those areas, only one margin of the continent is involved, and past plate interactions of either the Pacific or Atlantic worlds are the only ones of direct concern. The region of dual influence in the southern Cordillera extends from Wyoming to central Mexico, but the areas most affected have been the states of Arizona and New Mexico north of the border, and those of Sonora and Chihuahua south of the border.

Only an overview of the plate tectonic evolution of the southern Cordillera is presented here. Similar but much shorter summaries have been given by Coney (1978a), and by Woodward and Ingersoll (1979). Emphasis is placed upon inferences about the nature of plate interactions through time along the nearby continental margins, and upon the apparent relations in space and time between those interactions and tectonic events within the southern Cordillera. General ideas about the possible genetic associations of the two sets of phenomena are also explored briefly. However, no attempt is made to reach definitive conclusions about the nature of various geodynamic linkages between the peripheral plate interactions and internal structural deformation within the southern Cordillera.

Paleotectonic maps were drawn without any palinspastic restoration using the map of King (1969) as a base. The disadvantage of thus showing past tectonic elements incorrectly in space is outweighed here by the advantage that each tectonic element shown can be identified correctly in terms of present geography. Moreover, many unresolved questions are thereby avoided. These include principally the amount of crustal extension involved in the Basin-and-Range province, the amount of crustal contraction or telescoping involved in Cordilleran thrust systems, and the amount of torsional warping or tectonic rotation experienced by coastal domains and offshore islands (Beck, 1980).

The paleotectonic maps include many features and concepts presented and discussed previously

elsewhere (Graham and others, 1975; Dickinson, 1976, 1977, 1979; Dickinson and Seely, 1979; Dickinson and Snyder, 1978, 1979a, 1979b; Dickinson and others, 1979; Keith and Dickinson, 1979; Dickinson and Coney, 1980). Other ideas incorporated in the maps have arisen from discussions and field trips with many geologists in the southwest (see acknowledgments for partial list). Key depositional patterns that are depicted in generalized form were adapted from Cram (1971), Mallory (1972), or Cook and Bally (1975).

The captions of the six paleotectonic maps (see below) provide a thumbnail description of the succession of geologic settings through which the southern Cordillera passed during the Phanerozoic. The following text expands upon selected topics with emphasis upon features and concepts that are not clear from the map relations. Tectonic interpretations rely heavily upon concepts advanced initially by Hamilton (1969), Coney (1971, 1972), and various others. In this paper, however, specific citations generally are made by preference to the most recent literature that incorporates the latest information bearing upon each topic. No slight of earlier work is intended by this procedure.

TRANSFORM AND PALEOTRANSFORM OFFSETS

On each paleotectonic map, dotted lines indicate the locations of the main dextral transform strands of the Cenozoic San Andreas fault system, and the main sinistral transform strands of the Mesozoic Mojave-Sonora megashear system. In each case, older tectonic trends are offset now along these dotted lines, whereas younger tectonic trends are superimposed across them. To achieve a proper view of relations prior to offset, the displaced trends must be restored mentally to their positions of initial juxtaposition. Strands of the two transform systems with different ages and senses of motion lace partly through the same region in southern California, where original locations of displaced tectonic trends are thus especially difficult to establish.

The general geometry of the San Andreas transform system is well known, although many details of its history remain unclear. It came into being as the Pacific -American plate boundary when the Pacific-Farallon ridge was drawn into the Farallon-American trench during Late Oligocene time. Key fault strands that have accommodated significant proportions of the net dextral slip between the Pacific and American plates during the Neogene include: (a) the San Andreas fault proper and its San Gabriel branch (Crowell, 1975), (b) the San Gregorio-Hosgri fault trend along the central California coast (Graham and Dickinson, 1978a, b), (c) a fault between the inner and outer continental borderlands off southern California (Crouch, 1979), and (d) the Tosco-Abreojos fault near the shelf edge off Baja California (Spencer and Normark, 1979).

The Mojave-Sonora megashear is a more controversial feature whose location is imprecise or quite uncertain in many areas, and whose very existence is still doubted by many. It was inferred originally to explain the distribution of contrasting Precambrian plutonic terranes whose juxtaposition seemingly requires fault offsets across southeastern California, southwestern Arizona, and northwestern Sonora (Silver and Anderson, 1974). Certain puzzling aspects of the distribution of overlying Paleozoic and Mesozoic sedimentary sequences in the same region are also tentatively resolved by the megashear hypothesis (Anderson and Silver, 1979). Farther east, there is a curiously sharp jog or discontinuity in the trend of the Ouachita system within Mexico (Flawn and others, 1961, p.99-106). This anomalous feature also can be explained by fault offset if the sinistral megashear trend is extended to the southeast through the Torreon region toward the Gulf of Mexico.

The presumed course of the Mojave-Sonora megashear across Mexico provides a coherent and much-needed kinematic mechanism to resolve two outstanding problems of Caribbean plate tectonics (Dickinson and Coney, 1980): (a) the means by which Yucatan withdrew from Texas to form the oceanic region in the central Gulf of Mexico during the Jurassic, and (b) the means by which crustal overlap between southern Mexico and northwestern South America can be avoided for reconstructions of Triassic Pangaea (see also Silver and Anderson, 1974; Van der Voo and others, 1976; Coney, 1978a). The megashear trend is approximately parallel to the calculated vector of relative motion between North and South America during their initial separation in mid-Mesozoic time (Ladd, 1976). While the megashear was active as a paleotransform, Yucatan and southern Mexico thus moved coupled with South America as the Gulf of Mexico opened; when Yucatan and southern Mexico were later coupled to North America, continued motion of South America then opened the Caribbean oceanic region beyond Yucatan (see Fig. 1).

The presumed offset of the Ouachita front and the width of the Gulf of Mexico require 750-850 km of net aggregate slip along the Mojave-Sonora megashear system. However, the outcrop pattern of Paleozoic rocks in the Mojave region of California implies that the megashear split into at least two strands northwest of Sonora. Exposures in the El Paso Mountains beside the Garlock Fault suggest that a subordinate strand with total offset of perhaps 250-350 km passed along the eastern side of the Mojave block and northward along the trend of the modern Sierra Nevada (Poole and Christiansen, 1980). The nature of Paleozoic strata farther west (Stewart and Poole, 1975) indicate that the main strand or strands with about 500 km of additional displacement passed west of the Mojave block. Later dextral movements within the younger San Andreas system were subparallel to this latter path of the main megashear, and make sure recognition of the earlier sinistral movements difficult at best.

Acceptance of the Mojave-Sonora megashear as a significant tectonic feature renders inadequate most previous discussions of the tectonic history and plate tectonics of the southern Cordillera (cf. Davis and others, 1978). For example, acceptance of the megashear concept obviates the necessity to infer an early Mesozoic rift event or dextral Mesozoic truncation of the continental block to account for the abrupt termination of Paleozoic tectonic trends in central California (e.g., Burchfiel and Davis, 1972, 1975; Schweickert, 1976a).

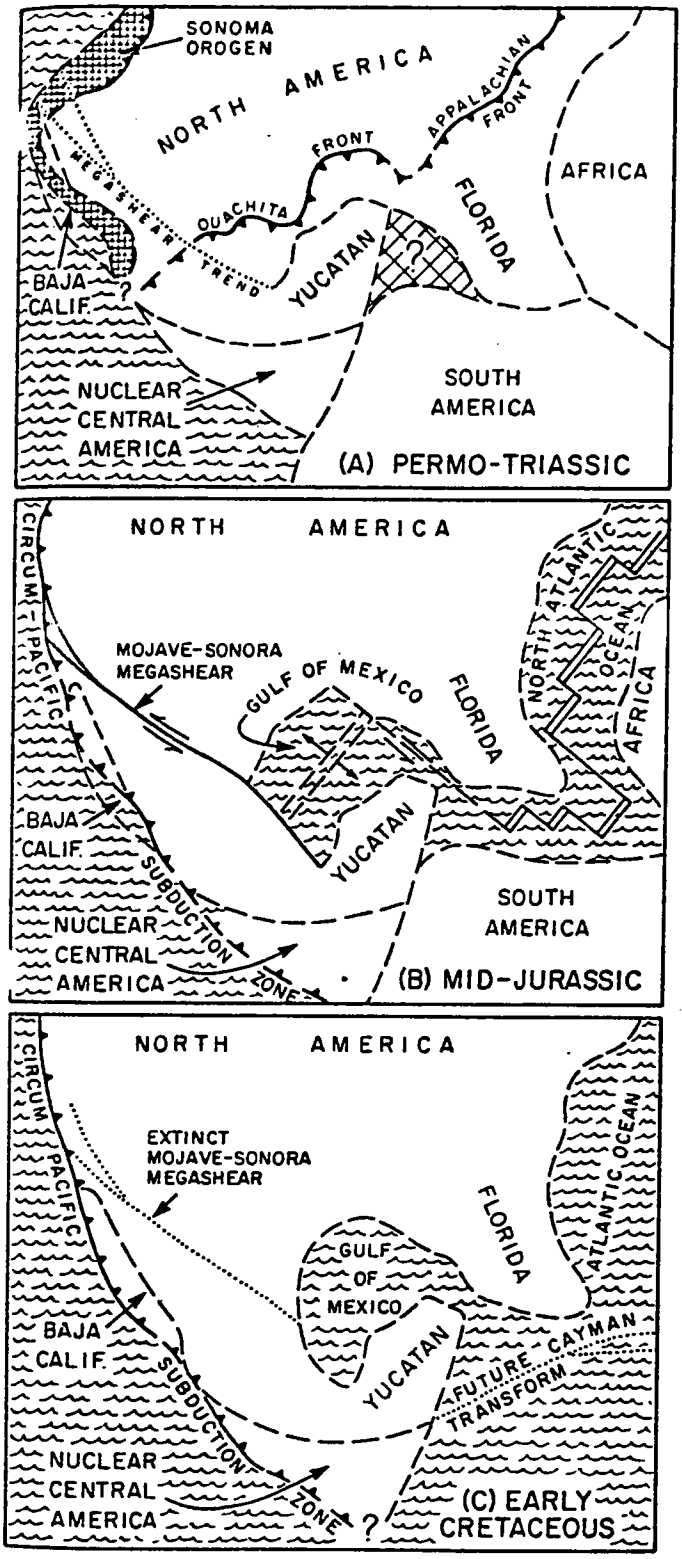

Figure 1. Sketch maps to illustrate relationship of paleotransform movement on Mojave-Sonora megashear to opening of Gulf of Mexico by Jurassic seafloor spreading (after Dickinson and Coney, 1980); oceanic regions stippled and continental blocks blank; Yucatan includes Campeche Bank; Florida includes surrounding shelves, banks and plateaus. Map A: configuration of Pangaea assembly following Permo-Carboniferous suturing of Gondwana to Laurasia along Appalachian and Ouachita segments of Hercynian orogenic belt; Permo-Triassic Sonoma orogen along Cordilleran margin includes suspect terranes accreted by mid-Triassic time; relations uncertain in queried area between Yucatan and Florida. Map B: active plate boundaries during opening of Gulf of Mexico by seafloor spreading between mid-Early and mid-Late Jurassic time; spreading systems schematic; circum-Pacific (Cordilleran) subduction zone and Mojave-Sonora megashear (paleotransform) intersect at unstable triple junction analogous geometrically to modern Cocos-American-Caribbean triple junction where Cayman transform meets Middle America trench between Mexico and Central America. Map C: relations after spreading ceased within Gulf of Mexico as South America continued to separate from North America; subsequent offset of nuclear Central America with respect to Mexico and Yucatan occurred by Cenozoic movement along Cayman transform trend.

LATEST PRECAMBRIAN AND EARLY TO MIDDLE PALEOZOIC

For most of the Precambrian, the plate tectonic environments of the southern Cordillera have not been delineated in detail. Extensive Proterozoic terranes include voluminous granitic batholiths, widespread calc-alkalic volcanics and associated metamorphic belts. These lithotectonic associations suggest that processes related to subduction were prevalent during petrogenesis (Shafiqullah and others, 1980). Local platform cover of less deformed sedimentary strata implies that Precambrian orogenesis formed a stable block of continental character. By late in the Proterozoic, the construction and assembly of crustal blocks had led to the formation of a supercontinent within which the North American craton was imbedded (Stewart, 1976). Rifting and subsequent continental drift in the latest Precambrian and early in the Paleozoic carved out the North American continental block, whose subsequent history can be followed in more detail.

The rifted continental margins of interest here were those along the Cordilleran and Ouachitan flanks of the craton (see Fig. 2). The exact time of rifting is not known with certainty in either case. Within the Cordilleran miogeocline, which was the continental terrace deposited upon the rifted Cordilleran margin, an unbroken record of sedimentation certainly extends back into the Precambrian. However, subsidence rates through time suggest, by analogy with relations along modern passive continental margins, that rifting occurred and deposition began in latest Precambrian time between 600 and 650 my BP (Stewart and Suczek, 1977). On the Ouachitan margin, volcanic rocks that form the floor of the Anadarko-Ardmore aulacogen, and thus roughly date the rift event, were erupted from 500 to 525 my BP in about Late Cambrian time (Ham and others, 1964; Burke and others, 1969).

Throughout the early Paleozoic, passive subsidence of both the Cordilleran and Ouachitan margins allowed conformable, or at least concordant, successions of shelf sediments to accumulate across broad belts flanking the craton. On the Cordilleran margin, a tract of thin platform cover passed westward across a hinge line into a wedge of miogeoclinal strata that thickened markedly westward. If such a feature were ever present along the Ouachitan margin, its location and nature have been obscured by later underthrusting beneath the Ouachita orogenic system. On Figure 2, the seaward margin of the

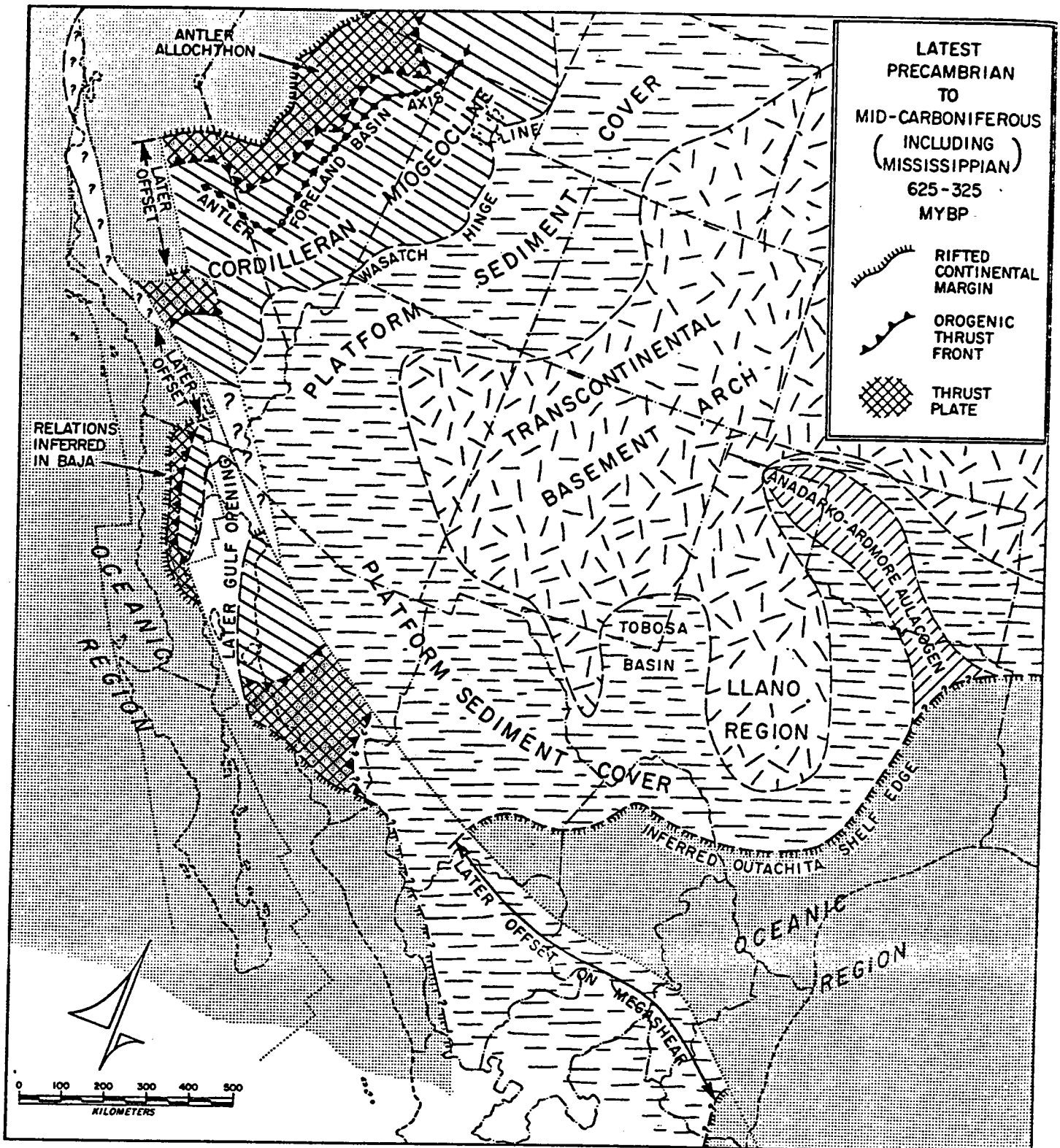

Figure 2. Paleotectonic map of southern Cordillera, latest Precambrian to mid-Carboniferous (Mississippian-Pennsylvanian boundary) time, 625-325 myBP. Rifted continental margins to northwest and southeast of transcontinental arch of Precambrian basement formed 600-650 myBP in Cordilleran region and 500-525 myBP (Late Cambrian) in Ouachitan region. Cordilleran miogeocline is continental terrace sequence deposited along passive continental margin from latest Precambrian to latest Devonian (350 myBP) time. Wasatch hinge line marks zone of gradation between miogeolinal wedge and thinner platform succession towards continental interior. Thrust plate riding over seaward margin of miogeocline is Roberts Mountains allochthon, a subduction complex of mainly oceanic strata emplaced during Antler orogeny near end of Devonian time. Deep Antler foreland basin formed in front of thrust complex in Nevada by depression of miogeoclinal terrace under the load of the nearby allochthon. On Ouachitan margin, Anadarko-Ardmore aulacogen and Tobosa basin formed by Cambrian incipient rifting of continental block inland from prominent re-entrants in rifted continental margin. Ouachita shelf edge inferred from extent of Ouachita system in subsurface. Relations in Mojave region and Mexico interpretive.

platform is taken to have been a shelf edge located now beneath the younger Ouachita allochthon.

Between the Cordilleran and Ouachitan margins, the transcontinental arch formed a projection of Precambrian basement that extended southwest from the core of the craton. This prong of Precambrian basement reaches across what is now the southern Cordillera into the heart of the circum-Pacific orogenic belt. In southern California, Precambrian basement rocks extend nearly to the shores of the Pacific. There is thus reason to wonder whether North America may once have extended some indeterminate distance to the southwest before a post-Paleozoic rift episode truncated the continental block. Figure 2 indicates that such was probably not the case. The general continuity of the belt of lower Paleozoic shelf and platform sediments, from Texas west across Arizona, suggests that the Cordilleran and Ouachitan rifted margins were connected around the end of the transcontinental arch. However, the complexity of tectonic overprints in Arizona (e.g., Peirce, 1976), and the paucity of data on the Paleozoic of Mexico (e.g., Lopez-Ramos, 1969) makes the nature of the connection still uncertain.

Near the end of Devonian time, the Antler orogeny along the Cordilleran margin deformed the outer flank of the miogeocline in Nevada, and thrust the Roberts Mountains allochthon of generally oceanic facies above the miogeoclinal strata from west to east. The allochthon contains abundant argillite, chert, and greenstone inferred to represent slices of oceanic crust. Associated quartzites probably are chiefly seafloor turbidites, but also include slope deposits, and possibly some shelf sediments as well. Emplacement of the Roberts Mountains allochthon imposed a tectonic load that depressed the edge of the continental block. Consequently, a deep foreland basin developed on top of the remaining undeformed portion of the miogeocline lying east of the thrust front. During Mississippian time, this Antler foreland basin was filled progressively by turbidite fans and deltaic complexes that were shed eastward from highlands within the allochthon along the orogenic flank of the basin (Harbaugh and Dickinson, 1981). The eastern flank of the foreland basin was marked by the fronts of Mississippian carbonate platforms that prograded westward from the margin of the craton (Rose, 1976).

Various hypotheses have been entertained for the plate tectonic setting of the Antler orogeny in Nevada (Nilsen and Stewart, 1980). Perhaps the most straightforward interpretation is the hypothesis of arc-continent collision (Dickinson, 1977). The overthrust allochthon is then interpreted as the subduction complex of an arriving arc-trench system, beneath which the miogeoclinal assemblage of the passive Cordilleran continental margin was underthrust by subduction. Recent information suggests that similar allochthonous terranes were emplaced in analogous fashion farther south, both in the Mojave region (Poole and Christiansen, 1980) and in central to southern Sonora (Peiffer-Rangin, 1979).

The greatest difficulty with the hypothesis of arc-continent collision as an explanation for the Antler orogeny is the lack of an identifiable arc terrane whose arrival at the continental margin can be attributed to an Antler collision event. Figure 3 shows schematically three possible sequels to arc-continent collision. For post-Antler evolution, Figure 3A is ruled out by the complete

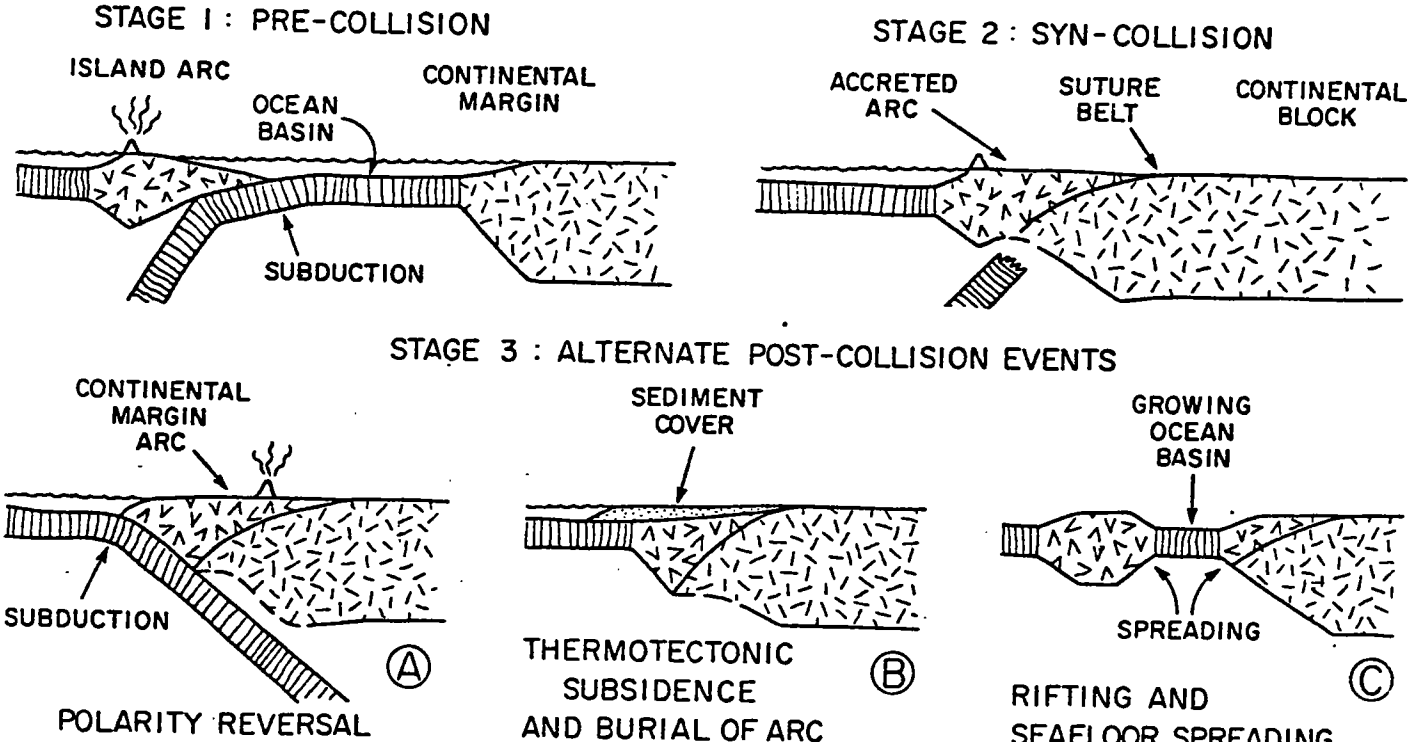

Figure 3. Schematic diagrams to illustrate alternate modes of inferred tectonic evolution following arc-continent collision orogeny. In sequel A, subduction continues following reversal of arc polarity to create new continental-margin magmatic arc. In sequel B, plates weld together and accreted arc subsides thermotectonically along modified continental margin. In sequel C, new rift tears most of arc orogen away from continental margin leaving only overthrust subduction complex behind as part of modified continental margin.

lack of subsequent arc magmatism locally. Figure 3B is conceivable, but is difficult to accept simply because intense post-Paleozoic deformation and erosion in Nevada have as yet exposed no vestige of the supposedly buried arc terrane. Figure 3C is fully compatible with known relations, and is an especially attractive alternative because oceanic facies and volcanic seafloor of late Paleozoic age form the younger Golconda allochthon emplaced locally during the Sonoma orogeny (see below). Post-Antler rifting is seemingly the only effective means to produce the requisite late Paleozoic oceanic crust nearby. Thus, the arc that collided with the Cordilleran margin during the Antler orogeny may well have been rifted away shortly afterward. If Figure 3C is not the correct scenario, we may expect eventually to discover some record of the buried arc postulated by Figure 3B. In the Antler case, this record would take the form of pre-Carboniferous arc volcanics incorporated as structural slices within the otherwise younger rocks of the Golconda allochthon (see below).

LATE PALEOZOIC AND EARLIEST MESOZOIC

Following the Antler orogeny, Pennsylvanian to Permian strata were deposited across the eroded Roberts Mountains allochthon as an overlap sequence (Silberling and Roberts, 1962). Initial nonmarine deposits were succeeded by marine strata, but facies patterns remained complex throughout the remainder of the Paleozoic along the Cordilleran margin (e.g., Stevens, 1979).

Meanwhile, the southern margin of North America was deformed by the Permo-Carboniferous Ouachita orogeny (see Fig. 4), an arc-continent or continent-continent collision event (Graham and others, 1975; Wickham and others, 1976). An allochthon of oceanic facies deformed into an imbricate subduction complex was emplaced from south to north across the depressed edge of the craton-fringing platform as the margin of the continent was underthrust beneath the flank of an arriving arc-trench system (Viele, 1979). The overthrust allochthon, known as the Ouachita system (Flawn and others, 1961), is composed mainly of argillites, cherts, and varied turbidites. The crustal elements that were sutured to North America south of the Ouachita system were formerly parts of Gondwanaland. They included the pre-Mesozoic basement block of present-day Yucatan and the Campeche Bank, together with poorly known pre-Mesozoic terranes still buried in the subsurface of the Gulf coastal plain (e.g., Woods and Addington, 1973). The Ouachita orogenic belt was thus part of the Hercynian system along which Laurasia and Gondwanaland were joined to form Pangaea. The dramatic offset of the Ouachita system from central Chihuahua to the vicinity of Ciudad Victoria in Tamaulipas is one of the most clearcut effects of major Mesozoic displacement along the Mojave-Sonora megashear (see Fig. 4).

In front of the Ouachita thrusts, major foreland basins subsided along the flank of the craton. More distant features related to the Ouachita collision orogeny were the intracratonic block uplifts and associated basins of the Ancestral Rockies system in the region of the southern Cordillera (Kluth and Coney, 1981). These largely Pennsylvanian but partly Early Permian tectonic elements were coeval in their development with the progress of the Ouachita orogeny. No correlation with tectonic events along the Cordilleran margin is indicated, because the Antler orogeny was completely over and the Sonoma orogeny had not yet begun when the Ancestral Rockies developed.

The Ancestral Rockies uplifts were basement-cored folds delimited in whole or in part by faults with normal, reverse, and wrench characteristics. The style of deformation was roughly analogous to the patterns of neotectonics observed in the interior of Eurasia as a result of its Cenozoic collision with the Indian subcontinent (Molnar and Tapponier, 1975). The intraplate deformation that produced the Ancestral Rockies is attributed similarly to the stresses induced within the North American lithosphere by the Ouachita collision. The associated sedimentary basins are an important type of intracontinental basin whose plate tectonic setting has not been well understood in the past.

The map pattern of the Ancestral Rockies system (see Fig. 4) suggests that irregularities in the shape of the pre-collision Ouachitan margin served to guide stresses along preferred paths across the transcontinental arch. For example, the Anadarko-Ardmore aulacogen was reactivated in the Ouachita foreland as a fault-bounded and internally wrenched basin (Ham and Wilson, 1967). The structural axes of the Pennsylvanian Anadarko basin and the adjacent Wichita uplift are aligned to the northwest with the structural trends of the main Ancestral Rockies uplifts in Colorado. Similarly, the late Paleozoic Permian Basin region of west Texas is superimposed above the Tobosa basin of early Paleozoic age (see Fig. 2), and local structural trends also continue northward into the Ancestral Rockies region.

The most distant basins now known within the Ancestral Rockies field are the Oquirrh basin on the northwest and the Pedregosa basin on the southwest (see Fig. 4). The Oquirrh basin lies mainly athwart the miogeoclinal belt along the Cordilleran margin, and thus marks a place where intraplate deformation caused by the Ouachita collision broke across the transcontinental arch to affect the opposite continental margin (Jordan and Douglas, 1980). The large but poorly known Pedregosa basin developed within the platform belt that had previously closed around the nose of the transcontinental arch (see Fig. 2). Its western termination is poorly known. In the Death Valley region, an Early Permian angular unconformity (Stone and others, 1980) that separates downfaulted turbidites from overlying shelf strata may reflect Ancestral Rockies deformation much farther west.

In Late Permian and Early Triassic time, an arc-continent collision along the Cordilleran margin occurred during the Sonoma orogeny (Speed, 1977). The deformed Golconda allochthon of Permo-Carboniferous oceanic strata was emplaced as a subduction complex above the underthrust Antler orogen and its thin cover in central Nevada. The rocks involved include cherts, argillites, greenstones, and turbidites. The oceanic sequence evidently accumulated in a post-Antler ocean basin that was probably formed by mid-Carboniferous rifting along the general trend of the Antler orogenic belt. Emplacement of the allochthon evidently terminated Early Triassic marine sedimentation that represented a continuation of Paleozoic depositional patterns (Collinson and Hasenmuller, 1978).

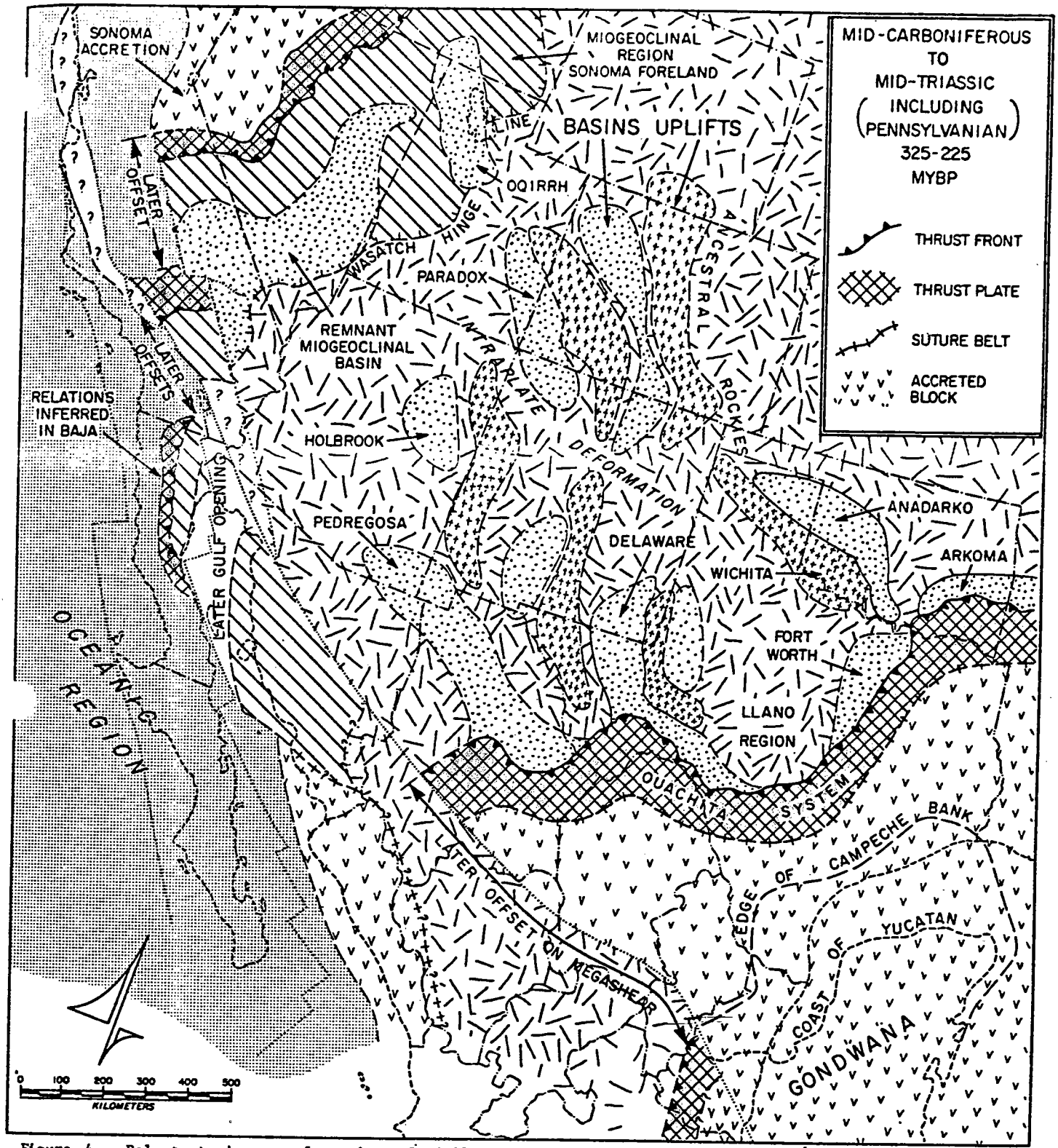

Figure 4. Paleotectonic map of southern Cordillera, mid-Carboniferous (Mississippian-Pennsylvanian boundary) to mid-Triassic (end of Middle Triassic) time, 325-225 myBP. On southeast, Ouachita system is subduction complex of Paleozoic oceanic strata thrust over previously passive continental margin during Ouachita orogeny in Pennsylvanian and earliest Permian time, 325-275 myBP (note Arkoma and Fort Worth foreland basins). Coast of modern Yucatan and edge of present Campeche Bank shown in approximate positions occupied within Pangaea, from mid-Permian to mid-Triassic time (275-225 myBP), after suturing of Gondwanan crustal blocks to the craton along the Ouachita collision belt. Pennsylvanian and Early Permian uplifts and basins of Ancestral Rockies and related systems across southern Cordillera as far as Oquirrh and Pedregosa basins formed by intraplate deformation under stresses induced by Ouachita collision orogeny. Younger thrust plate on Cordilleran margin is Golconda allochthon, a subduction complex of upper Paleozoic oceanic strata emplaced during Permo-Triassic Sonoma orogeny (275-225 myBP), when composite arc terranes were also accreted to the continental margin. Relations in Mojave region and Mexico interpretive or speculative, or both.

An extensive composite arc terrane was sutured to the Cordilleran margin during the Sonoma orogeny (Speed, 1979). In addition, local Lower Triassic magmatism like that in the Koipato volcanic center of central Nevada occurred during or just after the collision event in some areas. Middle Triassic strata of the Star Peak Group overlap the Golconda allochthon in Nevada and seemingly date the end of related accretion there (Silberling and Wallace, 1969; Nichols and Siberling, 1977). A reversal in arc polarity following the Sonoma collision probably initiated Cordilleran subduction in Late Triassic time as part of the nascent circum-Pacific orogenic belt (see Fig. 3A).

Recent work in the Mojave region indicates that major deformation and metamorphism, uplift and erosion, and deposition of both synorogenic and postorogenic clastics occurred there in association with the Sonoma orogeny (Miller, 1978; Burchfiel and others, 1980). Thrusting during the Sonoma orogeny was probably not restricted to emplacement of the Golconda allochthon, but also likely included pre-Jurassic thrusts of the Last Chance system (Stewart and others, 1966; Burchfiel and others, 1970; Dunne and others, 1978), which displaces slabs of miogeoclinal rocks. Although the latter types of thrusts have commonly been regarded as early precursors of the much younger Sevier thrust system of Cretaceous age, the fact that they are intruded locally by arc plutons of Early Jurassic age implies that they were part of the Sonoma deformation. Triassic thrusts of this type are currently well dated only in the Death Valley region. Logically, they may be present also farther northeast in Nevada and Utah where a general lack of preserved Mesozoic strata within the deformed miogeoclinal belt would make it difficult to distinguish suspected Triassic thrusts from younger Cretaceous thrusts.

LATE TRIASSIC AND JURASSIC

Between Late Triassic and Late Jurassic time, important changes in plate tectonic regimes adjacent to the southern Cordillera reflect the changing global patterns of continental drift and seafloor spreading that accompanied the breakup of Pangaea (cf. Coney, 1978b). Along the Cordilleran margin, subduction of seafloor and associated arc magmatism marked the beginning of the modern circum-Pacific orogenic system. In the Ouachita region, rifting and spreading related to the opening of the modern Atlantic formed the Gulf of Mexico as Yucatan pulled away from Texas. Coordinate transform motion along the Mojave-Sonora megashear displaced all pre-existing terranes across Mexico.

The oldest widespread plutons of the Mesozoic magmatic arc that intrude Precambrian basement and its Paleozoic cover in the southern Cordillera were emplaced about 150 to 190 my BP from mid-Early to mid-Late Jurassic time (e.g., Crowder and others, 1973; Dunne and others, 1978). Scattered plutons of Late Triassic and even older age are known locally in the Mojave region, and intermediate volcanics of Late Triassic age are locally prominent in the Sierra Nevada region (Schweickert, 1978). However, the mid-Lower to mid-Upper Jurassic granitic batholiths and associated arc volcanics form a coherent elongate belt that extends from the Sierra Nevada region (Schweickert, 1976b) across southeastern California and southern Arizona (Shafiqullah and others, 1980) into Sonora (see Fig. 5). Although rocks of the Jurassic arc terrane are displaced locally across the Mojave-Sonora megashear (Anderson and Silver, 1979), arc magmatism continued southward in Mexico. Subduction evidently proceeded under both blocks to either side of the paleotransform (Fig. 6), much as Mesoamerican subduction is underway now under both Mexico and Central America to either side of the active Cayman transform.

The time span of motion along the Mojave-Sonora megashear is not yet well constrained, but can be inferred closely from data on the opening of the Gulf of Mexico. Late Triassic rift valleys in the Texas subsurface may herald the first tentative breakup of Pangaea, but oceanic crust did not form in the Atlantic region until Jurassic time. The opening of the Gulf of Mexico by the movement of Yucatan probably occurred between mid-Early and mid-Late Jurassic time (Salvador, 1980). Logically, slip on the Mojave-Sonora megashear was confined mainly to the same time span, which is the period during which it was presumably active as a paleotransform.

The full geologic effects of slip on the megashear or paleotransform were doubtless complex, but are poorly understood. The triple junction at its western end was inherently migratory (see Fig. 6), and deformation of the adjacent continental crust was probably severe as the triple junction moved southward through time. Near the western end of the paleotransform, its trend lay subparallel to the circum-Pacific arc-trench system. Transpressional or transtensional deformation along the arc itself or within the forearc region may well have given rise to local uplifts or pull-apart basins in southern Arizona and the Mojave region. A promising topic for future study is a comparison of Upper Triassic and Lower Jurassic strata in southern Nevada (Reilly and others, 1980; Speed and Jones, 1969) with coeval strata in western Sonora (Gonzalez, 1979). The former were trapped in the backarc region behind the Jurassic arc, but the latter may well be offset equivalents that extended well into the forearc region and were carried far to the south by movements along the megashear.

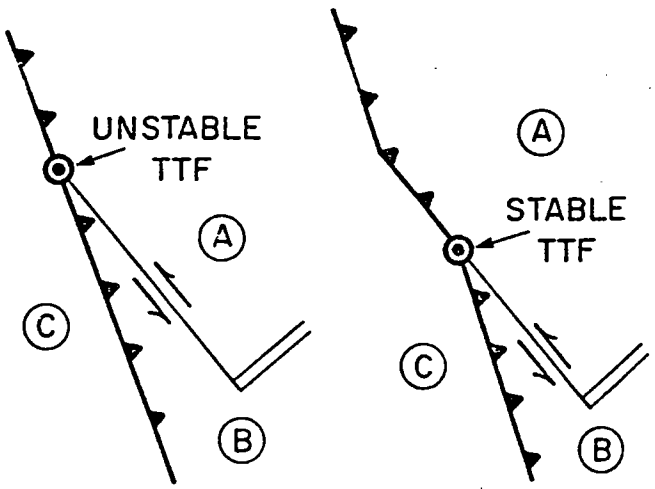

Figure 6. Diagrams of unstable (left) and stable (right) trench-trench-transform (TTF) triple junctions, the type developed where Mojave-Sonora megashear or paleotransform met circum-Pacific Cordilleran subduction zone; trench lengthens with time by addition of new central segments.

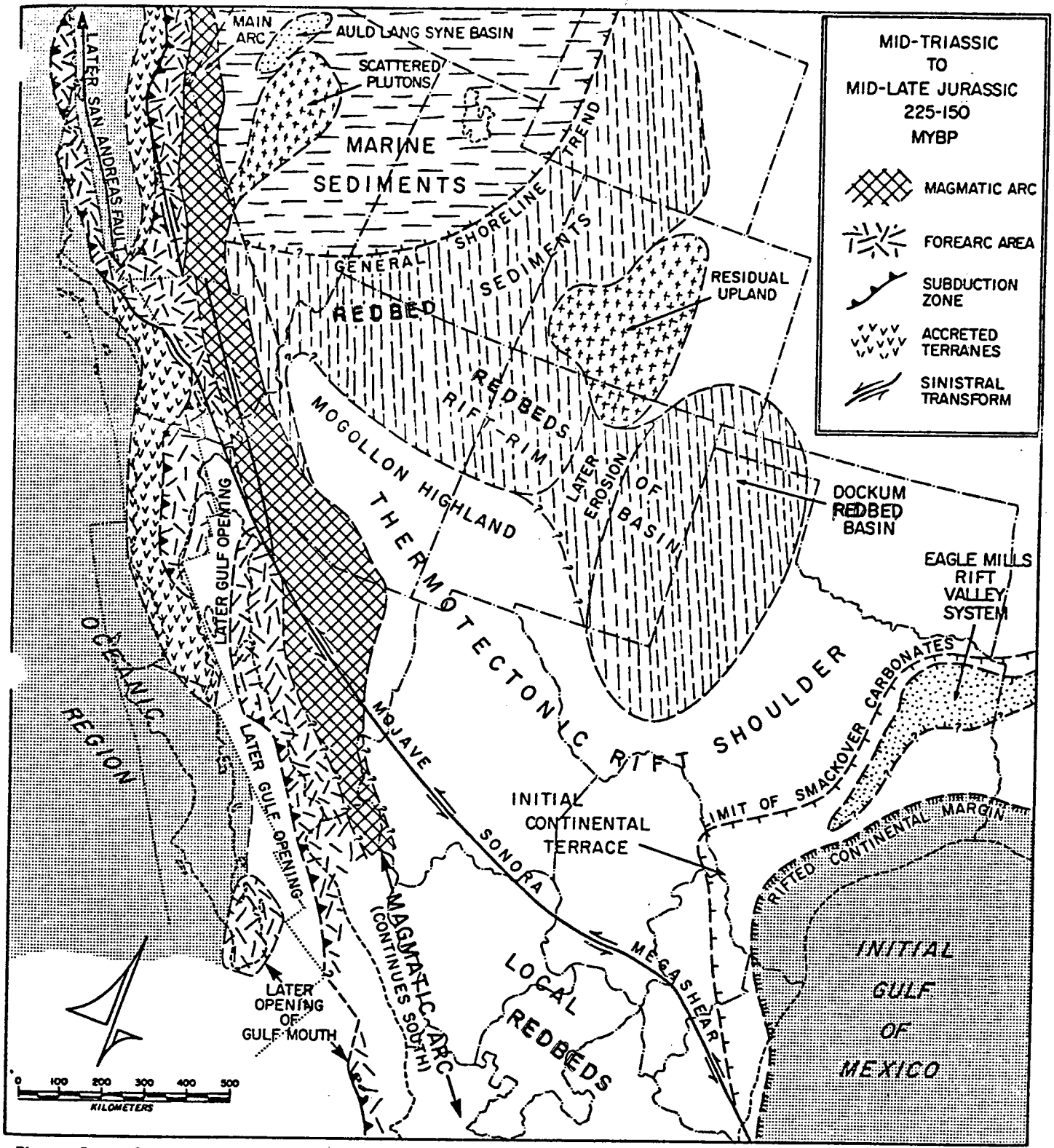

Figure 5. Paleotectonic map of southern Cordillera, mid-Triassic (end of Middle Triassic) to mid-Late Jurassic time, 225-150 myBP. In Texas, rift-valley clastics overlain by Upper Jurassic carbonates form basal horizons of Gulf Coast sediment prism whose deposition along rifted continental margin was initiated by Early to Middle Jurassic opening of oceanic Gulf of Mexico. Coordinate slip of 750-850 km on Mojave-Sonora megashear or paleotransform displaced pre-Late Jurassic terranes across Mexico. Thermotectonic uplift of edge of rifted continental block formed Mogollon highlands and related uplands separating the Gulf depression and related lowlands from an extensive rim basin, which filled with redbeds from the Colorado Plateau area to west Texas. Early to Middle Jurassic arc magmatism formed the initial volcanoplutonic complexes of the circum-Pacific arc-trench system along the Cordilleran margin. Mid-Late Jurassic accretion of intra-oceanic island arc terranes to the Cordilleran margin caused the subduction zone to step outward from locations now inland to locations near the present coast. Probable extension of Cordilleran magmatic arc southward into central Mexico not well controlled.

Farther north in Nevada, the origin of the Late Triassic to Early Jurassic basin in which the thick Auld Lang Syne Group was deposited remains unclear (Burke and Silberling, 1973). It formed after the Sonoma orogeny but before slip on the megashear. Also uncertain is the significance of scattered plutons of mid-Early to mid-Late Jurassic age in central Nevada, where they were emplaced between 150 and 180 my BP (Silberman and McKee, 1971; Erickson and others, 1978). Nearly all were intruded into ground that had previously been overridden by oceanic allochthons during the Antler and Sonoma orogenies.

In central Arizona, the Mogollon highlands that appeared in the Late Triassic served as a major sediment source for the fluvial clastics in the Upper Triassic Chinle Formation of the Colorado Plateau (Stewart and others, 1972). Other sources of redbed clastics lay in residual highlands inherited from the Ancestral Rockies system in Colorado. The origin of the Mogollon highlands to the south has long been a problem. They clearly lay behind the Jurassic arc terrane, and extended far to the east away from the Cordilleran margin. The regional tectonic relations suggest that the Mogollon highlands represented the western end of a broad thermotectonic uplift associated with rifting that formed the Gulf of Mexico and associated Mesozoic troughs farther west in Mexico.

The mid-Mesozoic redbed basin of the Colorado Plateau and the Dockum basin of Texas and eastern New Mexico thus together formed a broad rim basin (Veevers, 1977). This elongate depression lay between the more elevated interior of the continent and the thermotectonic uplift flanking troughs related to the Gulf of Mexico on the south. Later erosion has severed the continuity of the Upper Triassic redbed succession across the trend of the Rio Grande rift. Farther northwest, both Triassic and Jurassic redbeds pass gradationally into marine strata deposited along the Cordilleran margin.

Jurassic eolian units composed of dune sands that were blowing generally southward away from the shoreline trend are widespread on the Colorado Plateau (Stokes, 1961). Analogous and generally correlative strata are intercalated with Jurassic arc volcanics in the Mojave region (Miller and Carr, 1978) and in southern Arizona (Bilodeau and Keith, 1979). The continuity of this unique association of arc volcanics and quartzose dune sands across the trace of the eastern strand of the megashear implies that the largest and latest displacements occurred along the western strand of the megashear.

Subduction along the modified Cordilleran margin during the Jurassic led to the growth of a subduction complex along the present Sierra Nevada foothills. Along strike, deformed Triassic and Jurassic radiolarian cherts form parts of tectonic wedges that were underthrust beneath the flank of the continent in the Klamath Mountains (Irwin and others, 1978). In mid-Late Jurassic time, bulky oceanic island arcs apparently lodged in this subduction zone, which now lies inland, both in the Sierra Nevada foothills (Schweickert and Cowan, 1975) and in Baja California (Rangin, 1978; Gastil and others, 1978). The accretion of these crustal blocks apparently induced the subduction zone to step outward, into the site of the present California Coast Ranges and along coastal or offshore Baja California.

LATEST JURASSIC AND CRETACEOUS

Beginning in latest Jurassic time and continuing through the Cretaceous, the Franciscan subduction complex grew incrementally in width and bulk within coastal California and Baja California. Consequently, the subduction zone shifted gradually seaward, and major forearc basins developed at intervals along the arc-trench system (Ingersoll, 1979). Notable examples occupied the Great Valley of California and the Vizcaino lowlands in Baja California. The magmatic arc occupied a broad belt within which major composite batholiths were emplaced in the Sierra Nevada and the Peninsular Ranges (see Fig. 7). The trend of the igneous belt lay distinctly oceanward from its previous position in mid-Mesozoic time (Schweickert, 1976b; Coney and Reynolds, 1977).

The Franciscan assemblage has a complex internal structure marked especially by multiple thrust panels and imbricate slices of disparate terranes, and by the widespread development of intricately dislocated melanges. Subordinate components clearly represent dismembered fragments and slabs of oceanic lithosphere carried into the subduction zone from sites far out to sea. These include serpentinite altered from peridotite of the oceanic mantle, pillow basalt and related mafic igneous rocks of the oceanic crust, and radiolarian chert with minor pelagic limestone deposited on the open seafloor. However, the bulk of the Franciscan consists of graywacke and associated argillite. These turbidites probably represent trench fill and deposits of slope basins associated with the trench. The compositions of Franciscan graywackes are broadly comparable to the compositions of coeval sandstones in nearby forearc basins. Both clastic suites were derived from volcanic and plutonic sources in the nearby magmatic arc, which was undergoing dissection while igneous activity continued (Dickinson and others, 1981).

On the other side of the southern Cordillera, transgression spread shelf sediments across much of Texas and northeastern Mexico as the rifted margin of the Gulf of Mexico subsided thermotectonically. A structural arm of the Gulf depression also extended far to the northwest across Mexico toward the rear flank of the magmatic arc (see Fig. 7). Backarc deformation within the southern Cordillera varied widely from time to time and from place to place during the late Mesozoic. The most widespread effects of backarc deformation were two major sedimentary basins of regional extent: (1) in the south, the extensional Chihuahua Trough of Late Jurassic to mid-Cretaceous age connecting to the Gulf depression, and (2) in the north, a retroarc foreland basin of mid-Cretaceous to Late Cretaceous age adjacent to the Sevier thrust belt and connecting to the Alberta Basin. Let us here consider each in turn.

The Chihuahua Trough was continuous around the Coahuila Platform with the main expanse of the Gulf of Mexico. As the Gulf and its margins subsided thermotectonically following mid-Mesozoic rifting, marine waters advanced gradually up the Chihuahua Trough through Late Jurassic and Early Cretaceous time (de Czerna, 1971). The Bisbee Group of southeastern Arizona was deposited near the tip of this elongate basin farthest inland from the Gulf

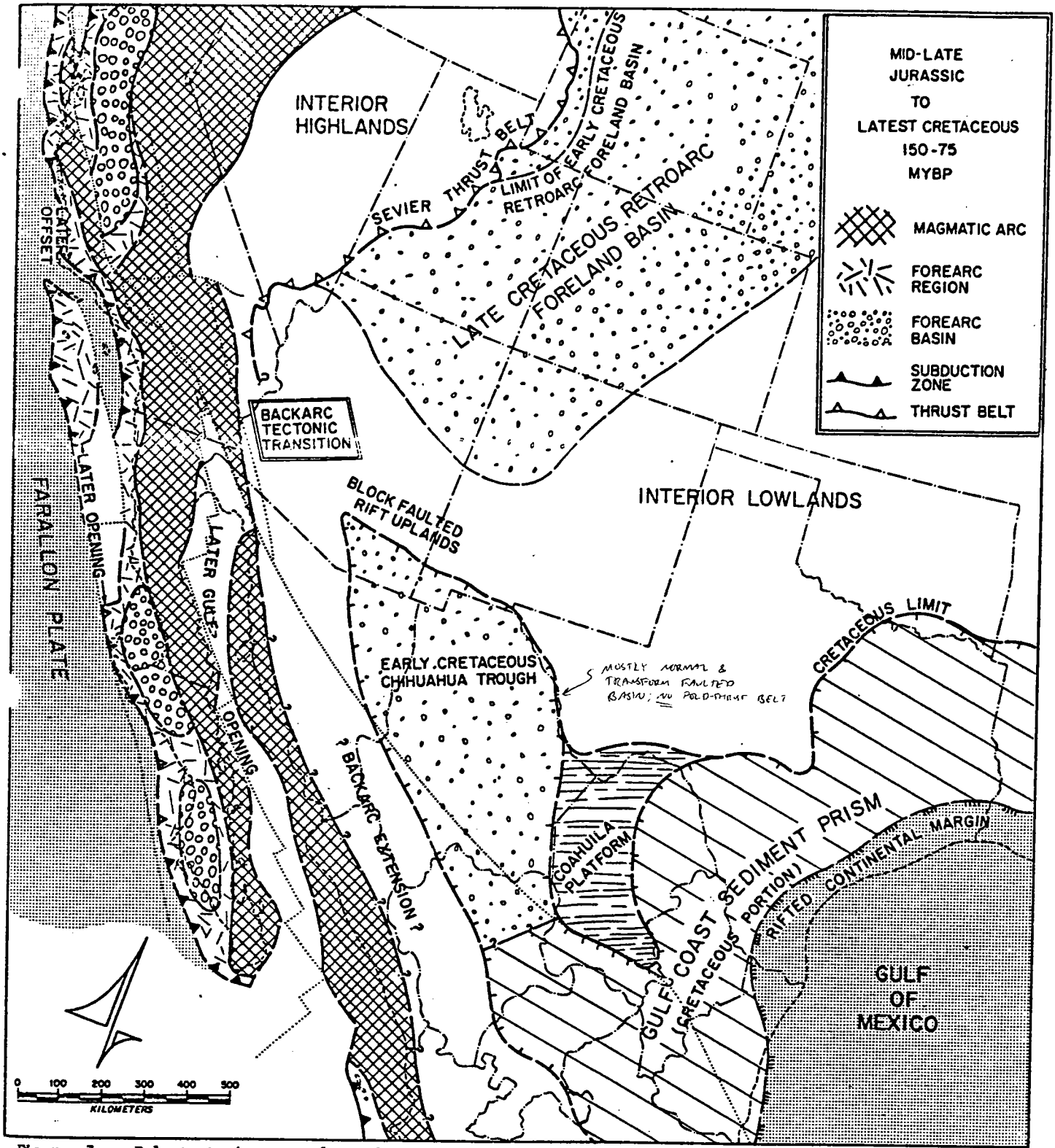

Figure 7. Paleotectonic map of southern Cordillera, mid-Late Jurassic to latest Cretaceous (Campanian-Maestrichtian boundary) time, 150-75 myBP. Continued subsidence of rifted continental margin adjacent to Gulf of Mexico was accompanied by marked Cretaceous transgression of flank of continental block. Marine invasion of Chihuahua Trough through passage connecting with Gulf of Mexico south of Coahuila Platform extended by mid-Cretaceous time (100 myBP) as far as region of backarc extension in Arizona where Bisbee Group was deposited. Farther north, backarc contraction along Sevier thrust belt induced mainly Late Cretaceous (100-75 myBP) subsidence in Rocky Mountain retroarc foreland basin as broad flank of continental block was flexed downward beneath tectonic load of foreland thrust sheets. Broad and continuous magmatic arc along Cordilleran margin formed major batholiths in Sierra Nevada and Peninsular Ranges, while major forearc basins developed in Great Valley of Alta California and beneath Vizcaino Desert in Baja California. Accretionary Franciscan subduction complex grew in bulk and width within Coast Ranges of Alta California and along coastal fringe of Baja California.

(Hayes, 1970; Cordoba and others, 1971). Marine conditions finally reached this distal region in the latter part of the Early Cretaceous, only to retreat again by mid-Cretaceous time. The Glance Conglomerate at the base of the Bisbee Group is a widespread unit of variable thickness representing coarse piedmont fans dumped into local basins from rugged nearby fault blocks forming a rift topography (Bilodeau, 1979b). The conglomerate fans and uplifted fault blocks were covered alike by finer grained fluvial and marine strata as bulk regional subsidence proceeded. The basin was essentially full to spill point with sediment by mid-Cretaceous time.

By contrast, the Late Cretaceous retroarc foreland basin of the Rocky Mountain region was associated with backarc contraction. The Sevier thrust sheets to the west formed a tectonic load that downflexed the adjacent part of the continental block to form the asymmetric foreland basin. At intervals during the evolution of the basin, Sevier thrust sheets also supplied piedmont conglomerates to the orogenic flank of the basin (Armstrong, 1968). Major deltaic complexes also prograded eastward across the basin as coastal plains built outward along the orogenic flank of the basin (Weimer, 1970). Major subsidence did not begin in Utah until about mid-Cretaceous time, although a foreland basin was present earlier farther north (Dickinson, 1976). Sedimentation continued through nearly all of the Late Cretaceous, but never extended southward across the relict Mogollon highlands of central Arizona.

The retroarc foreland basin to the north and the extensional backarc basin to the south were thus in large part of different ages, mainly Late Cretaceous in the north but Early Cretaceous in the south. At present, however, there is no indication that the two types and styles of basin tectonics were ever superimposed sequentially in the same place. Consequently, Figure 7 shows schematically a transition in backarc Cretaceous tectonics at about the latitude of the Mojave region. To the north, effects of contractional deformation were dominant, whereas effects of extensional deformation were dominant to the south.

Bilodeau (1979a) has proposed three alternate conceptual models to explain the presumed transition in backarc tectonics within the southern Cordillera during late Mesozoic time (Fig. 8). The three concepts are not mutually exclusive, and may be considered as possibly complimentary tectonic influences. Figure 8A depicts the Chihuahua Trough with its distal Bisbee basin as a segmented arm of a rift system extending as an aulacogen-like feature into the southern Cordillera from the Gulf of Mexico. Figure 8B postulates contraction to the north and extension to the south behind the Cordilleran magmatic arc as a function of different inclinations for the slab of lithosphere subducted beneath the Cordillera. The subducted slab is assumed to have been segmented or flexed (not shown) in the region of the tectonic transition of Figure 7. The significance of shallowing or steepening the angle of slab descent for tectonic regimes in the overriding plate is discussed

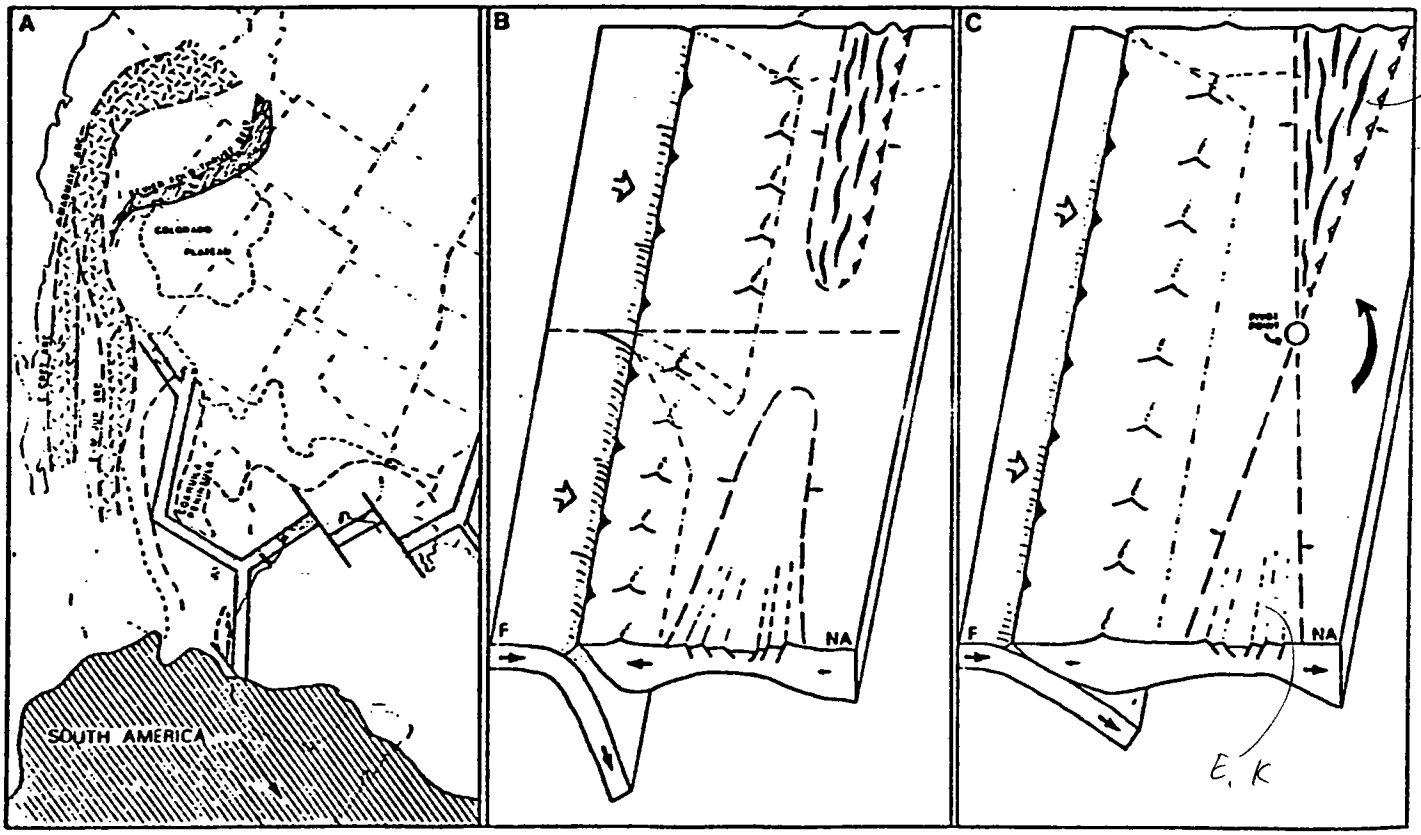

Figure 8. Alternate conceptual models (from Bilodeau, 1979a) to explain presumed transition in late Mesozoic backarc tectonics within the southern Cordillera: A (left) is aulacogen or intracontinental rift model, B (center) is model of segmented slab with variable dip, and C (right) is rotation model where absolute motion of over-riding plate varies. South America shown in Early Jurassic position (after Ladd, 1976) before rifting to open Gulf of Mexico; arc trends approximate.

further in later sections of this paper. Figure 8C attributes the tectonic transition instead to a rotational motion of the overriding plate about a pivot point located at the tectonic transition. The models of Figures 8B and 8C both involve changes in the nature of the interaction between the overriding plate and the zone of flexure or trench hinge in the plate being subducted, and either could contribute to evolution of the pattern of plate boundaries shown in Figure 8A.

The interpretation of contraction to the north and extension to the south is doubtless an oversimplified view when the factor of timing is taken into account. In western Arizona and adjacent parts of the Mojave region in California, metamorphosed Jurassic or Cretaceous redbeds were folded, together with older Paleozoic strata, into folds with southeasterly vergence during a deformational episode of probable Cretaceous age (Reynolds, 1980). In this region, earlier deposits of an extensional trough may have been crumpled by later contractional deformation. If so, perhaps the tectonic transition, between contraction to the north and extension to the south, migrated southward through Cretaceous time.

LATEST CRETACEOUS TO LATEST OLIGOCENE

Contractional deformation finally swept across the full width of the southern Cordillera along its whole length during latest Cretaceous and early Paleogene time. In a real sense, this Laramide event defined the extent of the southern Cordillera as we know it today. The inland limit of orogenic deformation migrated well toward the craton, beyond the axes of the Cretaceous sedimentary basins that previously had lain behind the magmatic arc (see Fig. 9). As orogenic deformation thus spread to interior parts of the Cordilleran belt, arc magmatism also shifted progressively eastward and waned in intensity (Armstrong, 1974; Coney, 1976; Snyder and others, 1976). The mid-Paleocene to mid-Eocene peak of deformation in the Wyoming and Colorado Rockies along the inland fringe of the Laramide orogenic belt coincided roughly with a prominent gap or null in arc magmatism within the intermontane region farther west.

Both the eastward migration of arc magmatism and orogenic deformation toward the interior of the continent, and the coordinate reduction in overall magmatic activity, can be attributed to a decrease in the dip of the subducted slab at depth beneath the southern Cordillera (Coney, 1978a; Dickinson and Snyder, 1978). Several related conditions contributed to these effects (see Fig. 10A):

1) Flattening of the angle of slab descent shifted the locus of melting near the top of the slab farther away from the subduction zone along the coast (Coney and Reynolds, 1977; Keith, 1978). Consequently, magmatism shifted inland.

2) As the inclination of the subducted slab in the mantle became subhorizontal, magma generation was suppressed because the slab did not penetrate well into the asthenosphere (cf. Barazangi and Isacks, 1976). Consequently, arc magmatism waned.

3) Shallower descent of the slab increased the degree of interaction between the subducted slab and the overriding plate by keeping the two in shear contact for longer distances inland from the coastal subduction zone (cf. Barazangi and Isacks, 1976). Consequently, the belt of Cordilleran tectonics widened.

4) Decrease in slab dip is associated with net convergence between the interior of the overriding plate and the line of flexure or trench hinge in the place being subducted (Dickinson, 1980; Dewey, 1980). Consequently, contractional tectonic features were dominant across the Cordilleran belt.

Details of the geometry of structures developed during Laramide deformation, and of the mechanics that produced them, have long been controversial. In the classic Laramide region of the Wyoming and Colorado Rockies, the dispute has centered upon the question of whether the fault-bounded basement uplifts reflect basement contraction or purely vertical tectonics (Matthews, 1978). Modern data from seismic reflection show unequivocally that key faults separating uplifts from basins are major thrusts that penetrate deep into basement at shallow dips (Smithson and others, 1979). The controversy is thus now resolved in favor of basement contraction, and the monoclines of the Colorado Plateau farther west can be viewed as less extreme products of similar contractional tectonics (e.g., Coney, 1976).

Near the Mexican border in southern Arizona and adjacent New Mexico, a different sort of

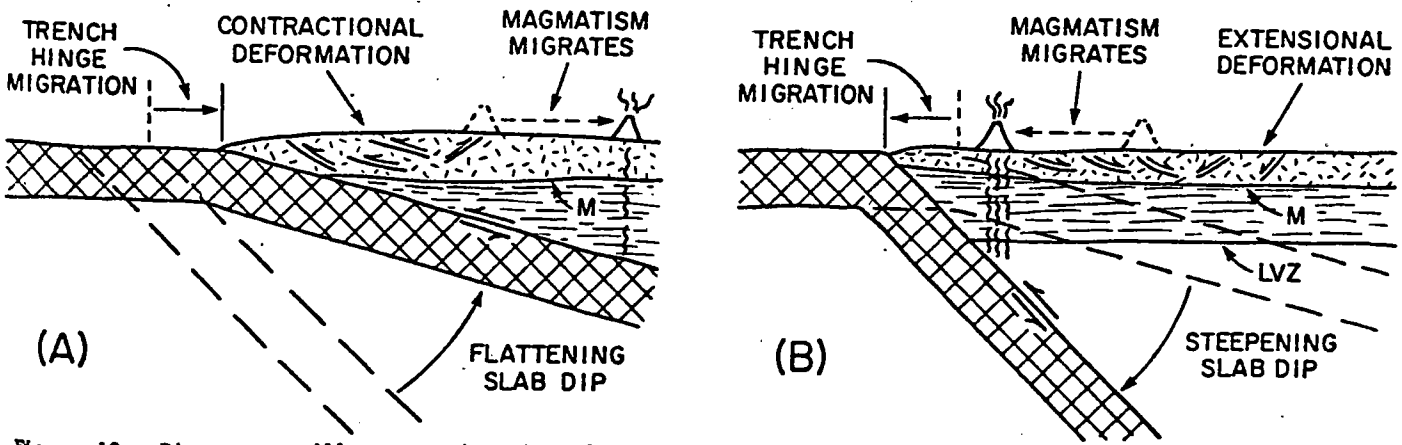

Figure 10. Diagrams to illustrate migration of arc magmatism and changing tectonic regimes within over-riding plate in response to changing dip of subducted oceanic slab. See text for discussion.

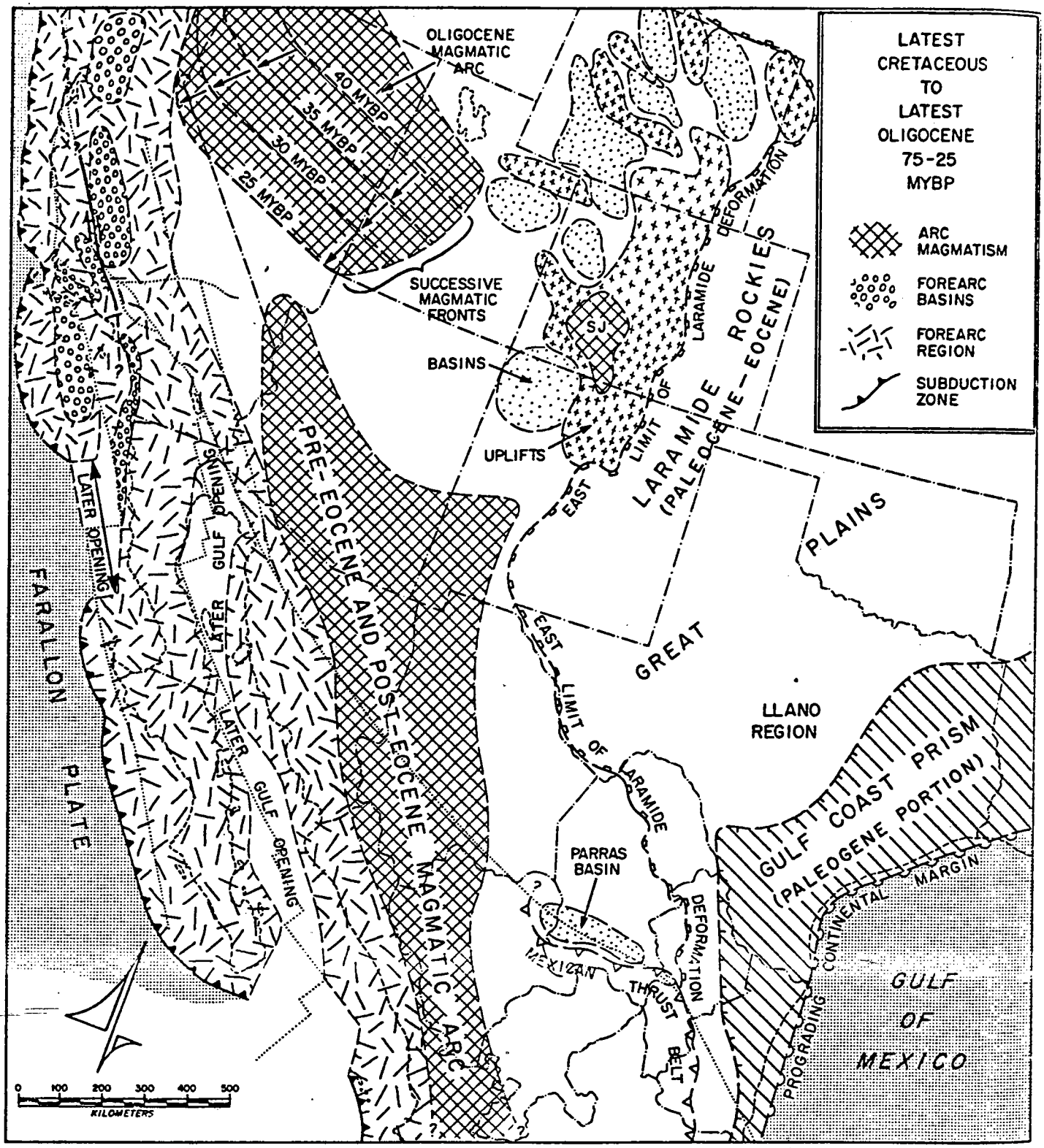

Figure 9. Paleotectonic map of southern Cordillera, latest Cretaceous (Campanian-Maestrichtian boundary) to latest Oligocene time, 75-25 my BP. Broad forearc region developed along Cordilleran margin as shallow descent of subducted Farallon plate beneath the southern Cordillera caused arc magmatism to shift eastward and wane from latest Cretaceous to mid-Eocene time (75-50 my BP). Simultaneously, contractional deformation expanded eastward to form broad Laramide orogen. Peak of intracontinental deformation to form uplifts and basins of Laramide Rockies by breakage of over-riding plate was roughly coincident with regional null in arc magmatism about mid-Eocene time (50 myBP). Arc magmatism swept back westward in Oligocene time as angle of descent of subducted Farallon plate steepened beneath the southern Cordillera, but Oligocene arc still lay inland from Cretaceous arc. Re-establishment of arc magmatism locally was accompanied by extensional deformation associated with Cordilleran metamorphic core complexes. On the Gulf Coast, progradational sedimentation advanced the shelf edge throughout Paleogene time, but latest Cretaceous to earliest Paleogene backarc thrusting in Mexico disrupted inland flank of Gulf Coast sediment prism, and formed Parras retroarc foreland.

controversy exists concerning Laramide structures (e.g., Drewes, 1976; Keith and Barrett, 1976). Local accumulations of latest Cretaceous volcanic and sedimentary rocks (Hayes and Drewes, 1978) are involved with older strata in complex folds and faults whose geometry is not yet fully resolved. There is no doubt that the structures reflect contractional tectonics, but two contrasting views of their structural style exist:

1) Drewes (1978) concludes that major exposed faults are segments of deformed thrusts whose regional attitude is essentially subhorizontal. These regional thrusts are held to delineate thin-skinned thrust sheets that experienced lateral tectonic transport of major proportions with consistent vergence toward the interior of the continent. In this view, the main difference between the observed tectonic style and the well-known style of the somewhat older Sevier thrust sheets farther north lies in the fact that the thrust panels incorporate slabs of basement rock not encountered within the Sevier thrust belt.

2) Davis (1979) concludes that major exposed faults are more local thrusts and reverse faults that bound basement-cored uplifts. The vergence of these structures is interpreted to have been controlled by the flanks of the uplifts, and thus vergence is held to be variable, both away from the interior of the continent as well as toward it. In this view, the observed tectonic style resembles that of the classic Laramide region in the Wyoming and Colorado Rockies, except that the scale of the individual uplifts is somewhat smaller.

The latter view is preferred here for two main reasons: (a) the sort of repetitive imbrication of cover rocks so typical of thin-skinned thrust belts elsewhere is not observed locally (e.g. Drewes, 1980), and (b) no broad foreland basin like that observed in Alberta or in the Cretaceous of the Rocky Mountain region is present in New Mexico between the deformed belt and the craton. Without imbrication of the cover rocks either within or adjacent to the deformed belt, it is unclear how the surficial shortening required by regional overthrusting could be accommodated. In the absence of a depressed foreland region, it is unclear how the lithosphere might have adjusted to the tectonic load imposed by the emplacement of major regional thrust sheets. However, the issue is complicated by the fact that generally coeval thrusting farther south in Mexico did lead to the development of the Parras basin, which appears to exhibit the attributes expected for a retroarc foreland basin (McBride and others, 1974).

In the Mojave region farther to the west, Laramide events are even more poorly understood. The Pelona-Orocopia schist terrane (Haxel and Dillon, 1978) was apparently metamorphosed between mid-Paleocene and mid-Eocene time. The protoliths of these rocks constitute an oceanic assemblage of graywacke accompanied by subordinate argillite, chert, and greenstone. This terrane was probably underthrust bodily beneath the whole Mojave region from the subduction zone along the edge of the continent during the Laramide interval of shallow plate descent. In effect, the pre-existing lower crust within that region was stripped back beneath the continental block and replaced by the underthrust subduction complex. Coordinate intense deformation of the over-riding upper crust may be reflected by complex thrusting and metamorphism of generally Laramide age in southwestern Arizona (Reynolds and others, 1980; Haxel and others, 1980). Proto-San Andreas strike slip near the coast (see Fig. 9) may have been induced by partial coupling of underthrust lithosphere, which was subducted obliquely, to the thin overthrust lip at the tapering edge of the over-riding continental block (Dickinson and others, 1979).

Following the period of Laramide deformation, arc magmatism was re-established within the intermontane region along a trend lying roughly parallel to the coastal subduction zone. During the Oligocene, arc activity swept progressively westward in a pattern that mimics in reverse the inward sweep of arc magmatism which accompanied the onset of Laramide deformation (Coney and Reynolds, 1977; Dickinson and Snyder, 1978; Keith, 1978). By analogy, this backswing can be attributed to a gradual increase in the dip of the subducted slab at depth beneath the southern Cordillera (see Fig. 10B). Steepening of the angle of slab descent shifted the locus of melting where the slab penetrated the asthenosphere back toward the coast, and at the same time intensified arc magmatism as full penetration of the asthenosphere by the descending slab was achieved once again. However, the Oligocene magmatic arc remained inland from the position that the main Cretaceous magmatic arc had occupied.

MID-CENOZOIC DEFORMATION

The increase in the dip of the subducted slab was associated with pronounced tectonic effects locally. Whereas flattening of slab dip produced widespread contractional tectonics, steepening of slab dip evidently induced prominent extensional tectonics, whose full implications are not yet understood. As these poorly known processes began in the Oligocene but continued into the Miocene, they pertain in part to two of the accompanying paleotectonic maps (Figs. 9 and 11), hence are discussed separately here. Damon and Bikerman (1964) were the first to argue the importance of mid-Cenozoic tectonic and magmatic events that were post-Laramide, yet preceded classic Basin-and-Range development.

One can infer that an increase in slab dip reflects coordinate retrograde motion, or rollback, of the line of flexure at the trench hinge in the plate being subducted (Dickinson, 1980; Dewey, 1980). This geotectonic feature thus tends to retreat from the interior of the over-riding continental plate back toward the center of the adjacent ocean basin. The rollback vector represents a potential for crustal divergence within the previously contracted Cordilleran lithosphere where crustal convergence had been dominant. In effect, the change in slab behavior from a flattening mode to a steepening mode may have achieved a significant relaxation of orogenic stresses. If so, a period of extensional tectonics and crustal thinning within the southern Cordillera might well be expected to have succeeded the previous episode of contractional tectonics during which crustal thickening presumably had occurred (see Fig. 10). Even so, subduction was still underway at the convergent plate boundary along the continental margin. Thus, the potential for further orogenic deformation had not been entirely removed in the manner that would prevail along a

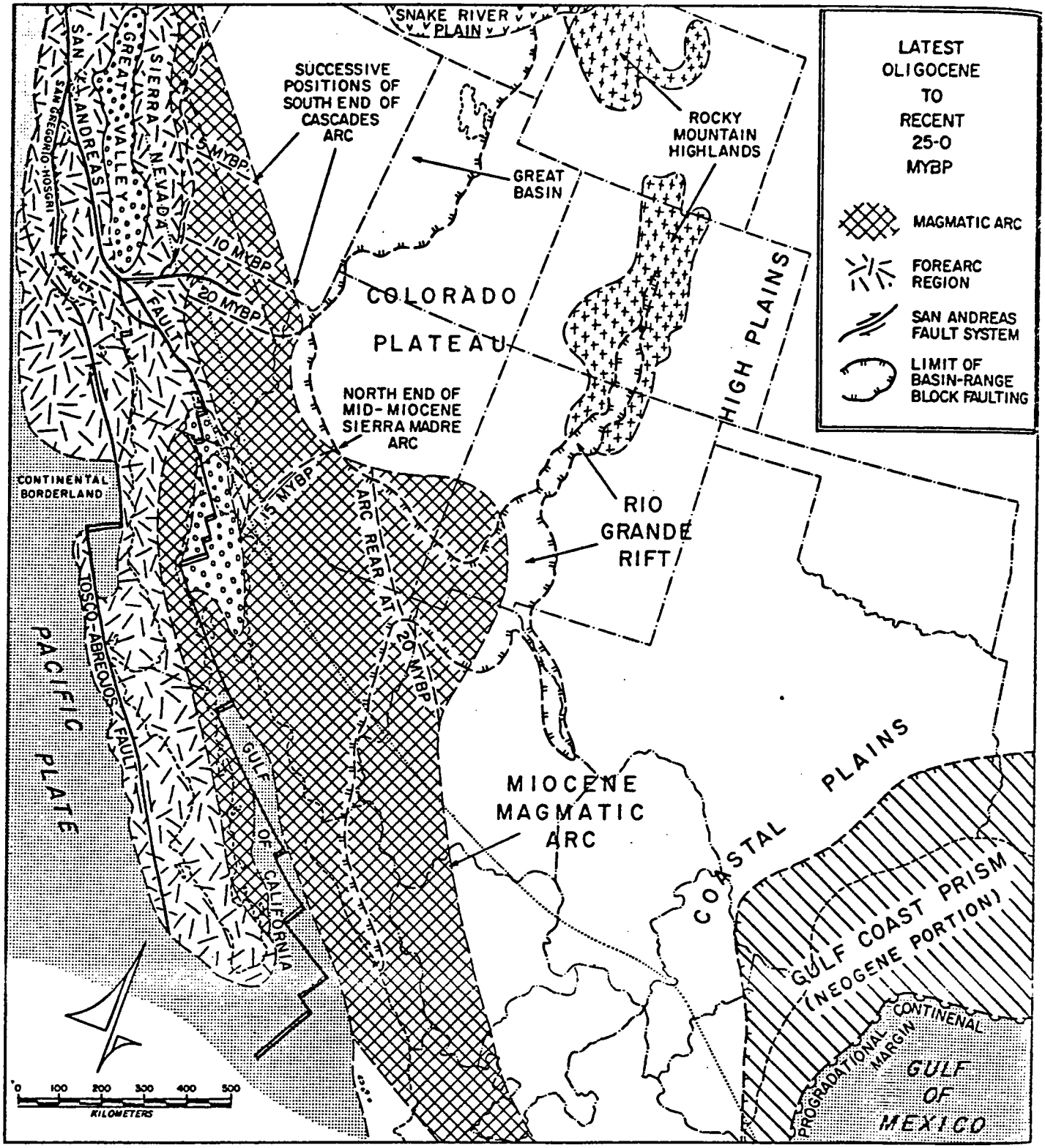

Figure 11. Paleotectonic map of southern Cordillera, latest Oligocene to Recent time, 25-0 myBP. Miocene magmatic arc had its greatest extent at the beginning of Miocene time (22.5 myBP). Since then, it has been progressively extinguished throughout the region shown as intervening segments of Farallon plate were consumed to bring Pacific and American plates into contact along San Andreas transform system. Transpressional San Andreas fault proper in California Coast Ranges and transtensional fault system within Gulf of California have been active mainly in post-Miocene time (5-0 myBP), whereas other key strands of San Andreas system along shore and offshore were most active during Miocene time. Extensional deformation within Basin-and-Range province to form typical horsts, grabens, and tilted blocks has occurred mainly since mid-Miocene time (15-0 myBP), but listric normal faulting with extreme tilting occurred earlier in Arizona. Such extensional fragmentation of the Cordilleran continental margin is restricted to the segment where no subduction zone is present and no plate consumption occurs along San Andreas transform system. Sedimentary progradation of continental margin continues along Gulf Coast.

divergent plate boundary of simple rifting.

South of the Colorado Plateau, post-Laramide arc magmatism returned to the region stretching from New Mexico to California at various times during the Oligocene (Deal and others, 1980; Shafiqullah and others, 1978, 1980; Crowe and others, 1979). Over wide areas in southern Arizona and adjacent California, the mid-Cenozoic volcanics were offset and strongly tilted, together with generally coeval clastics, by movement along listric normal faults or subhorizontal detachment surfaces (Crowe, 1978; Davis and others, 1979; Reynolds, 1980; Rehrig and others, 1980; Shafiqullah and others, 1980). This style of extensional tectonics was prevalent from latest Oligocene to approximately mid-Miocene time. Similar features of similar age are known also from the Great Basin farther north (Anderson, 1971; Proffett, 1977). Inferred directions of extensional movement are generally normal to Laramide or older Cordilleran structural trends (e.g., Rehrig and Heidrick, 1976).

Metamorphic core complexes (Coney, 1979, 1980) are associated regionally, and in places locally, with the fields of listric normal faults, and also with the surficial detachment surfaces, some of which constitute upper structural levels of exposed core complexes. Evidence for mid-Cenozoic tectonic denudation is characteristic for the metamorphic core complexes in the southern Cordillera (Davis and Coney, 1979). Many also harbor mid-Cenozoic plutons (Banks, 1980; Reynolds, 1980; Todd, 1980), and the correlation in space and time between Cordilleran core complexes and the flare-up of mid-Cenozoic arc magmatism is clear (Coney, 1979, 1980). Accordingly, the Cordilleran metamorphic core complexes are regarded here as the structurally complicated but tectonically informative record of significant mid-Cenozoic crustal extension that coincided with steepening slab dip and renewed arc magmatism (Davis, 1980; Rehrig and Reynolds, 1980).

Extension in a direction roughly colinear with the direction of earlier Laramide contraction is suggested for many areas (e.g., Rehrig and Heidrick, 1976). One factor that may complicate local structural interpretations is the possibility that subhorizontal thrust surfaces, which developed originally during Laramide contraction, may later have served to guide subhorizontal dislocations during the mid-Cenozoic extensional event (e.g., Davis and others, 1979; Shafiqullah and others, 1980). Some of the metamorphic fabrics within the core complexes may be inherited from the time of Laramide deformation (Davis and others, 1980; Keith and others, 1980). Perhaps it is even conceivable that basement thrusts along which movement accomplished crustal thickening during Laramide contraction served later as the soles of listric fault systems along which movement accomplished crustal thinning during subsequent mid-Cenozoic extension.

During the mid-Cenozoic, a broad belt along the edge of the continental block experienced wholesale uplift that produced a widespread late Paleogene erosion surface upon which the mid-Cenozoic volcanics were erupted (Epis and Chapin, 1975). This effect was produced by the subduction of successively younger and more buoyant oceanic lithosphere as the trench along the continental margin gradually encroached upon the Pacific-Farallon spreading center (Damon, 1979).

LATEST OLIGOCENE TO RECENT

In late Cenozoic time, three related processes have dominated the tectonic evolution of the southern Cordillera (see Fig. 11): (1) the extinction of subduction along the continental margin and the growth of the San Andreas transform fault system, (2) the termination of subduction-related arc magmatism and its replacement by scattered basaltic and rhyolitic volcanic centers, and (3) the development of the Basin-and-Range province of extensional tectonism within that portion of the continental block adjacent to the San Andreas transform.

Evolution of the San Andreas transform began in the Late Oligocene when the Pacific-Farallon ridge first began to encounter the Farallon-American trench near the latitude of the Mexican border. The resulting Pacific-American transform has gradually lengthened with time, although various fault strands have absorbed the main slip at different times during its long evolution (Dickinson and Snyder, 1979a). The major slip zone was probably along the continental margin until mid-Miocene time, when it stepped inland to various faults along the California coast, within the offshore borderland, and along the shelf off Baja California. The present San Andreas fault proper did not become the principle strand of the transform system until about the beginning of Pliocene time. Since then, opening of the Gulf of California has split apart the Miocene arc volcanics of the mainland from those of the peninsula (Gastil and others, 1979).

As the San Andreas transform evolved along the continental margin, arc volcanism was progressively extinguished inland because no lithosphere is subducted along a transform plate boundary. Geometric analysis of the plate motions involved indicates that a region lacking a subducted slab developed first where the San Andreas transform was initiated, and then expanded with time as a roughly triangular area lying adjacent to the growing transform with its apex well inland (Dickinson and Snyder, 1979b). The resulting absence of a subducted slab beneath the segment of the Cordillera adjacent to the San Andreas transform can be viewed as a breach or window in the subducted slab otherwise present in the mantle beneath the southern Cordillera. As this slab window expanded through time, it eventually passed beneath the magmatic arc and thus extinguished arc magmatism. The pattern of extinction observed was close to that predicted from a knowledge of relative plate motions.

In Early Miocene time, a continuous magmatic arc existed along the flank of the whole southern Cordillera (see Fig. 11). By mid-Miocene time, northward retreat of the southern end of the Cascades arc and southward retreat of the northern end of the Mexican arc were well underway. At present, no arc volcanism is present within the region. Instead, largely basaltic volcanism accompanied by some less mafic igneous activity occurs at centers scattered unsystematically throughout the region. This type of volcanism is associated in space and time with extensional tectonics of Basin-and-Range style.

The characteristic structures of Basin-and-Range tectonism are horsts, grabens, and tilt-blocks bounded by steeply-dipping normal faults, which may become listric at depth (Stewart, 1978). Major crustal extension is clearly involved. The present topographic grain within the Basin-and-Range province developed after mid-Miocene time (Eberly and Stanley, 1978; Stewart, 1978; Shafiqullah and others, 1980), during the period when expansion of a slab window beneath the southern Cordillera was progressively extinguishing arc magmatism. Much of the deformation in southern Arizona was complete by the end of Miocene time, whereas nearly all the deformation in the Great Basin to the north has occurred since latest Miocene time (Dickinson and Snyder, 1979a).

These relations suggest that upwelling of asthenosphere through the slab window may have triggered uplift and extension within the Basin-and-Range province (see Fig. 12). The inferred extent of the region lacking a subducted slab beneath it is virtually coextensive with the main Basin-and-Range province augmented by the Colorado Plateau and the Rio Grande rift (Dickinson and Snyder, 1979b). The present elevation of the southern Cordillera is compatible with the view that a subducted slab of lithosphere is present beneath the Great Plains, but tapers westward to a feather edge near the Rio Grande rift (Damon, 1979). Farther west, the elevated tracts of the intermontane region are underlain by more buoyant mantle, for differences in crustal thickness are not adequate to explain the elevation difference between regions like the Colorado Plateau and the Great Plains (Thompson and Zoback, 1979). The high mountain knots of central Colorado and northwest Wyoming may owe their extreme elevations to especially pronounced thermotectonic uplift around the apices of the Snake River plain and the Rio Grande rift.

In any case, the present elevated character of the southern Cordillera cannot be a property inherited from past plate configurations or orogenies. Most of the uplift of the modern Great Plains has occurred since latest Miocene time (Trimble, 1980). The broad regional uplift is thus presumably due to thermotectonic effects related to subduction of a spreading center in late Cenozoic time (Damon, 1979).

why is Colorado Plateau so high?

ACKNOWELDGMENTS

I thank the following for helpful discussions and field trips (but none of them should be held responsible for the thoughts that I have expressed): T.H. Anderson, W.L. Bilodeau, R.C. Blakey, B.C. Burchfiel, M.D. Carr, P.J. Coney, P.E. Damon, L.T. Grose, W.B. Hamilton, L.E. Harding, P.L. Heller, R.V. Ingersoll, W.S. Jefferson, S.B. Keith, C.F. Kluth, T.A. Lawton, J.F. Longoria, E.L. Miller, H.W. Peirce, R.E. Powell, S.J. Reynolds, S.M. Richard, L.T. Silver, J.E. Spencer, and G.W. Viele. Current research that contributed to the construction of the paleotectonic maps and the preparation of this paper was supported in part by the Earth Sciences Section of the National Science Foundation with NSF Grants EAR79-22848 and EAR80-18231, and also in part by Projects LOG-1 and LOG-2 of the Laboratory of Geotectonics in the Department of Geosciences at the University of Arizona. Earlier and less complete versions of this paper were presented in a Sandia Colloquium at the University of New Mexico in 1979, and before the Arizona Geological Society in 1980. I wish especially to thank A.K. Loring for encouragement.

REFERENCES CITED

Anderson, R.E., 1971, Thin skin distension in Tertiary rocks of southeastern Nevada: Geol. Soc. America Bull., v.82, p.43-58.

Anderson, T.H., and Silver, L.T., 1979, The role of the Mojave-Sonora megashear in the tectonic evolution of northern Sonora, in Anderson, T.H., and Roldan-Quintana, J., eds, Geology of northern Sonora: Geol. Soc. America Ann. Mtg. Field Trip Guide No. 27, p.59-68.

Armstrong, R.L., 1968, Sevier orogenic belt in Nevada and Utah: Geol. Soc. America Bull., v.79, p.429-458.

Armstrong, R.L., 1974, Magmatism, orogenic timing, and orogenic diachronism in the Cordillera from Mexico to Canada: Nature, v.247, p.348-351.

Banks, N.G., 1980, Geology of a zone of metamorphic core complexes in southeastern Arizona: Geol. Soc. America Mem. 153, p. 177-215.

Barazangi, M., and Isacks, B.L., 1976, Spatial distribution of earthquakes and subduction of the Nazca plate beneath South America: Geology, v. 4, p. 686-692.

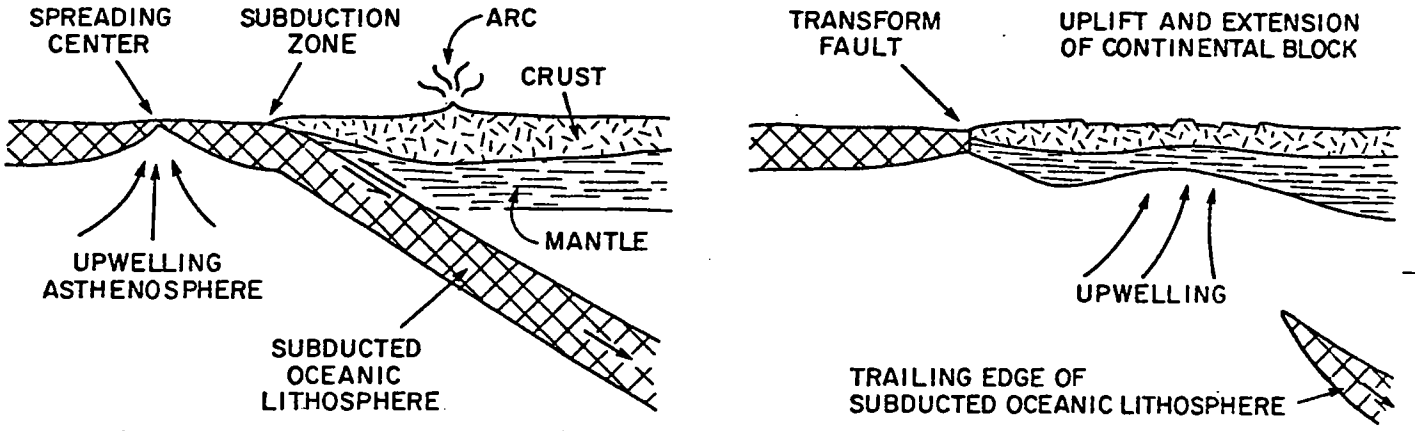

Figure 12. Diagram to illustrate concept of mantle upwelling through slab window to cause uplift and extension of over-riding plate. At left, oceanic spreading rise approaches subduction zone at trench along continental margin. At right, encounter of rise and trench has produced transform fault as trailing edge of subducted slab continues to descend, thus producing slab window through which asthenosphere then rises.

Beck, M.E., Jr., 1980, Paleomagnetic record of plate-margin tectonic processes along the western edge of North America: Jour. Geophys. Res., v.85, p.7115-7131.

Bilodeau, W.L., 1979a, Early Cretaceous tectonics and deposition of the Glance Conglomerate, southeastern Arizona: Stanford Univ. Ph.D. Dissert., Stanford, Calif., 145p.

Bilodeau, W.L., 1979b, The Glance Conglomerate, a Lower Cretaceous syntectonic deposit in southeastern Arizona, in Callender, J.F., Wilt, J.C., and Clemons, R.E., eds, Land of Cochise: N.Mex. Geol. Soc. 29th Field Conf. Guidebook, p.209-214.

Bilodeau, W.L., and Keith, S.B., 1979, Intercalated volcanics and eolian "Aztec-Navajo-like" sandstones in southeast Arizona: another clue to the Jurassic-Triassic paleotectonic puzzle of the southwestern U.S.: Geol. Soc. America Abs. With Programs, v.11, no.3, p.70.

Burchfiel, B.C., Cameron, C.S., Guth, P.L., Spencer, J.E., Carr, M.D., Miller, E.L., and McCulloh, T.H., 1980, A Triassic overlap assemblage in northern Mojave/Death Valley region, California: an interpretation: Geol. Soc. America Abs. With Programs, v.12, no.7, p.395.

Burchfiel, B.C., and Davis, G.A., 1972, Structural framework and evolution of the southern part of the Cordilleran orogen, western United States: Am. Jour. Sci., v.272, p.97-118.

Burchfiel, B.C. and Davis, G.A., 1975, Nature and controls of Cordilleran orogenesis, western United States: extensions of an earlier synthesis: Am. Jour. Sci., v.275-A, p.363-396.

Burchfiel, B.C., Pelton, P.J., and Stewart, J.H., 1970, An early Mesozoic deformation belt in south-central Nevada-southeastern California: Geol. Soc. America Bull., v.81, p.211-215.

Burke, D.B., and Silberling, N.J., 1973, The Auld Lang Syne Group of Late Triassic and Jurassic (?) age, north-central Nevada: U.S. Geol. Survey Bull. 1394-E, p.E1-E14.

Burke, W.H., Otto, J.B., and Denison, R.E., 1969, Potassium-argon dating of basaltic rocks: Jour. Geophys. Res., v.74, p.1082-1086.

Collinson, J.R., and Hasenmueller, W.A., 1978, Early Triassic paleogeography and biostratigraphy of the Cordilleran miogeosycline, in Howell, D.G., and McDougall, K.A., eds, Mesozoic paleogeography of western United States: Soc. Econ. Paleontologists and Mineralogists, Pacific Sec., Pacific Coast Paleogeography Symp. 2, p.175-188.

Coney, P.J., 1971, Cordilleran tectonic transitions and motions of the North American plate: Nature, v.233, p.462-465.

Coney, P.J., 1972, Cordilleran tectonics and North American plate motion: Am. Jour. Sci., v.272, p.603-628.

Coney, P.J., 1976, Plate tectonics and the Laramide orogeny, in Woodward, L.A., and Northrop, S.A., eds, Tectonics and mineral resources of southwestern North America: N. Mex. Geol. Soc. Special Pub. No. 6, p.5-10.

Coney, P.J., 1978a, The plate tectonic setting of southeastern Arizona, in Callender, J.F., Wilt, J.C., and Clemons, R.E., eds., Land of Cochise: N. Mex. Geol. Soc. 29th Field Conf. Guidebook, p. 285-290.

Coney, P.J., 1978b, Mesozoic-Cenozoic Cordilleran plate tectonics: Geol. Soc. America Mem. 152, p.33-50.

Coney, P.J., 1979, Tertiary evolution of Cordilleran metamorphic core complexes, in Armentrout, J.M., Cole, M.R., and TerBest, H., Jr., Cenozoic paleogeography of the western United States: Soc. Econ. Paleontologists and Mineralogists, Pacific Sec., Pacific Coast Paleogeography Symp. 3, p.14-28.

Coney, P.J., 1980, Cordilleran metamorphic core complexes: an overview: Geol. Soc. America Mem. 153, p.7-31.

Coney, P.J., and Reynolds, S.J., 1977, Cordilleran Benioff zones: Nature, v.270, p.403-406.

Cook, T.D., and Bally, A.W., eds, 1975, Stratigraphic atlas of North and Central America: Princeton Univ. Press, Princeton, N.J., 272p.

Cordoba, D.A., Rodriguez-Torres, R., and Guerrero-Garcia, J., 1971, Mesozoic stratigraphy of the northern portion of the Chihuahua Trough, in Seewald, K., and Sundeen, D., eds, The geologic framework of the Chihuahua tectonic belt: West Tex. Geol. Soc. Pub. 71-59, p.83-97.

Cram, I.H., 1971, Future petroleum provinces of the United States, their geology and potential: Am. Assoc. Petroleum Geologists Mem. 15, 1496p.

Crouch, J.K., 1979, Neogene tectonic evolution of the California continental borderland and western Transverse Ranges: Geol. Soc. America Bull., v.90, p.338-345.

Crowder, D.F., McKee, E.H., Ross, D.C., and Krauskopf, K.B., 1973, Granitic rocks of the White Mountains area, California-Nevada: age and regional significance: Geol. Soc. America Bull., v.84, p.285-296.

Crowe, B.M., 1978, Cenozoic volcanic geology and probable age of inception of basin-range faulting in the southeasternmost Chocolate Mountains, California: Geol. Soc. America Bull., v.89, p.251-264.

Crowe, B.M., Crowell, J.C., and Krummenacher, D., 1979, Regional stratigraphy, K-Ar ages, and tectonic implications of Cenozoic volcanic rocks, southeastern California: Am. Jour. Sci., v.279, p.186-216.

Crowell, J.C., ed, 1975, San Andreas fault in southern California: Calif. Div. Mines and Geology Special Rpt. 118, 272p.

Damon, P.E., 1979, Continental uplift at convergent boundaries: Tectonophysics, v.61, p.307-319.

Damon, P.E., and Bikerman, M., 1964, Potassium-argon dating of post-Laramide plutonic and volcanic rocks within the Basin and Range province of southeastern Arizona and adjacent areas: Ariz. Geol. Soc. Digest, v.7, p.63-78.

Davis, G.A., Anderson, J.L, Frost, E.G., and Shackelford, T.J., 1979, Regional Miocene detachment faulting and early Tertiary (?) mylonitization, Whipple-Buckskin-Rawhide Mountains, Southeastern California and western Arizona, in Abbott, P.L., ed, Geological excursions in the southern California area: Dept. Geol. Sci., San Diego State Univ., San Diego, Calif., p.75-108.

Davis, G.A., Anderson, J.L., Frost, E.G., and Shackelford, T.J., 1980, Mylonitization and detachment faulting in the Whipple-Rawhide-Buckskin Mountains terrane, southeastern California and western Arizona: Geol. Soc. America Mem. 153, p.79-129.

Davis, G.A., Monger, J.W.H., and Burchfiel, B.C., 1978, Mesozoic construction of the Cordilleran "collage", central British Columbia to central

California, in Howell, D.G., and McDougall, K.A., eds, Mesozoic paleogeography of the western United States: Soc. Eon. Paleontologists and Mineralogists, Pacific Sec., Pacific Coast Paleogeography Symp. 2, p.1-32.

Davis, G.H., 1979, Laramide folding and faulting in southeastern Arizona: Am. Jour. Sci., v.279, p.543-569.

Davis, G.H., 1980, Structural characteristics of metamorphic core complexes, southern Arizona: Geol. Soc. America Mem. 153, p.35-77.

Davis, G.H., and Coney, P.J., 1979, Geologic development of the Cordilleran metamorphic core complexes: Geology, v.7, p.120-124.

Deal, E.G., Elston, W.E., Erb, E.E., Peterson, S.L., Reiter, D.E., Damon, P.E., and Shafiqullah, M., 1978, Cenozoic volcanic geology of the Basin and Range province in Hidalgo County, New Mexico, in Callender, J.F., Wilt, J.C., and Clemons, R.E., eds, Land of Cochise: N. Mex. Geol. Soc. 29th Field Conf. Guidebook, p.219-230.

deCzerna, Z., 1971, Mesozoic sedimentation, magmatic activity and deformation in northern Mexico, in Seewald, K., and Sundeen, D., eds, The geologic framework of the Chihuahua tectonic belt: West Tex. Geol. Soc. Pub. 71-59, p.99-117.

Dewey, J.F., 1980, Episodicity, sequence and style at convergent plate boundaries, in Strangway, D.W., ed, The continental crust and its mineral deposits: Geol. Assoc. Canada Special Pap. 20, p.553-574.

Dickinson, W.R., 1976, Sedimentary basins developed during evolution of Mesozoic-Cenozoic arc-trench system in western North America: Can. Jour. Earth Sci., v.13, p.1268-1287.

Dickinson, W.R., 1977, Paleozoic plate tectonics and the evolution of the Cordilleran continental margin, in Stewart, J.H., Stevens, C.H., and Fritsche, A.E., eds, Paleozoic paleogeography of the western United States: Soc. Econ. Paleontologists and Mineralogists, Pacific Sec., Pacific Coast Paleogeography Symp. 1, p.137-155.

Dickinson, W.R., 1979, Cenozoic plate tectonic setting of the Cordilleran region in the United States, in Armentrout, J.M., Cole, M.R., and TerBest, H., Jr., eds, Cenozoic paleogeography of the western United States: Soc. Econ. Paleontologists and Mineralogists, Pacific Sec., Pacific Coast Paleogeography Symp. 3, p.1-13.

Dickinson, W.R., 1980, Plate tectonics and key petrologic associations, in Strangway, D.W., ed, The continental crust and its mineral deposits: Geol. Assoc. Canada Special Pap.20, p.341-360.

Dickinson, W.R., and Coney, P.J., 1980, Plate tectonic constraints on the origin of the Gulf of Mexico, in Pilger, R.H., Jr., ed, The origin of the Gulf of Mexico and the early opening of the central North Atlantic Ocean: School of Geoscience, Louisiana State Univ., Baton Rouge, La., p.27-36.

Dickinson, W.R., Ingersoll, R.V., Cowan, D.S., Helmold, K.P., and Suczek, C.A., 1981, Provenance of Franciscan graywackes in coastal California: Geol. Soc. America Bull., in press.

Dickinson, W.R., Ingersoll, R.V., and Graham, S.A., 1979, Paleogene sediment dispersal and paleotectonics in northern California: Geol. Soc. America Bull., v.90, Pt.I, p.897-898; Pt.II, p.1458-1528.

Dickinson, W.R., and Seely, D.S., 1979, Structure and stratigraphy of forearc regions: Am. Assoc. Petroleum Geologists Bull., v.63, p.2-31.

Dickinson, W.R., and Snyder, W.S., 1978, Plate tectonics of the Laramide orogeny: Geol. Soc. America Mem. 151, p.355-366.

Dickinson, W.R., and Snyder, W.S., 1979a, Geometry of triple junctions related to San Andreas transform: Jour. Geophys. Res., v.84, p.561-572.

Dickinson, W.R., and Snyder, W.S., 1979b, Geometry of subducted slabs related to San Andreas transform: Jour. Geology, v.87, p.609-627.

Drewes, H., 1976, Laramide tectonics from Paradise to Hells Gate, southeastern Arizona: Ariz. Geol. Soc. Digest, v.10, p.151-168.

Drewes, H., 1978, The Cordilleran orogenic belt between Nevada and Chihuahua: Geol. Soc. America Bull., v.89, p.641-657.

Drewes, H., 1980, Tectonic map of southeast Arizona: U.S. Geol. Survey Misc. Inv. Map I-1109, 1:125,000.

Dunne, G.C., Gulliver, R.M., and Sylvester, A.G., 1978, Mesozoic evolution of rocks of the White, Inyo, Argus, and Slate Ranges, eastern California, in Howell, D.G., and McDougall, K.A., eds, Mesozoic paleogeography of the western United States: Soc. Econ. Paleontologists and Mineralogists, Pacific Sec., Pacific Coast Paleogeography Symp. 2, p.189-208.

Eberly, L.D., and Stanley, T.B., Jr., 1978, Cenozoic stratigraphy and geologic history of southwestern Arizona: Geol. Soc. America Bull., v.89, p.921-940.

Epis, R.C., and Chapin, C.E., 1975, Geomorphic and tectonic implications of the post-Laramide, late Eocene erosion surface in the southern Rocky Mountains: Geol. Soc. America Mem. 144, P.45-74.

Erickson, R.L., Silberman, M.L., and Marsh, S.P., 1978, Age and composition of igneous rocks, Edna Mountain quadrangle, Humboldt County, Nevada: U.S. Geol. Survey Jour. Research, v.6, p.727-743.

Flawn, P.T., Goldstein, A., Jr., King, P.B., and Weaver, C.E., 1961, The Ouachita system: Univ. Tex. Bur. Econ. Geology Pub. No. 6120, 401p.

Gastil, G., Krummenacher, D., and Minch, J., 1979, The record of Cenozoic volcanism around the Gulf of California: Geol. Soc. America Bull., v.90, p.839-857.

Gastil, G., Morgan, G.J., and Krummenacher, D., 1978, Mesozoic history of peninsular California and related areas east of the Gulf of California, in Howell, D.G., and McDougall, K.A., eds, Mesozoic paleogeography of the western United States: Soc. Econ. Paleontologists and Mineralogists, Pacific Sec., Pacific Coast Paleogeography Symp. 2, p.107-116.

Gonzalez, C., 1979, Geology of the Sierra del Alamo, in Anderson, T.H., and Roldan-Quintana, J., eds, Geology of northern Sonora: Geol. Soc. America Ann. Mtg. Field Trip No. 27,p.23-31.

Graham, S.A., Dickinson, W.R., and Ingersoll, R.V., 1975, Himalayan-Bengal model for flysch dispersal in the Appalachian-Ouachita system: Geol. Soc. America Bull., v.86, p.273-286.

Graham, S.A., and Dickinson, W.R., 1978a, Evidence

for 115 kilometers of right-slip on the San Gregorio-Hosgri fault trend: Science, v.199, p.179-181.

Graham, S.A., and Dickinson, W.R., 1978b, Apparent offsets of on-land geologic features across the San Gregorio-Hosgri fault trend: Calif. Div. Mines and Geology Special Rpt. 137, p.13-24.

Ham, W.E., Denison, R.E., and Merritt, C.A., 1964, Basement rocks and structural evolution of southern Oklahoma: Okla. Geol. Survey Bull. 95, 302p.

Ham, W.E., and Wilson, J.L., 1967, Paleozoic epeirogeny and orogeny in the central United States: Am. Jour. Sci., v.265, p.332-407.

Hamilton, W., 1969, Mesozoic California and the underflow of the Pacific mantle: Geol. Soc. America Bull., v.80, p.2409-2430.

Harbaugh, D.W., and Dickinson, W.R., 1981, Depositional facies of Mississippian clastics, Antler foreland basin, central Diamond Mountains, Nevada: Jour. Sed. Petrology, v.51, in press.

Haxel, G., and Dillon J.,1978 The Pelona-Orocopia Schist and Vincent-Chocolate Mountain thrust system, southern California, in Howell, D.G., and McDougall, K.A., eds, Mesozoic paleogeography of western United States: Soc. Econ. Paleontologists and Mineralogists, Pacific Sec., Pacific Coast Paleogeography Symp.2, p.453-469.

Haxel, G., Wright, J.E., May, D.J., and Tosdal, R.M., 1980, Reconnaissance geology of the Mesozoic and lower Cenozoic rocks of the southern Papago Indian Reservation, Arizona: Ariz. Geol. Soc. Digest, v.12, p.17-30.

Hayes, P.T., 1970, Cretaceous paleogeography of southeastern Arizona and adjacent areas: U.S. Geol. Survey Prof. Paper 658-B, 42p.

Hayes, P.T., and Drewes, H., 1978, Mesozoic depositional history of southeastern Arizona, in Callender, J.F., Wilt, J.C., and Clemons, R.E., eds, Land of Cochise: N. Mex. Geol. Soc. 29th Field Conf. Guidebook, p.201-207.

Ingersoll, R.V., 1979, Evolution of the Late Cretaceous forearc basin, northern and central California: Geol. Soc. America Bull., v.90, p. 813-826.

Irwin, W.P., Jones, D.L., and Kaplan, T.A., 1978, Radiolarians from pre-Nevadan rocks of the Klamath Mountains, California and Oregon, in Howell, D.G., and McDougall, K.A., eds, Mesozoic paleogeography of the western United States: Soc. Econ. Paleontologists and Mineralogists, Pacific Sec., Pacific Coast Paleogeography Symp. 2, p. 303-310.

Jordan, T.E., and Douglas, R.C., 1980, Paleogeography and structural development of the Late Pennsylvanian to Early Permian Oquirrh basin, northwestern Utah, in Fouch, T.D., and Magathan, E.R., eds, Paleozoic paleogeography of the west-central United States: Soc. Econ. Paleontologists and Mineralogists, Rocky Mountain Sec., Rocky Mountain Paleogeography Symp. 1, p.217-238.

Keith, S.B., 1978, Paleosubduction geometries inferred from Cretaceous and Tertiary magmatic patterns in southwestern North America: Geology, v.6, p.516-521.

Keith, S.B., and Barrett, L.F., 1976, Tectonics of the central Dragoon Mountains: a new look: Ariz. Geol. Soc. Digest, v.10, p.169-204.

Keith, S.B., and Dickinson, W.R., 1979, Transition from subduction to transform tectonics in southwestern North America (22-8 myBP): Geol. Soc. America Abs. With Programs, v.11, No.7, p.455.

Keith, S.B., Reynolds, S.J., Damon, P.E., Shafiqullah, M., Livingston, D.E., and Pushkar, P.D., 1980, Evidence for multiple intrusion and deformation within the Santa Catalina-Rincon-Tortolita crystalline complex, southeastern Arizona: Geol. Soc. America Mem. 153, p. 217-267.

King, P.B., 1969, Tectonic map of North America: U.S. Geol. Survey, 1:5,000,000.

Kluth, C.F., and Coney, P.J., 1981, Plate tectonics of the ancestral Rocky Mountains: Geology, v.9, p.10-15.

Ladd, J.W., 1976, Relative motion of South America with respect to North America and Caribbean tectonics: Geol. Soc. America Bull., v.87, p.969-976.

Lopez-Ramos, E., 1969, Marine Paleozoic rocks of Mexico: Am. Assoc. Petroleum Geologists Bull., v.53, p.2399-2417.

Mallory, W.W., ed, 1972, Geologic atlas of the Rocky Mountain region: Rocky Mtn. Assoc. Geologists, Denver, Colo., 331p.

Matthews, V., III, ed, 1978, Laramide folding associated with basement block faulting in the western United States: Geol. Soc. America Memoir 151, 370p.

McBride, E.F., Weidie, A.E., Wolleben, J.A., and Laudon, R.C., 1974, Stratigraphy and structure of the Parras and La Popa basins, northeastern Mexico: Geol. Soc. America Bull., v.84, p.1603-1622.

Miller, E.L., 1978, The Fairview Valley Formation: a Mesozoic intraorogenic deposit in the southwestern Mojave desert, in Howell, D.G., and McDougall, K.A., eds, Mesozoic paleogeography of the western United States: Soc. Econ. Paleontologists and Mineralogists, Pacific Sec., Pacific Coast Paleogeography Symp. 2, p.277-282.

Miller, E.L., and Carr, M.D., 1978, Recognition of possible Aztec-equivalent sandstones and associated Mesozoic metasedimentary deposits within the Mesozoic magmatic arc in the southwestern Mojave Desert, California, in Howell, D.G., and McDougall, K.A., eds, Mesozoic paleogeography of the western United States: Soc. Econ. Paleontologists and Mineralogists, Pacific Sec., Pacific Coast Paleogeography Symp. 2, p.283-290.

Molnar, P., and Tapponier, P., 1975, Cenozoic tectonics of Asia: effects of a continental collision: Science, v.189, p.419-426.

Nichols, K.M., and Silberling, N.J., 1977, Stratigraphy and depositional history of the Star Peak Group (Triassic), northwestern Nevada: Geol. Soc. America Special Pap. 178, 73p.

Nilsen, T.H., and Stewart, J.H., 1980, The Antler orogeny, mid-Paleozoic tectonism in western North America: Geology, v.8, p.298-302.

Peiffer-Rangin, F., 1979, Les zones isopiques du Paleozoique inferieur du nord-ouest mexicain, temoins du relais entre les Appalaches et la cordillere ouest-americaine: Compte Rendu Acad. Sci. Paris, Ser. D, v.288, p.1517-1519.

Peirce, H.W., 1976, Elements of Paleozoic tectonics in Arizona: Ariz. Geol. Soc. Digest, v.10, p.37-58.

Poole, F.G., and Christiansen, R.L., 1980, Allochthonous lower and middle Paleozoic eugeosynclinal rocks in El Paso Mountains, northwestern Mojave Desert, California: Geol.

Soc. America Abs. With Programs, v.12, No.3, p.147.

Proffett, J.M., Jr., 1977, Cenozoic geology of the Yerington District, Nevada, and implications for the origin and nature of Basin and Range faulting: Geol. Soc. America Bull., v.88, p.247-266.

Rangin, C., 1978, Speculative model of Mesozoic geodynamics, central Baja California to northeastern Sonora (Mexico), in Howell, D.G., and McDougall, K.A., eds, Mesozoic paleogeography of western United States: Soc. Econ. Paleontologists and Mineralogists, Pacific Sec., Pacific Coast Paleogeography Symp. 2, p.85-106.

Rehrig, W.A., and Heidrick, T.L., 1976, Regional tectonic stress during the Laramide and late Tertiary intrusive periods, Basin and Range province, Arizona: Ariz. Geol. Soc. Digest, v.10, p.205-228

Rehrig, W.A., and Reynolds, S.J., 1980, Geologic and geochronologic reconnaissance of a northwest-trending zone of metamorphic core complexes in southern and western Arizona: Geol. Soc. America Mem. 153, p.131-157

Rehrig, W.A., Shafiqullah, M., and Damon, P.E., 1980, Geochronology, geology, and listric normal faulting of the Vulture Mountains, Maricopa County, Arizona: Ariz. Geol. Soc. Digest, v.12, p.89-110.

Reilly, M.B., Breyer, J.A., and Oldow, J.S., 1980, Petrographic provinces and provenance of the Upper Triassic Luning Formation, west-central Nevada: Geol. Soc. America Bull., v.90, Pt. I, p.573-575; Pt. II, p.2112-2151.

Reynolds, S.J., 1980, Geologic framework of west-central Arizona: Ariz. Geol. Soc. Digest, v.12,p.1-16.

Reynolds, S.J., Keith, S.B., and Coney, P.J., 1980, Stacked overthrusts of Precambrian crystalline basement and inverted Paleozoic sections emplaced over Mesozoic strata, west-central Arizona: Ariz. Geol. Soc. Digest, v.12, p.45-52.

Reynolds, S.J., and Rehrig, W.A., 1980, Mid-Tertiary plutonism and mylonitization, South Mountain, Central Arizona: Geol. Soc. America Mem. 153, p.159-175.

Rose, P.R., 1976, Mississippian carbonate shelf margins, western United States: U.S. Geol. Survey Jour. Research, v.4, p.449-466.

Salvador, A., 1980, Late Triassic-Jurassic paleogeography and the origin of the Gulf of Mexico, in Pilger, R.H., Jr., ed, The origin of the Gulf of Mexico and the early opening of the central North Atlantic Ocean: School of Geoscience, Louisiana State Univ., Baton Rouge, La., p.101.

Schweickert, R.A., 1976a, Early Mesozoic rifting and fragmentation of the Cordilleran orogen in the western U.S.A.: Nature, v.260, p.586-591.

Schweickert, R.A., 1976b, Shallow-level plutonic complexes in the eastern Sierra Nevada, California, and their tectonic implications: Geol. Soc. America Special Pap. 176, 58p.

Schweickert, R.A., 1978, Triassic and Jurassic paleogeography of the Sierra Nevada and adjacent regions, California and western Nevada, in Howell, D.G., and McDougall, K.A., eds, Mesozoic paleogeography of western United States: Soc. Econ. Paleontologists and Mineralogists, Pacific Sec., Pacific Coast Paleogeography Symp. 2, p.361-384.

Schweickert, R.A., and Cowan, D.S., 1975, Early Mesozoic tectonic evolution of the western Sierra Nevada, California: Geol. Soc. America Bull., v.86, p.1329-1336.

Shafiqullah, M., Damon, P.E., Lynch, D.J., and Kuck, P.H., 1978, Mid-Tertiary magmatism in southeastern Arizona, in Callender, J.F., Wilt, J.C., and Clemons, R.E., eds, Land of Cochise: N. Mex. Geol. Soc. 29th Field Conf. Guidebook, p.231-242.

Shafiqullah, M., Damon, P.E., Lynch, D.J., Reynolds, S.J., Rehrig, W.A., and Raymond, R.H., 1980, K-Ar geochronology and geologic history of southwestern Arizona and adjacent areas: Ariz. Geol. Soc. Digest, v.12, p.201-260.

Silberling, N.J., and Roberts, R.J., 1962, Pre-Tertiary stratigraphy and structure of northwestern Nevada: Geol. Soc. America Special Pap. 72, 58p.

Silberling, N.J., and Wallace, R.E., 1969, Stratigraphy of the Star Peak Group (Triassic) and overlying lower Mesozoic rocks, Humboldt Range, Nevada: U.S. Geol. Survey Prof. Paper 592, 50p.

Silberman, M.L., and McKee, E.H., 1971, K-Ar ages of granitic plutons in north-central Nevada: Isochron/West, no.1, p.15-32.

Silver, L.T., and Anderson, T.H., 1974, Possible left-lateral early to middle Mesozoic disruption of the southwestern North American craton margin: Geol. Soc. America Abs. With Programs, v.6, No.7, p.955-956.

Smithson, S.B., Brewer, J.A., Kaufman, S., Oliver, J.E., and Hurich, C.A., 1979, Structure of the Laramide Wind River uplift, Wyoming, from COCORP deep reflection data and fram gravity data: Jour. Geophys. Res., v.84, p.5955-5972.

Snyder, W.S., Dickinson, W.R., and Silberman, M.L., 1976, Tectonic implications of space-time patterns of Cenozoic magmatism in the western United States: Earth Planet. Sci. Lettrs., v.32, p.91-106.

Speed, R.C., 1977, Island-arc and other paleogeographic terranes of late Paleozoic age in the western Great Basin, in Stewart, J.H., Stevens, C.H., and Fritsche, A.E., eds, Paleozoic paleogeography of the western United States: Soc. Econ. Paleontologists and Mineralogists, Pacific Sec., Pacific Coast Paleogeography Symp. 1, p.349-362.

Speed, R.C., 1979, Collided Paleozoic microplate in the western United States: Jour. Geology, v.87, p.279-292.

Speed, R.C., and Jones, T.A., 1969, Synorogenic quartz sandstone in the Jurassic mobile belt of western Nevada: Boyer Ranch Formation: Geol. Soc. America Bull., v.80, p.2551-2584.

Spencer, J.E., and Normark, W.R., 1979, Tosco-Abreojos fault zone: A Neogene transform plate boundary within the Pacific margin of southern Baja California, Mexico: Geology, v.7, p.554-557.

Stevens, C.H., 1979, Lower Permian of the central Cordilleran miogeosyncline: Geol. Soc. America Bull., v.90, Pt. I, p.140-142; Pt. II, p.381-455.

Stewart, J.H., 1976, Late Precambrian evolution of North America: plate tectonics implication: Geology, v.4, p.11-15.

Stewart, J.H., 1978, Basin-Range structure in western North America: a review: Geol. Soc. America Mem. 152, p.1-32.

Stewart, J.H., and Poole, F.G., 1975, Extension of the Cordilleran miogeosynclinal belt to the San

Andreas fault, southern California: Geol. Soc. America Bull., v.86, p.205-212.

Stewart, J.H., Poole, F.G., and Wilson, R.F., 1972, Stratigraphy and origin of the Chinle Formation and related Upper Triassic strata in the Colorado Plateau region: U.S. Geol. Survey Prof. Paper 690, 336p.

Stewart, J.H., Ross, D.C., Nelson, C.A., and Burchfiel, B.C., 1966, Last Chance thrust -- a major fault in the eastern part of Inyo County, California: U.S. Geol. Survey Prof. Paper 550-D, p.D23-D34.

Stewart, J.H., and Suczek, C.A., 1977, Cambrian and latest Precambrian paleogeography and tectonics in the western United States,. in Stewart, J.H., Stevens, C.H., and Fritsche, A.E., eds, Paleozoic paleogeography of the western United States: Soc. Econ. Paleontologists and Mineralogists, Pacific Sec., Pacific Coast Paleogeography Symp. 1, p.1-18.

Stone, P., Stevens, C.H., and Cavit, C.D., 1980, A regional Early Permian angular unconformity in eastern California: Geol. Soc. America Abs. With Programs, v.12, No.3, p.154.

Stokes, W.L., 1961, Fluvial and eolian sandstone bodies in Colorado Plateau, in Peterson, J.A., and Osmond, J.C., eds, Geometry of sandstone bodies: Am. Assoc. Petroleum Geologists, Tulsa, Okla., p.151-178.

Thompson, G.A., and Zoback, M.L., 1979, Regional geophysics of the Colorado Plateau: Tectonophysics, v.61, p.149-181.

Todd, V.R., 1980, Structure and petrology of a Tertiary gneiss complex in northwestern Utah: Geol. Soc. America Mem. 153, p.349-383.

Trimble, D.E., 1980, Cenozoic tectonic history of the Great Plains contrasted with that of the southern Rocky Mountains: a synthesis: Mtn. Geologist, v.17, p.59-69.

Van der Voo, R., Mauk, F.J., and French, R.B., 1976, Permian-Triassic continental configurations and the origin of the Gulf of Mexico: Geology, v.4, p.177-180.

Veevers, J.J., 1977, Rifted arch basins and post-breakup rim basins on passive continental margins: Tectonophysics, v.41, p.T1-T15.

Viele, G.W., 1979, Geologic map and cross section, eastern Ouachita Mountains, Arkansas: map summary: Geol. Soc. America Bull., v.90, Pt.I, p.1096-1099.

Weimer, R.J., 1970, Rates of deltaic sedimentation and intrabasin deformation, Upper Cretaceous of Rocky Mountain region, in Morgan, J.P., ed, Deltaic sedimentation, modern and ancient: Soc. Econ. Paleontologists and Mineralogists Special Pub. No.15, p.270-292.

Wickham, J., Roeder, D., and Briggs, G., 1976, Plate tectonics models for the Ouachita foldbelt: Geology, v.4, p.173-176.

Woods, R.D., and Addington, J.W., 1973, Pre-Jurassic geologic framework, northern Gulf basin: Gulf Coast Assoc. Geol. Soc. Trans., v.23,p.92-108.

Woodward, L.A., and Ingersoll, R.V., 1979, Phanerozoic tectonic setting of Santa Fe country, in Ingersoll, R.V., ed, Santa Fe country: N. Mex. Geol. Soc. 30th Field Conf. Guidebook, p.51-58.

VOLUME 93 NUMBER 6

THE JOURNAL OF GEOLOGY

November 1985

BASEMENT AND SEDIMENTARY RECYCLING—2: TIME DIMENSION TO GLOBAL TECTONICS[1]

JÁN VEIZER[2] AND SIEGFRIED L. JANSEN
Derry Laboratory, Department of Geology, University of Ottawa, Ottawa, Ontario, K1N 6N5, Canada
and Department of Systems and Computer Engineering, Carleton University, Ottawa, Ontario, K1S 5B6, Canada

ABSTRACT

If plotted on mass (volume, area, tonnage) vs. time diagrams, geologic entities—for example, continental and oceanic crust, sediments, and mineral resources—display an exponential (power law) relationship, with entity per unit time increasing toward the present. This relationship is consistent with the concept of recycling and can be simulated mathematically. The authors' approach is based on the plate tectonic theory and considers area-age or mass-age distributions of crystalline basement and sediments for major global tectonic realms. Each tectonic realm is characterized by a specific lifespan, which is an inverse function of its recycling rate (b). The estimated average half-area or half-mass ages (τ_{50}) are the following: basins of active margins ~30 Ma, oceanic sediments ~40 Ma, oceanic crust ~55 Ma, basins of passive margins ~80 Ma, immature orogenic belts ~100 Ma, mature orogenic belts ~380 Ma, and platforms ~380 Ma. The corresponding parameters for continental crust are ~690 Ma for K/Ar, and ~1200 Ma for Rb/Sr and U-Th/Pb dating pairs. For Sm/Nd τ_{50} is $\lesssim$ 1800 Ma, suggesting either that continental crust was growing during geologic history and/or its recycling via mantle (or lower crust) was more vigorous prior to 2500 Ma ago. The estimated maximal survival (or oblivion) ages for these tectonic realms are ~3–3.5 times longer than their τ_{50}. Tectonic diversity preserved in the geologic record is therefore a function of time, with oceanic tectonic realms, because of their rapid recycling, underrepresented in the rocks older than ~300 Ma. Sm/Nd isotopic systematics of sediments suggests that, for a near steady-state post-Archean sedimentary mass, recycling is ~90 ± 5% cannibalistic. This yields an estimated upper limit on crust-mantle exchange via sediment subduction of $\sim 1.1 \pm 0.5 \times 10^{15}$ g a^{-1} (~0.5 ± 0.2 km^3 a^{-1}); considerably less than demanded by isotopic constraints. The discrepancy may indicate the existence of additional loci, such as orogenic belts, for significant crust-mantle interaction.

INTRODUCTION

The evolution of the Earth is characterized by a combination of recurring (cyclic) and superimposed unidirectional phenomena. The recurring, short-term phenomena leave behind only residual records, and the long-term trends, as they appear to us, are usually a compound picture of such residual records. For example, the present-day continental crust is a result of agglomeration of remnants from recurring episodes of orogenesis. In order to understand this long-term evolution, it is essential to appreciate the time scales of the repetitive phenomena and the probabilities of their preservation over geologic time.

This dynamic understanding of the Earth is inherent in the concept of global plate tectonics. We are aware that tectonic realms associated with the oceanic crust are, geologically speaking, euphemeral features with low probabilities of preservation. In contrast, tectonic realms within present-day continents are characterized by expanded records. This suggests a long-term frequency for the generation and destruction of continental tectonic

[1] Manuscript received October 18, 1984; revised April 26, 1985.
[2] Publication XX-85 of the Ottawa-Carleton Centre for Geoscience Studies.

[JOURNAL OF GEOLOGY, 1985, vol. 93, p. 625–643]

0022-1376/85/9306-002$1.00

realms. In this contribution we would like to demonstrate that recycling is amenable to systematic conceptual treatment. Furthermore, we shall propose estimates for the average net rates of generation and/or destruction of major global tectonic realms. This, in turn, predicts their probabilities of preservation over geologic time, and hence their lifespans.

CONCEPTUAL APPROACH

Our present approach is analogous to that of population dynamics in living systems. A natural population, characterized by a continuous birth/death cycle, is usually typified by an age distribution similar to that in figure 1. The proportion of progressively older constituent units, such as human individuals, decreases exponentially. This exponential (power law) decrease is due to mortality usually being proportional to, or a first-order function of, the size of the given age group. A cumulative curve of such an age histogram defines all necessary attributes of a given population. These are its *size* A (here 100%), *half-life* τ_{50}, *mean age* τ_{MEAN}, and *oblivion age* τ_{MAX} (fig. 1 and appendix 1). The above τ_{50}, τ_{MEAN}, and τ_{MAX}, and thus the slope of the cumulative curve, are an inverse function of the mortality rate; the faster the rate the steeper the slope, because older individuals have a lower chance of survival. For a steady-state extant population, natality per unit time equals combined mortality for all age groups during the same time interval. Consequently, the cumulative slope remains the same but propagates into the future (fig. 1 bottom). This natality (= mortality) rate is designated as the *average recycling proportionality parameter* **b**. For growing, non-steady-state populations, the given **b** relates directly to a specific population *growth model* **n** (fig. 2). Usually, the **b**'s for most realistic growth models ($n \leq 3$) in fast cycling populations are similar to those for the steady-state ($n = 1/\infty$), but the integrated *recycled quantities* of constituents **D** decrease with increasing **n**. For slowly cycling systems, the results in the subsequent text are tabulated, and the **b**'s and **D**'s for specific **n**'s can be read either directly or extrapolated from the tables. Furthermore, the *beginnings* t_0 (fig. 2) of population growth and recycling for geological applications are allowed to vary between 4.5 and 2.7 Ga ago for all theoretical growth models. We have to point out, however, that other things being equal, the calculated **b**'s are inversely related to time resolution; a relationship of particular importance for fast-cycling systems. For example, time resolution of 10 yrs will not even register many individuals who were born and died before their first census. It is therefore essential to select the simulation *time increment* (= *resolution*) **T** as close as possible to the frequencies of natural systems. The selected **T**, in million years, is identified in the text as a superscript (e.g., $\mathbf{b}^{20}$ signifies a **b** derived for T = 20 Ma). As a final point, there is a fundamental dichotomy between the modes of creation/destruction of oceanic and continental domains. Subduction of the oceanic crust is consuming preferentially, although not exclusively, its oldest portions, while in the continental domain (and at its margins) it is the youngest components that contribute the bulk of recycled material. Consequently

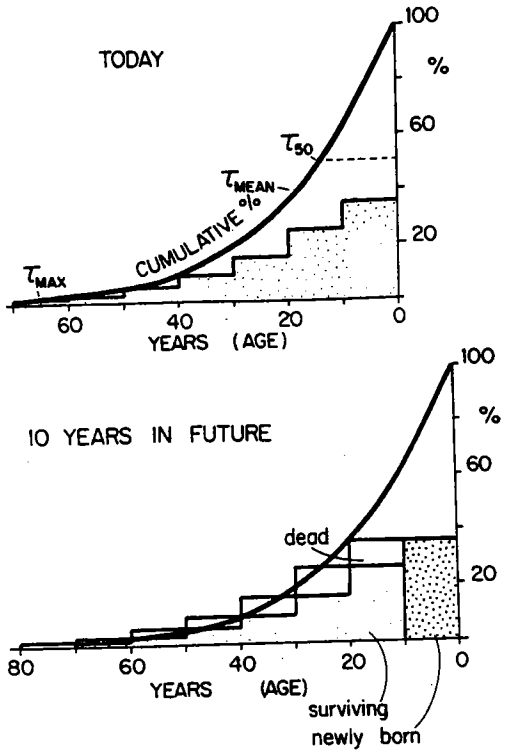

FIG. 1.—Theoretical age distribution for a steady-state living system. τ_{50}, τ_{MEAN}, and τ_{MAX} as in appendix 1. In this case, the natality/mortality rate is 35% of the total population for a 10-year interval ($\mathbf{b} = 35 \times 10^{-3}\ a^{-1}$).

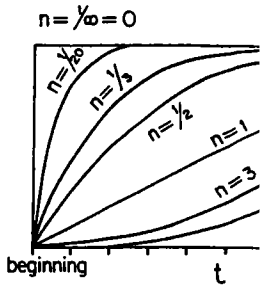

FIG. 2.—Model populati
The modeled **n**'s represer
growth patterns from an i
of the total population at t_0
a steady-state, to linear gr
stantaneous generation at
models for decreasing po
creasing size of continents
sidered here. For fast cyc
ments and oceanic domain
models are analogous to **n**

the preferred T for th
long (≥20 Ma), while f
main it is short (≤20 M

The mathematics of tl
presented in Veizer an
the glossary of terms is
dix 1. The most impor
tions to the concept of r
burg (1961), Armstrong
(1970, 1980, 1985), Ga
(1971*a*, 1971*b*), Li (197
lack (1980), Sclater et
sons (1981, 1982), Dace
and Thompson (1984).

The calculated mo
specifically the **b**'s, a
squares fitting of the t
age distributions to the
conceptual geological
the context and will be
We are keenly aware
tion is episodic rather
that intervals of growth
ternate with quiescent i
tions in our models a
essarily the sole pos
particularly for partia
The scatter of points
mulative curve is prob
factor. Such deviation
portance for evaluati
creation vs. destructi
sedimentation/erosion,

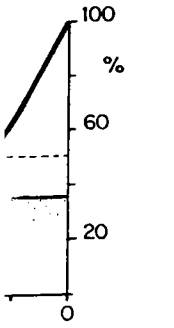

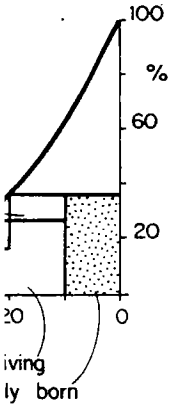

ribution for a
AN, and τ_{MAX} as
atality/mortality
n for a 10-year

al growth mod-
however, that
calculated **b**'s
solution; a re-
tance for fast-
, time resolu-
register many
id died before
refore essen-
ime increment
ossible to the
. The selected
l in the text as
a **b** derived for
ere is a funda-
modes of cre-
nd continental
ceanic crust is
ough not exclu-
le in the conti-
rgins) it is the
contribute the
Consequently

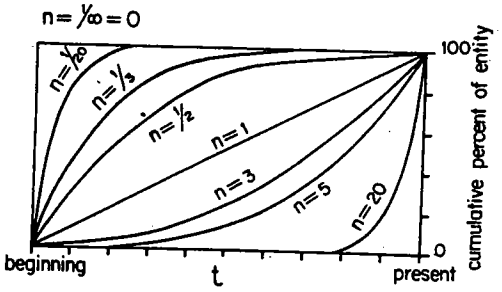

FIG. 2.—Model population growth patterns (**n**). The modeled **n**'s represent an infinite number of growth patterns from an instantaneous generation of the total population at t_0 ($n = 1/\infty$), representing a steady-state, to linear growth ($n = 1$), to an instantaneous generation at present ($n = \infty$). The models for decreasing population size (e.g., decreasing size of continents with time) are not considered here. For fast cycling systems (e.g., sediments and oceanic domain), solutions for **b** in such models are analogous to $n = 1/\infty$.

the preferred **T** for the oceanic domain is long (≥20 Ma), while for the continental domain it is short (≤20 Ma).

The mathematics of this approach has been presented in Veizer and Jansen (1979), and the glossary of terms is summarized in appendix 1. The most important recent contributions to the concept of recycling are: Wasserburg (1961), Armstrong (1968, 1981), Gregor (1970, 1980, 1985), Garrels and Mackenzie (1971*a*, 1971*b*), Li (1972), Sprague and Pollack (1980), Sclater et al. (1980, 1981), Parsons (1981, 1982), Dacey and Lerman (1983), and Thompson (1984).

The calculated model parameters, and specifically the **b**'s, are derived by least-squares fitting of the theoretical cumulative age distributions to the ones observed. The conceptual geological meaning depends on the context and will be specified in the text. We are keenly aware that geological evolution is episodic rather than continuous and that intervals of growth and/or destruction alternate with quiescent intervals. The assumptions in our models are therefore not necessarily the sole possible approximations, particularly for partial short-term records. The scatter of points around the overall cumulative curve is probably due mostly to this factor. Such deviations are of paramount importance for evaluation of *partial* rates of creation vs. destruction (e.g., the rates of sedimentation/erosion, faunal extinction, generation/dispersal of mineral resources, etc.), but they do not preclude calculation of the long-term overall average rates (cf. Veizer 1984).

The term *recycling*, as employed in this contribution, designates any process causing apparent rejuvenation of a given geologic entity. If the process conserves the matter, it is termed *closed system* (or *cannibalistic*) recycling. At the opposite end of the spectrum, a continuous generation and destruction of an entity via an external reservoir is termed an *open system* recycling. In nature, most cycles are neither entirely closed nor open. As an example, the sedimentary cycle approaches the former and the generation/destruction of the oceanic crust the latter alternative.

The rates of recycling proposed in the subsequent text must be considered as first-order approximations only. Future improved data base and theoretical treatment will yield more sophisticated solutions. It is our hope that this contribution will stimulate accumulation of relevant data and a reappraisal of the conceptual understanding of the geological evolution of the Earth.

THEORETICAL RECYCLING RATES

In this section only the theoretical average recycling proportionality constants (**b**'s) will be presented. Their direct geological meaning will be discussed in the subsequent text.

Oceanic Crust.—The present-day area (mass, volume)-age distribution of the oceanic crust is summarized in table 1 and has been discussed previously by Berger and Winterer (1974), Sprague and Pollack (1980), Sclater et al. (1980, 1981), and Parsons (1981, 1982). The observed distributions (fig. 3) indeed approximate the previously discussed exponential pattern. In this paper, we shall deal with the subject solely to derive the appropriate model parameters for our systematics. The calculated $\mathbf{b}^{\geq 20}$ is $110 \pm 5 \times 10^{-10}$ a^{-1} for all realistic growth models ($n \leq 10$). This translates into an average generation/destruction of oceanic crust of 3.4 ± 0.2 km^2 a^{-1} or 20.4 ± 0.9 km^3 a^{-1} ($67.3 \pm 3.1 \times 10^{15}$ g a^{-1}); in accord with the results of Sclater et al. (1981), Parsons (1982), Turcotte and Schubert (1982), and Dewey and Windley (1981).

Continental Crust.—The distribution of age provinces in the continental crust is

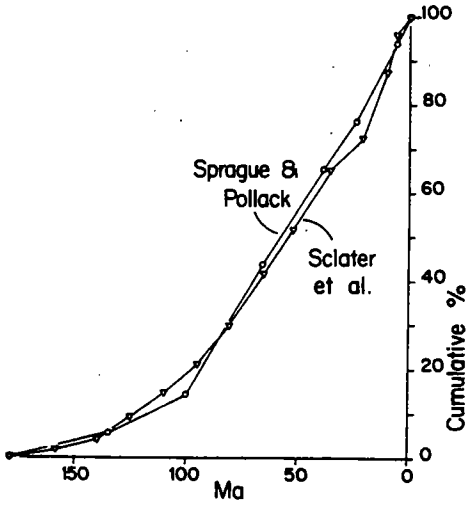

FIG. 3.—Present-day area-age distribution of oceanic crust.

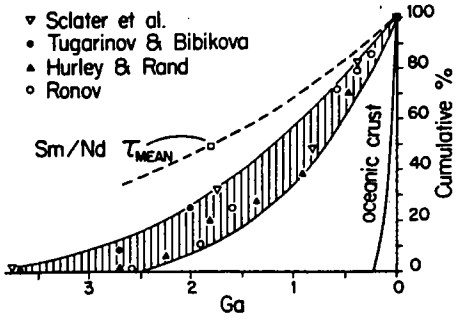

FIG. 4.—Present-day area-age distribution of continental crust. The points of Tugarinov and Bibikova, Hurley and Rand, and Ronov as in table 1 of Veizer and Jansen (1979). The points of Sclater et al. (1981) for 0–250, 250–800, 800–1560, 1560–3700, and ≥3700 Ma are 100, 82, 47, 34 and 0 cum %, respectively. The curve for oceanic crust is from figure 3 for comparison. The Sm/Nd mean age is from McCulloch and Wasserburg (1978) and Goldstein and O'Nions (1982). This τ_{MEAN} is assumed to equal τ_{50}, because the areal distribution of Sm/Nd age provinces is not known. The area of subaerially exposed continents is at present 150 × 10^6 km^2 (Sclater et al. 1981), but inclusion of submarine portions gives a total area of 200 × 10^6 km^2 (Turcotte and Schubert 1982). Taking this latter figure and the average thickness of 38 km (Reymer and Schubert 1984), the total volume is 7600 × 10^6 km^3 and the corresponding mass is 20900 × 10^{21} g. The submerged portion of the continental crust is assumed to have age distribution comparable to that on land.

poorly known for the upper crust and not at all for the lower crust. Veizer and Jansen (1979) and Sclater et al. (1981) compiled the available literature data (fig. 4).

Model solutions for continental crust are summarized in tables 3 and 4, and they clearly depend on the assumed growth model (**n**). In our *preferred growth model*, formation of the continental crust was initiated (or the crust started to be preserved) at ~4 Ga ago, and the major period of growth is believed to have occurred ~3–2 Ga ago (Veizer and Jansen 1979; Allègre 1982; Allègre and Rousseau 1984). The solutions for this "preferred" model are $\mathbf{b}^{\leq 50} = -3.7 \pm 1.3 \times 10^{-10}\,a^{-1}$ for the top enveloping curve, and $-8.5 \pm 0.7 \times 10^{-10}\,a^{-1}$ for the bottom one. For alternative growth models the solutions can be extrapolated directly from tables 2 and 3.

TABLE 1

AREA-AGE DISTRIBUTION OF THE OCEAN FLOOR

Sclater et al. (1981)		Sprague and Pollack (1980)	
Age (in Ma)	Cum. %	Age (in Ma)	Cum. %
0–4	100.00	0–5	100.1
4–9	95.7	5–23	94.4
9–20	87.9	23–38	76.7
20–35	77.9	38–65	65.5
35–52	65.5	65–100	48.9
52–65	51.7	100–135	14.5
65–80	42.2	135–180	5.7
80–95	30.2	>180	0
95–110	22.4		
110–125	14.7		
125–140	9.0		
140–160	4.3		
160–180	1.7		
>180	0		

Total area = 309 × 10^6 km^2 (Sclater et al. 1981).
Volume = 1854 × 10^6 km^3. At average thickness of 6 km (Reid and Jackson 1981).
Mass = 6118 × 10^{21} g. At specific density of 3.3 g cm^{-3}.

For the indicated Sm/Nd curve, the solution for the steady-state model (**n** = 1/∞) is $\mathbf{b}^{\leq 50} = -4 \times 10^{-10}\,a^{-1}$, while for the "preferred" growth model it is $-2.1 \pm 1.0 \times 10^{-10}\,a^{-1}$.

Global Sedimentary Mass.—The present-day age distribution of the global sedimentary mass is summarized in table 4 and figure 5. The major uncertainty is in the pre-1600 Ma value, but to the best of our knowledge no better data is available. The calculated model parameters are summarized in table 5.

Although essential for balance calculations, the global recycling parameters are nevertheless somewhat misleading as they represent an amalgam of two sedimentary

TABLE 2

UPPER ENVELOPE SIMULATION RECYCLING OF THE CONTINENTAL CRUST AREAL DISTRIBUTION

t_0 (Ma)		n = 1/∞	1/20	1/10	1/5	1/3	1/2	1	2	3	5	10
4500	b	7.0	7.0	6.8	6.4	5.9	5.3	3.5	.4	...	...	...
	D	3.15	3.0	2.8	2.4	2.0	1.6	.8	.1	...	...	...
4050	b	7.0	6.9	6.7	6.1	5.5	4.8	3.0	...	...	...	...
	D	2.8	2.7	2.5	2.1	1.9	1.3	.6	...	...	...	...

NOTE.—Definition of terms is given in Appendix 1. An example of reading is as follows: For a linearly growing continental crust (n = 1), starting at the time of the formation of the Earth (t_0 = 4500 Ma B.P.) the average recycling parameter b, required to generate the present-day distribution of age provinces (fig. 4), is $\sim 3.5 \times 10^{-10}$ a^{-1}, and the recycled quantity D is equivalent to 0.8 of the present-day continental area (mass, volume). The results of simulations for fast cycling systems (e.g., oceanic crust) are not tabulated, because all realistic solutions result in identical b. These solutions are therefore discussed in the text only. Recycling increment T = 10 Ma, but the solutions are similar for T = 1–50 Ma.

TABLE 3

LOWER ENVELOPE SIMULATION RECYCLING OF THE CONTINENTAL CRUST AREAL DISTRIBUTION

t_0 (in Ma)		n = 1/∞	1/20	1/10	1/5	1/3	1/2	1	2	3	5
4500	b	10.2	10.0	9.9	9.6	9.2	8.7	7.4	4.7	2.1	...
	D	4.6	4.3	4.0	3.6	3.1	2.6	1.7	.7	.2	...
4050	b	10.2	10.0	9.8	9.5	9.1	8.5	6.9	3.9	1.1	...
	D	4.1	3.9	3.6	3.2	2.8	2.3	1.4	.5	.1	...

NOTE.—Explanations as in table 2. Recycling increment T = 10 Ma, but the solutions are similar for T = 1–50 Ma.

systems, continent- and ocean-based. The former is liable to be recycled at a slower and the latter at a faster rate than the global average.

Continental Sedimentary Mass.—The age distribution of continental sediments is summarized in table 4 and figure 5. The calculated model parameters are presented in table 6. However, the size of the continental (and global) sedimentary mass is principally a function of the extent and freebord of the buoyant continental crust (Veizer and Jansen 1979; Veizer 1983). It is therefore reasonable to assume that the growth of the continental sedimentary mass approximated that of the continental crust itself. If our "preferred" growth pattern is accepted as the first-order approximation of **n**, the calculated $\mathbf{b}^{\leq 10} = \sim 16.2 \pm 1.1 \times 10^{-10}$ a^{-1} and the respective recycled **D** equals $\sim 3.7 \pm 0.5$ times the present-day continental sedimentary mass. This translates into recycling of $\sim 3.0 \pm 0.3 \times 10^{15}$ g ($\sim 1.2 \pm 0.1$ km^3) of sediments per year.

The above rates are, however, only average values for the entire continental sedimentary column. Within this sedimentary pile,

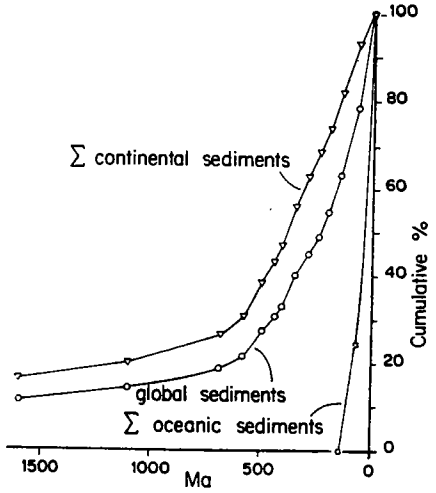

FIG. 5.—Present-day mass-age distributions of global, continental, and oceanic sediments.

the deeply buried sediments may have been recycled at the same slow rate as the underlying basement (**b** $\sim 8.5 \pm 0.7 \times 10^{-10}$ a^{-1}), while the uppermost layer (10–100 m thick) has been cycled at a much faster rate, $\sim 70 \pm 20 \times 10^{-10}$ a^{-1}. The latter value has been

TABLE 4

PRESENT-DAY MASS-AGE DISTRIBUTION OF GLOBAL, CONTINENTAL, AND OCEANIC UNMETAMORPHOSED SEDIMENTS

	Age (Ma)	Global Sediments		Continental Sediments		Oceanic Sediments[b]	
		Mass (10^{21}g)	Cum. %	Mass (10^{21}g)	Cum. %	Mass (10^{21}g)	Cum. %
Cenozoic	0–66	576.9	100.1	140.0	100.1	284.7	100.0
Cretaceous	66–132	428.5	78.7	205.4	92.7	90.1	24.3
Jurassic	132–185	228.2	62.8	152.1	81.8	1.1	.3
Triassic	185–235	140.8	54.3	105.1	73.7		
Permian	235–280	108.8	49.1	99.6	68.1		
Carboniferous	280–345	137.7	45.1	129.7	62.8		
Devonian	345–400	181.6	40.0	166.7	55.9		
Silurian	400–435	67.8	33.3	65.1	47.0		
Ordovician	435–490	97.8	30.8	92.6	43.5		
Cambrian	490–570	157.4	27.2	150.0	38.6		
Vendian	570–680	75.1	21.4	75.1	30.6		
U. Riphean	680–1100	124.3	18.6	124.3	26.6		
L. & M. Riphean	1100–1600	66.4	14.0	66.4	20.0		
	>1600	310.0	11.5	310.0[a]	16.5		
	Σ	2701.3		1882.1		375.9	

SOURCES.—The Phanerozoic part after Gregor (1985), and the Precambrian part after Ronov (1980, table 7).

[a] The mass of sediments older than 1600 m.y. has been obtained as a difference between the total mass of sediments on continents (1.89×10^{24}g) and the mass of sediments on continents younger than 1600 Ma (1.57×10^{24}g) (Ronov 1980, tables 10 and 7, respectively). The sum of Phanerozoic sediments on continents by Gregor is 0.1×10^{24}g higher than that of Ronov.

[b] Passive margins excluded.

calcula
surficia
Blatt ar
1979) fc
Ocea
bution c
table 4
~142 ×
≥30 Ma
because
ments a
rate of
ceeds, b
continer
therefor
and the
geologic
sedimen

t_0 (in Ma	
4500	

NOTE.—

2700	
3150	
3600	
4050	

t_0 (in M	
450	

NOTE.

2700	
3150	
3600	
405	

TABLE 5

SIMULATION OF RECYCLING FOR GLOBAL SEDIMENTARY MASS

t_0 (in Ma)		n										
		1/∞	1/20	1/10	1/5	1/3	1/2	1	2	3	5	10
4500	b	42.8	42.8	42.6	42.4	42.1	41.7	40.6	38.3	35.9	31.3	19.8
	D	19.3	18.3	17.4	15.9	14.2	12.5	9.1	5.7	4.0	2.4	0.8
4050	b	42.8	42.8	42.6	42.4	42.0	41.6	40.3	37.7	35.1	30.0	17.1
	D	17.3	16.5	15.7	14.3	12.8	11.2	8.2	5.1	3.6	2.0	0.6
3600	b	42.7	42.7	42.6	42.3	41.9	41.4	40.0	37.0	34.1	28.3	13.7
	D	15.4	14.7	13.9	12.7	11.3	10.0	7.2	4.4	3.1	1.7	0.5
3150	b	42.7	42.7	42.5	42.2	41.8	41.2	39.5	36.1	32.8	26.0	9.2
	D	13.5	12.8	12.2	11.1	9.9	8.7	6.2	3.8	2.6	1.4	0.3
2700	b	42.7	42.7	42.5	42.1	41.6	40.9	38.9	34.9	31.0	23.0	3.2
	D	11.5	11.0	10.4	9.5	8.4	7.4	5.3	3.1	2.1	1.0	0.1

NOTE.—Explanations as in table 2. Recycling increment is 1 Ma, but the results for T = 1–10 Ma differ only marginally.

TABLE 6

SIMULATION OF RECYCLING FOR CONTINENTAL SEDIMENTS

t_0 (in Ma)		n										
		1/∞	1/20	1/10	1/5	1/3	1/2	1	2	3	5	10
4500	b	13.9	13.3	13.2	13.0	12.8	12.5	11.6	10.0	8.6	6.1	0.0
	D	6.3	5.7	5.4	4.9	4.3	3.7	2.6	1.5	1.0	0.5	0.0
4050	b	13.9	13.3	13.2	13.0	12.7	12.4	11.5	10.0	8.8	5.9	0.0
	D	5.4	5.1	4.8	4.4	3.9	3.3	2.3	1.3	0.9	0.4	0.0
3600	b	13.9	13.3	13.2	13.0	12.7	12.3	11.4	10.2	9.1	5.4	
	D	4.8	4.5	4.3	3.9	3.4	2.9	2.0	1.2	0.8	0.3	*
3150	b	13.4	13.3	13.2	12.9	12.6	12.3	11.6	10.8	9.2	4.4	*
	D	4.2	3.9	3.7	3.4	3.0	2.6	1.8	1.1	0.7	0.2	
2700	b	13.4	13.3	13.2	12.9	12.7	12.5	12.5	11.5	9.0	2.7	*
	D	3.6	3.4	3.2	2.9	2.5	2.2	1.7	1.0	0.6	0.1	

NOTE.—Explanations as in table 2. Recycling increment T = 1 Ma.

calculated from area-age distribution of surficial sediments (Higgs and Gilluly and Blatt and Jones curves in Veizer and Jansen 1979) for 1 Ma incremental recycling.

Oceanic Sediments.—The mass-age distribution of oceanic sediments is summarized in table 4 and figure 5. The model average **b** is $\sim 142 \times 10^{-10}\ a^{-1}$ for increments of recycling ≥30 Ma. These long increments are essential because, as with oceanic crust, older sediments are preferentially recycled. Thus, the rate of recycling of oceanic sediments exceeds, by one order of magnitude, that of the continental sediments. The recycled mass is, therefore, $\sim 5.3 \times 10^{15}\ g\ a^{-1}$ ($\sim 2.1\ km^3\ a^{-1}$) and the minimal **D**, recycled during the entire geologic history, is ≥64 present-day oceanic sediment masses.

GLOBAL TECTONIC REALMS AND THEIR RECYCLING RATES

The previously discussed total continental and oceanic rates are of considerable importance for global balance calculations. They do not, however, give a proper appreciation of the constraints for major tectonic realms, as defined by the tenets of global plate tectonics. In the subsequent discussion we shall recognize the following tectonic realms (Sclater et al. 1980; Gregor 1985; Ronov et al. 1980): (1) deep ocean floor, comprising abyssal and pelagic environments and covering $281.7 \times 10^6\ km^2$; (2) active margin basins, separated from (1) by tectonic barriers (e.g., backarc basins, Caribbean, Mediterranean) and accounting for $26.9 \times 10^6\ km^2$; (3) passive margin basins with the area of 52.2×10^6

km^2; (4) orogenic belts (geosynclines) with the subaerial extent of 27×10^6 km^2; and (5) platforms, with the subaerial extent of 123×10^6 km^2. From the above tectonic realms, the types (1) and (2) are mostly developed on oceanic crust, and the types (3) to (5) on continental crust.

Sediments of the Abyssal and Pelagic Realm.—The present-day mass-age distribution of abyssal and pelagic sediments is summarized in table 7 and figure 6. The lack of sediments older than Jurassic clearly points to a fast recycling rate, if compared to the terrestrial time scale. It is therefore not surprising that, for any marginally realistic growth model, the calculated rates of recycling (**b**'s) at ≥30 Ma increments are practically unchanged. The post-Triassic steady-state **b** is therefore $\sim 126 \times 10^{-10}$ a^{-1}. This is only slightly faster than that of the oceanic crust ($110 \pm 5 \times 10^{-10}$ a^{-1}). This agreement is not surprising, since ocean floor creation and destruction is the major cause of sediment recycling. The above **b**'s suggest that ≥87% of sediment recycling is due to this cause, with the remainder related to other factors such as bottom current scouring and dissolution of biogenic sediments (see also Moore and Heath 1977). In addition, the bulk of these sediments has been deposited on the already aged ocean floor, thus leading to a shorter lifespan (faster recycling).

Sediments in Basins of Active Margins.—Sediments of this tectonic realm form a heterogeneous assemblage related not only to intraoceanic back-arc basins, but also to relic ancient oceans with a substantial sialic component (e.g., the Mediterranean) and their mass-age distribution is summarized in table 7 and figure 6.

The calculated **b** depends strongly on the duration of the simulation increment **T**. The proximity to continental margin, causing preferential recycling of the youngest sediments, favors a **T** of short duration. In rare instances, however, the associated ocean floor spreading, coupled with subduction, may demand a long **T** component. For simulation increments of 1–35 Ma, the possible **b** values are $\sim 223 \pm 51 \times 10^{-10}$ a^{-1}. This suggests $\sim 3.2 \pm 0.9 \times 10^{15}$ g a^{-1} (1.3 ± 0.3 km^3 a^{-1}) as the recycled amount.

Sediments in Basins of Passive Margins.—The mass-age distribution of sediments in this tectonic realm is also summarized in table 7 and figure 6. The calculated $\mathbf{b}^{\leq 35}$ is $88 \pm 8 \times 10^{-10}$ a^{-1}. This translates to a recycling flux of $\sim 3.0 \pm 0.2 \times 10^{15}$ g a^{-1} ($\sim 1.2 \pm 0.1$ km^3 a^{-1}).

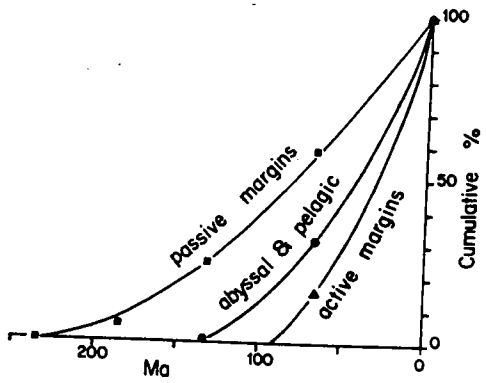

FIG. 6.—Present-day mass-age distributions of sediments in abyssal and pelagic realm, active margin basins, and passive margin basins.

Sediments in Other Tectonic Settings.—Sediments assigned to the residual oceanic environments, principally deep sea fans, constitute only a small portion of the sedimentary mass (table 7). Although their rate of recycling is fast (**b** $\sim 230 \pm 55 \times 10^{-10}$ a^{-1}), they are of subordinate significance in the overall budget. However, the similarity of the calculated **b** to that for sediments in basins of active margins may not be entirely fortuitous.

Sediments in Continental Orogenic Belts.—The present-day mass-age distribution of sediments in orogenic belts subaerially exposed within the confines of today's continents is summarized in table 7 and figure 7. Model solutions are presented in table 8. However, the continents have been growing via accretion of successive orogenic belts. Consequently our "preferred" growth model is considered to be the most likely approximation of **n**. In this case $\mathbf{b}^{10} = 18.4 \pm 0.5 \times 10^{-10}$ a^{-1}, and the corresponding $\mathbf{D} = 4.3 \pm 1.0$. This **b** translates into recycling of $\sim 2.5 \times 10^{15}$ g a^{-1} (~ 1 km^3 a^{-1}).

Sediments on Platforms.—The mass-age distribution of platformal sediments (table 7 and fig. 7) mimics that of the orogenic belts, and the calculated parameters are therefore almost identical (table 9). The $\mathbf{b}^{10}$ for our "preferred" growth pattern is $\sim 18.6 \pm 0.5 \times 10^{-10}$ a^{-1}, giving a recycled mass of $1.0 \times$

TABLE 7

MASS-AGE DISTRIBUTION OF SEDIMENTS IN MAJOR TECTONIC REALMS

	Age (in Ma)	Abyssal and pelagic sediments[a]		Active margin basins[a]		Other oceanic sediments (deep sea fans)[a]		Passive margin basins[a]		Continental orogenic belts[b]		Platforms[b]	
		Mass (10^{21} g)	Cum. %	Mass (10^{21} g)	Cum. %	Mass (10^{21} g)	Cum. %	Mass (10^{21} g)	Cum. %	Mass (10^{21} g)	Cum. %	Mass (10^{21} g)	Cum. %
Cenozoic	0–66	149.7	100.0	121.8	100.0	13.2	100.0	140.4	100.0	87	100.0	46	100.0
Cretaceous	66–132	65.7	30.8	22.2	15.4	2.2	14.3	114.3	58.3	121	93.6	81	91.5
Jurassic	132–185	1.1	.5	...	...	...	...	65.3	24.4	92	84.6	49	76.5
Triassic	185–235	...	...					16.8	5.0	83	77.8	35	67.4
Permian	235–280							...	...	79	71.7	27	60.9
Carboniferous	280–345									106	65.8	28	55.9
Devonian	345–400									150	57.9	36	50.7
Silurian	400–435									47	46.8	11	44.0
Ordovician	435–490									72	43.3	19	42.0
Cambrian	490–570									99	38.0	39	38.5
Vendian	570–680									414[c]	30.7	169[d]	31.3
U. Riphean	680–1100												
L. & M. Riphean	1100–1600												
	>1600												
	Σ	216.5		144.0		15.4		336.8		1350[4]		540[4]	

[a] Gregor (1985); [b] Ronov et al. (1980, table 1). Volume data recalculated to mass and prorated to give a Phanerozoic sedimentary mass of 1306 × 10^{21} g (see continental sediments in table 4). The discrepancies with table 1 of Ronov et al. (1980) are likely due to the inclusion of volcanics in their table; [c] Estimated as a difference between the totals (1350 and 540 × 10^{21} g respectively) and the sums of Phanerozoic masses; [d] Ronov (1980, table 7). See also table 4 for additional explanations.

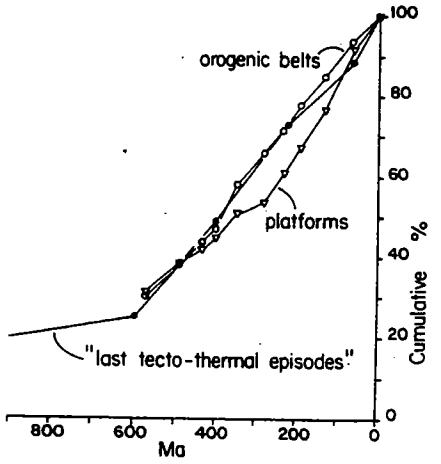

FIG. 7.—Present-day mass-age distributions of sediments in orogenic belts and platforms. "Last tectono-thermal episodes" from Sprague and Pollack (1980).

10^{15} g a^{-1} (0.4 km^3 a^{-1}). These observations are surprising, since geological intuition favors higher rates of erosion and/or (ultra)metamorphism for orogenic belts than platforms. This may be due to the fact that the sediments of immature orogenic belts (e.g., the Andean, Cordilleran, and similar types of mountain chains), which contribute to the bulk of erosion, account for only a subordinate part of the total mass of sediments in orogenic belts. If so, and providing the estimates of Ronov (1980) are correct, mature and worn down orogenic belts and platforms are both integral parts of the stable continental crust. They therefore respond in a similar manner to perturbations. These perturbations appear to have been tectonically induced since the curve of the so called "last tectonothermal" episodes for a given area of continental crust (fig. 7) has a similar, or only slightly steeper, slope to that of platform and geosynclinal sediments. The calculated **b** for this curve is $\sim 19 \pm 3 \times 10^{-10}$ a^{-1}.

Immature Orogenic Belts.—Because of the lack of direct measurements, the rate of recycling for immature orogenic belts must be estimated through other criteria such as the age distribution pattern of associated ores. The volcano-plutonic activity in emerging orogenic belts is accompanied by the development of an aureole of hydrothermal vein deposits such as Pb, Zn, Cu, Au, Sn, and Fe. These deposits have been formed originally at depths of ~3–10 km (Laznicka 1973). With continuing isostatic uplift of young mountain chains, the progressively deeper erosion levels lead to dispersal of the associated ores as well. This causes a decrease of reserves with increasing age. Since the uplift is rapid at first, and declines exponentially with time as the permanent thickness for a stable continental crust is approached, the age-distribution of ore reserves should approximate an exponential function, as indeed is the case (table 10 and fig. 8).

The calculated $\mathbf{b}^{\leq 10}$ is $118 \pm 8 \times 10^{-10}$ a^{-1} for the lower envelope and $51 \pm 3 \times 10^{-10}$ a^{-1} for the upper envelope (fig. 8). This gives an average **b** of $\sim 85 \pm 35 \times 10^{-10}$ a^{-1}, a value indistinguishable from that of the passive margins. Consequently, passive margins

TABLE 8

SIMULATION OF RECYCLING FOR OROGENIC BELTS

t_0 (in Ma)		n 1/∞	1/20	1/10	1/7	1/5	1/3	1/2	1	2	3	5	10
4500	b	19.3	19.2	19.1	19.0	18.9	18.5	18.2	17.0	14.7	12.3	7.7	*
	D	8.7	8.2	7.8	7.5	7.1	6.3	5.4	3.8	2.2	1.4	0.6	*
4050	b	19.3	19.2	19.1	18.9	18.8	18.5	18.0	16.7	14.1	11.5	6.3	*
	D	7.8	7.4	7.0	6.7	6.3	5.6	4.9	3.4	1.9	1.2	.4	*
3600	b	19.3	19.2	19.0	18.9	18.7	18.3	17.8	16.4	13.4	10.4	4.5	*
	D	7.0	6.6	6.2	5.9	5.6	4.9	4.3	2.9	1.6	.9	.3	*
3750	b	19.3	19.1	19.0	18.8	18.6	18.2	17.6	15.9	12.5	9.0	2.1	*
	D	6.1	5.7	5.4	5.2	4.9	4.3	3.7	2.5	1.3	.7	.1	*
2700	b	19.3	19.1	18.9	18.7	18.5	18.0	17.3	15.3	11.2	7.1	*	
	D	5.2	4.9	4.6	4.4	4.2	3.6	3.1	2.1	1.0	.5	*	

NOTE.—Explanations as in table 2. Recycling increment T = 10 Ma.

BASE

t_0 (in Ma)		1/∞	1/2
4500	b	19.0	18.
	D	8.5	8.
4050	b	19.0	18.
	D	7.7	7.
3600	b	19.0	18.
	D	6.9	6.

NOTE.—Explanations as in table 2

and young mountain bel
pressions of the same qua
of sedimentation, orogene
at the continent-ocean in

SYNOPSIS OF RECYCLING R
OF TECTONIC

The summary of reser
rates, fluxes, and half-liv
11. We emphasize that th
10^6–10^7 years' resolution
for time scales with sh
larger than the quoted v
sentation of recycling rat
(τ_{50}), as taken from figu
the theoretically predic
values are in good agree
steady-state situation (n
ment is nearly complete,
deviation at fast recyclin
sis is consistent with the e
damental *tectonic domai*

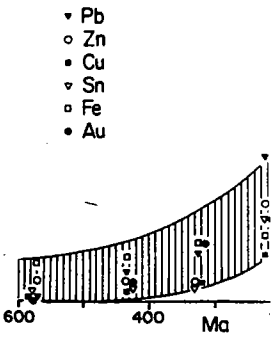

FIG. 8.—Present-day rese
of hydrothermal vein deposi

TABLE 9

SIMULATION OF RECYCLING FOR PLATFORMS

t_0 (in Ma)		n											
		1/∞	1/20	1/10	1/7	1/5	1/3	1/2	1	2	3	5	10
4500	b	19.0	18.9	18.8	18.7	18.5	18.2	17.8	16.7	14.3	12.0	7.3	*
	D	8.5	8.1	7.7	7.3	6.9	6.1	5.3	3.7	2.1	1.3	.6	*
4050	b	19.0	18.9	18.7	18.6	18.5	18.1	17.7	16.4	13.8	11.2	5.9	*
	D	7.7	7.3	6.9	6.6	6.2	5.5	4.8	3.3	1.9	1.1	.4	*
3600	b	19.0	18.8	18.7	18.6	18.4	18.0	17.5	16.0	13.1	10.1	4.1	*
	D	6.9	6.4	6.1	5.8	5.5	4.9	4.2	2.9	1.6	.9	.3	*

NOTE.—Explanations as in table 2. Recycling increment T = 10 Ma.

and young mountain belts are only two expressions of the same quasi-continuous cycle of sedimentation, orogenesis, and destruction at the continent-ocean interface.

SYNOPSIS OF RECYCLING RATES AND LIFESPANS OF TECTONIC REALMS

The summary of reservoir sizes, recycling rates, fluxes, and half-lives is given in table 11. We emphasize that these are net rates for 10^6–10^7 years' resolution, and the net fluxes for time scales with shorter resolution are larger than the quoted values. Graphic presentation of recycling rates (**b**) and half-lives (τ_{50}), as taken from figures 3–8, shows that the theoretically predicted and measured values are in good agreement (fig. 9). For a steady-state situation (**n** = 1/∞) the agreement is nearly complete, except for a slight deviation at fast recycling rates. This synopsis is consistent with the existence of two fundamental *tectonic domains*, the *continental* and the *oceanic* one, with a transition at **b** ~40 × 10^{-10} a^{-1} and τ_{50} ~225 Ma. Since global sediments are an amalgam of continental and oceanic ones, it is not surprising that they plot on this intercept. Furthermore, the results suggest that mountain building, as exemplified by immature orogenic belts, is related to the oceanic and not the continental tectonic domain. If so, sea floor spreading and peripheral orogenies are coupled and, following the uplift, mountain ranges are eroded back into the ocean. Sprague and Pollack (1980) hinted at this solution by proposing that their age distribution of "last tectono-thermal events" on continents was coupled to sea floor spreading by a factor of 0.15.

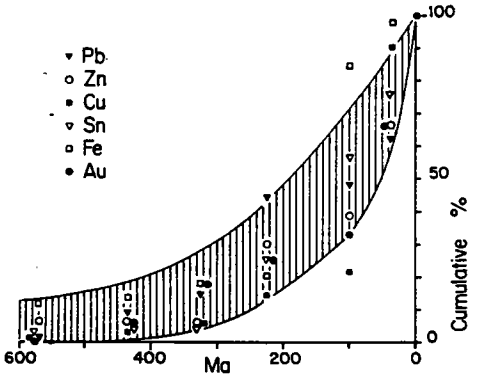

FIG. 8.—Present-day reserves-age distributions of hydrothermal vein deposits.

The above relationship (table 11, fig. 9) also predicts the likely maximum lifespan, or oblivion age τ_{MAX}, for a given tectonic realm. Empirically, τ_{MAX} is 3 to 3.5 times τ_{50}. Consequently basins of active margins will completely succumb to destructive forces of combined erosion, tectonic shortening, metamorphism, magmatism, plutonism, and subduction in less than ~100 Ma, oceanic sediments in ~130 Ma, oceanic crust in ~180 Ma, passive margin basins in ~270 Ma, and immature orogenic belts in ≤300 Ma. In contrast, ~1300 Ma is required for obliteration of newly deposited platform sequences and of the residual roots of former orogens, through surface erosion and deep-seated (ultra)metamorphism. The consequences for the continental crystalline basement will be discussed in a subsequent section.

The general shift to somewhat lesser **b**'s than the theoretical ones (fig. 9) is mostly a consequence of model considerations. For

TABLE 10

AGE DISTRIBUTION OF HYDROTHERMAL VEIN DEPOSITS ASSOCIATED WITH OROGENIC VOLCANO-PLUTONIC COMPLEXES

Age (in Ma)	Cum. %					
	Pb	Zn	Cu	Sn	Fe	Au[a]
0–38	99.9	100.1	100.0	100.0	100.0	100.0
38–100	62.9	66.8	90.2	76.2	98.8	66.3
100–225	48.8	39.7	21.1	57.3	84.2	33.5
225–325	44.2	30.2	13.8	25.2	20.1	25.6
325–435	14.5	7.3	6.2	5.7	18.1	18.8
435–570	8.3	7.0	3.0	3.9	14.5	5.3
570–900	1.3	6.8	1.5	3.4	12.2	...
900–1500	.9	.8	1.0	1.7	7.3	...
1500–2000	.7	.3	.9	.9	...	...
2000–2500	.2	...	.3	.4	...	...
2500–3000	.2	...	.1	.2	...	...
>3000	...	...	...	...	...	...
$\Sigma(10^3 t)$	98659	130651	282420	8376	1233	25141

NOTE.—Cumulative percentages with respect to known global reserves for this type of ores. Based on MANIFILE (Laznicka 1973, 1981) and personal file of P. Laznicka.

[a] Au ores of this type show a distinct bimodal distribution (two subtypes), with a break during the 570–900 Ma interval. Only the Phanerozoic population is included here.

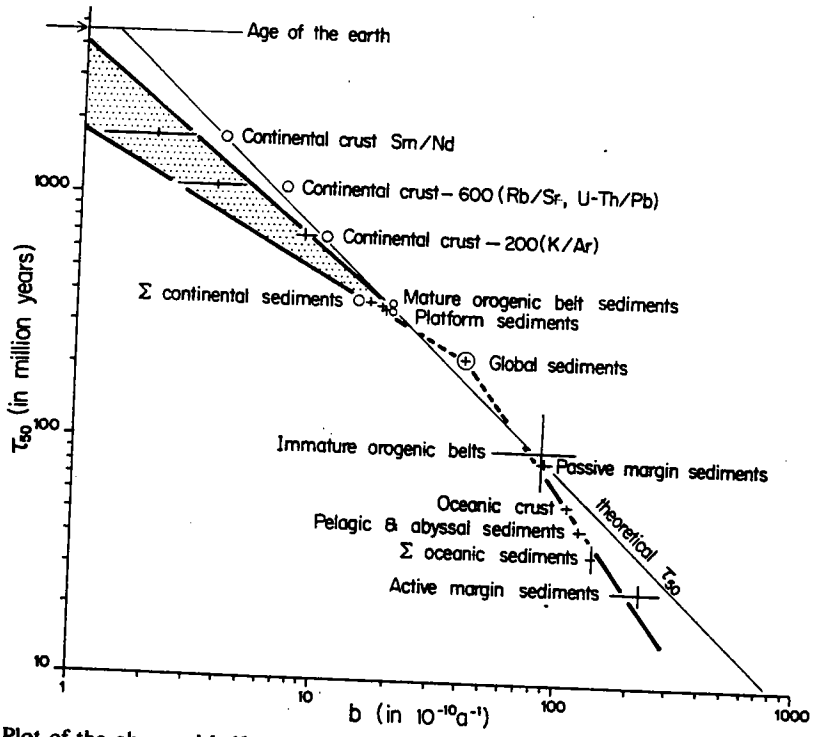

FIG. 9.—Plot of the observed half-mass and half-area ages (τ_{50}) and of recycling rates for major global tectonic realms. Crosses represent solutions for the "preferred" model of continental growth, while the circles give results for the steady-state alternative ($\mathbf{n} = 1/\infty$; $t_0 = 4.5$ Ga). The two limiting solutions are identical at $\mathbf{b} \geq 40 \times 10^{-10}\ a^{-1}$. Continental crust −200, −600, and Sm/Nd represent solutions for the bottom enveloping curve, the top enveloping curve, and the Sm/Nd curve in figure 4, respectively.

TABLE 11

SIZES OF RESERVOIRS, THEIR RECYCLING RATES, FLUXES, AND HALF-LIVES

Size	"Preferred" recycling constant b	Absolute quantity recycled	Observed τ_{50}[a]

TABLE 11

SIZES OF RESERVOIRS, THEIR RECYCLING RATES, FLUXES, AND HALF-LIVES

Reservoir	Size ($\times 10^{21}$ g)	"Preferred" recycling constant b ($\times 10^{-10}$ a^{-1})	Absolute quantity recycled ($\times 10^{15}$ g a^{-1})	Observed τ_{50}[a] (Ma)
Oceanic crust	6118	110 ± 5	67.3 ± 3.1	~55
Continental crust	20900 [200 × 10^6 km^2]			
I recycled via mantle (Sm/Nd)		2.1 ± 1.0	.04 ± .02 km^2 a^{-1}	≲1800
II involved in high-grade metamorphism (≥600°C) + I		3.7 ± 1.3	.07 ± .03 km^2 a^{-1}	~1200
III involved in low-grade metamorphism (≥200°C) + I + II		8.5 ± .7	.17 ± .1 km^2 a^{-1}	~690
Sediments				
global sediments	2701	40 ± 3	10.8 ± .8	~235
continental sediments	1882	16.2 ± 1.1	3.0 ± .3	~375
oceanic sediments (minus passive margins)	376	142	5.3	~45
Global tectonic realms (sediments)				
abyssal and pelagic	217	126	2.7	~40
active margin basins	144	223 ± 51	3.2 ± .9	~30
deep sea fans	15	230 ± 55	0.3 ± .1	~25
passive margin basins	337	88 ± 8	3.0 ± .2	~80
immature orogenic belts		85 ± 35		~100 (50–190)
mature orogenic belts	≲1350	18.4 ± .5	≲2.5	~380
platforms	540	18.6 ± .5	1.0	~380

[a] Figures 2–8.

continental tectonic domain, the recycling rates necessary to generate the present-day observed age distributions are less for growing (e.g., the "preferred" growth mode of $n = 0.5–2$) than for instantaneously generated steady-state continents. At rates of recycling $\geq 20 \times 10^{-10}$ a^{-1}, the solutions are independent of growth assumptions but become sensitive to the length of simulation interval T. Longer T, as employed in the simulation of recycling within the oceanic domain (see the section Conceptual Approach), results in lesser **b**.

CONTINENTAL BASEMENT AND ITS RECYCLING

It is likely that some continental crystalline basement is reinjected into the mantle either via erosion and sediment subduction or possibly in a more direct manner. However, the major mode of basement recycling is intracrustal rejuvenation (resetting) of radiometric ages by melting and metamorphic events. From figure 4 it is evident that the apparent mean ages τ_{MEAN} of the continental crust (~0.9 and ~1.4 Ga respectively for the bottom and top envelopes) are considerably less than τ_{MEAN} values of ~2–3 Ga based on crust-mantle isotopic balance calculations (e.g., Zartman and Doe 1981; Jacobsen and Wasserburg 1981; Allègre 1982; Taylor and McLennan 1985). Although this discrepancy may partially be blamed on the unsatisfactory data base, the major culprit is likely the above intracrustal resetting of radiometric ages. Crust-mantle transport models are insensitive to this consideration.

The closure temperatures for K/Ar in feldspars and micas at intermediate cooling rates are ~210 ± 50°C (Harrison et al. 1979), and for Rb/Sr (and perhaps U-Th/Pb) they are at near-melting metamorphic pressures and temperatures of ≥600°C (Van Breemen and Dallmeyer 1984). Today's near-surface rocks are statistically more likely to have been subjected to a temperature of ≥210°C (zeolite facies) than ≥600°C (amphibolite-granulite facies), and the rate of intracrustal rejuvenation of K/Ar ages should therefore exceed that of Rb/Sr (and U-Th/Pb). The Sm/Nd dating pair should essentially be impervious to intracrustal resetting (e.g., McCulloch and Wasserburg 1978). If so, τ_{MEAN} for areal extent of tectonic provinces should decrease in the sequence Sm/Nd > U-Th/Pb ≥ Rb/Sr > K/Ar.

The tentative age distribution pattern in figure 4 is consistent with this proposition. The steeper bottom curve reflects stabilizing and cooling episodes (cratonization) (Ronov 1976), as encoded chiefly in K/Ar age provinces (Hurley and Rand 1969). The upper curve may represent the areal distribution of age provinces as defined by the more retentive U-Th/Pb and Rb/Sr dating techniques. In accord with the theory, the indicated Sm/Nd τ_{MEAN} (McCulloch and Wasserburg 1978; Allègre and Rousseau 1984; Goldstein et al. 1984) exceeds both of the above estimates and approaches the estimates from isotopic transport models.

The calculated recycling parameters for the advocated interpretation are collated in table 11. Because of the lack of knowledge of the age structure in the deeper crust, it is impossible to convert these values into volumetric estimates. However, the indicated Sm/Nd τ_{MEAN} ($\sim\tau_{50}$) places some constraints on the evolution of the continental crust. Accepting an instantaneous crustal generation at 4.5 Ga ago, the steady-state **b** would have to be ~4 $\times 10^{-10}$ a^{-1}. In such a population, any random sampling of continental crust should result in ~20% of all Sm/Nd ages being in the 4.5–3.5 Ga range. This, quite evidently, is not the case. Consequently, either the continents were growing during geologic history, or the rate of their recycling into the mantle (or lower crust) prior to the Proterozoic has exceeded the steady-state value of **b**.

LIFESPAN OF IMMATURE OROGENIC BELTS

As stated previously, the oblivion age τ_{MAX} for a given tectonic realm is usually a factor of 3–3.5 of its τ_{50}. The predicted and observed oblivion ages for most realms are comparable (cf. figs. 3–7 with table 11), but the age distribution of hydrothermal vein deposits (fig. 8) is a notable exception. Theoretically, the τ_{MAX} of immature orogenic belts should be ~300 Ma. This theoretical limit is supported also by the observation that thermal perturbations have no effect in the continental lithosphere over time spans greater than ~200–300 Ma (Sclater et al. 1981). Consequently, the upper crustal materials, with elevated concentrations of heat generating elements, have been eroded within this time constant. As discussed previously (see Immature Orogenic Belts), the local erosion of a

BA

specific orogenic belt
tially with time, since
down as the equilibri
approached. The **b*** is
time and of **b** and ca
formula in appendix 1
recycling proportiona
immature orogenic be
is only the total relief t
applied that is diminis
sion is always confine
highest mountain chai
able a near-constant
while at the same tim
sion for a single chain
tially as this chain ag
erosion continues to di
b* would eventually ha
the erosion rates for
down, former orogeni
(fig. 10). This is an unli
with the attainment of
ness (~35 km), the ren
mer immature orogeni
of the continental dor
newly accreted portion
its recycling rate will b
tectonic realm (mature
newly accreted block
the continent itself, the
(fig. 10 and appendix 1
~180 Ma.

In the more likely alt
continent, both realms
at an equal apparent
t_E) (fig. 10 and appenc
yields ~230 Ma. Thus
well within the rang
theoretical limits. Con
vation of associated c
limit (fig. 8) is a consec

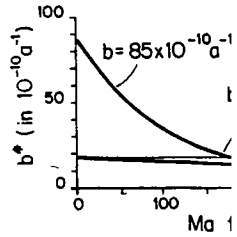

FIG. 10.—Variation of
with time. Time of transiti
ity (t_E) as in the text and
increment 10 Ma.

specific orogenic belt (**b***) declines exponentially with time, since the rate of uplift slows down as the equilibrium crustal thickness is approached. The **b*** is therefore a function of time and of **b** and can be calculated from a formula in appendix 1. Note that the average recycling proportionality parameter, **b**, for immature orogenic belts is a constant, and it is only the total relief to which this constant is applied that is diminishing. The bulk of erosion is always confined to the youngest and highest mountain chains. These dynamics enable a near-constant global erosional flux, while at the same time the local rate of erosion for a single chain (**b***) declines exponentially as this chain ages. If the rate of local erosion continues to diminish at a given **b**, the **b*** would eventually have to become less than the erosion rates for the adjacent, worn-down, former orogenic belts and platforms (fig. 10). This is an unlikely proposition, since with the attainment of an equilibrium thickness (~35 km), the remaining root of the former immature orogenic belt will become part of the continental domain and behave as a newly accreted portion of it. In other words, its recycling rate will be that of the successor tectonic realm (mature orogenic belt). If the newly accreted block were decoupled from the continent itself, the time of transition (τ_T) (fig. 10 and appendix 1) would be reached at ~180 Ma.

In the more likely alternative of coupling to continent, both realms will eventually recycle at an equal apparent rate (time of equality t_E) (fig. 10 and appendix 1). Solution for t_E yields ~230 Ma. Thus, both estimates are well within the range of the anticipated theoretical limits. Consequently the preservation of associated ores beyond this age limit (fig. 8) is a consequence of the transfer of a residual root section of the former immature orogenic belt into continental domain.

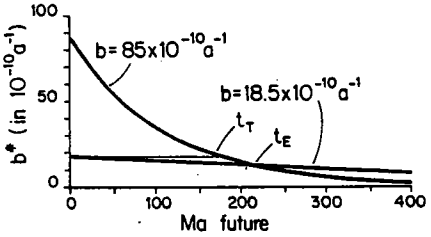

FIG. 10.—Variation of local erosional rate **b*** with time. Time of transition (t_T) and time of equality (t_E) as in the text and Appendix 1. Recycling increment 10 Ma.

CANNIBALISM OF SEDIMENTARY CYCLE AND CRUST-MANTLE FLUX

In our previous paper (fig. 12 in Veizer and Jansen 1979) we proposed that Sm/Nd model ages of multicycle sediments must exceed their stratigraphic ages and the age difference **Δ** (Appendix 1) should increase toward the present. The Sm/Nd model age records the time of the derivation of a sediment precursor from the chondritic mantle. Since subsequent crustal history does not alter the Sm/Nd ratio (McCulloch and Wasserburg 1978), this age will be perpetuated despite later intracrustal and sedimentary recycling. With repeated recycling, the **Δ** will grow as the sediment becomes stratigraphically younger. Subsequent analytical work (O'Nions et al. 1983; Allègre and Rousseau 1984; Goldstein et al. 1984; Michard et al. 1985) confirmed our predictions, and these measurements are summarized in figure 11. The measurements indicate that the **Δ** is ≤250 Ma for sediments older than ~2.0–2.5 Ga and increases afterwards to ~1.4 ± 0.4 Ga for modern sediments. The above authors interpreted their data in terms of crustal residence ages, with an implication that they reflect the evolution of the crystalline crustal source. We concur that the ~1.4 ± 0.4 Ga is a measure of the average ultimate provenance and thus of the τ_{MEAN} of the continental crust. We dissent, however, with the proposition that the observed post-Archean pattern records details of crustal evolution. The rate of sediment-sediment recycling is much faster than the cycle of metamorphism-erosion in the crystalline basement (see sediments vs. continental crust −200 and −600 in fig. 9). The overall post-Archean secular evolution of **Δ** is therefore essentially a function of the degree of cannibalism in the sedimentary cycle. In order to lower the Sm/Nd age, and thus the **Δ**, it is essential to add material to the sediments from a younger mantle-derived precursor. The amount of young material that can be incorporated into sedimentary cycle is, however, constrained by the degree of cannibalism. The more cannibalistic (less open) the sedimentary system, the less the contribution of young materials to "new" sediments and the steeper the age slope of the **Δ**.

The first-order features in figure 11 can be explained if the Archean were dominated mostly by the growth of the first cycle sedimentary mass from erosion of the contemporaneous young (≤250 Ma old) igneous precursors. Subsequent to a large degree of cratonization, and establishment of a near present-day global sedimentary mass at ~2.5 ± 0.3 Ga ago, recycling became the dominant feature of sediment evolution (cf. also Veizer 1983; Goldstein et al. 1984; Michard et al. 1985). With the **b** for the global sedimentary mass of $\sim 40 \times 10^{-10}\ a^{-1}$, the degree of cannibalism required to produce the observed ~1.4 ± 0.4 Ga Δ for Recent sediments is ~90 ± 5%.

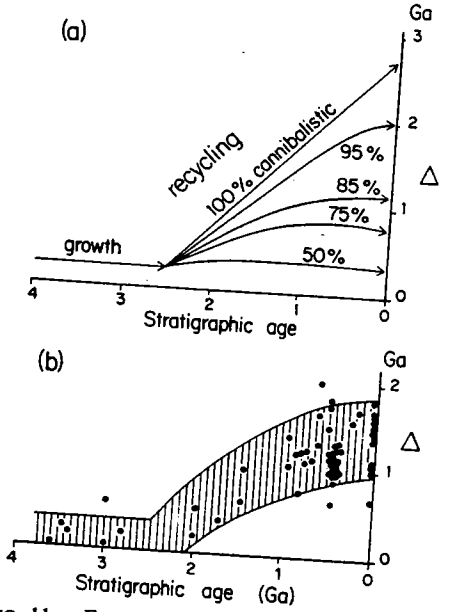

FIG. 11.—Excess of Sm/Nd model ages for sediments over their stratigraphic ages (Δ). (a) Theoretical calculations of the Δ-age slopes are based on the following assumptions. With the establishment of a near present-day global sedimentary mass (**n** = 1/∞) at ~2.5 Ga ago, the recycling proceeded at $\mathbf{b} = 40 \times 10^{-10}\ a^{-1}$ (table 11) and the slopes represent degrees of cannibalism in percents. The recycling increment is 250 Ma. Shorter increments lead to shallower slopes, thus compounding the difficulty of retaining large Δ's. The advocated degree of cannibalism is therefore a minimal estimate. The flatter curves (lesser degrees of cannibalism) in Veizer and Jansen (1979) were a consequence of a slower **b** utilized in their previous modeling. (b) Δ calculated for experimental data of O'Nions et al. (1983), Hamilton et al. (1983), McCulloch and Wasserburg (1978), Goldstein and O'Nions (1982), Taylor et al. (1983), and Allègre and Rousseau (1984). Recent publications of Goldstein et al. (1984) and Michard et al. (1985) only reinforce the above first-order pattern.

The above estimate simultaneously sets an upper limit of $\sim 1.1 \pm 0.5 \times 10^{15}\ g\ a^{-1}$ (10 ± 5% of global sedimentary mass) on the quantity of sediments available for crust-mantle exchange. In contrast, crust-mantle isotopic transport models (Armstrong 1981; DePaolo 1983) suggest 4–6 times larger fluxes. This discrepancy may be a consequence of the restrictive assumptions of isotopic model estimates (cf. also Patchett and Chauvell 1984). Alternatively, and more likely, it may indicate that a significant amount of the continental crust-mantle exchange is accomplished by means other than via subduction of sediments (e.g., at the base of orogenic belts or cratons).

CONCLUDING REMARKS

The above treatment of recycling demonstrated that first-order features of global plate tectonics are amenable to theoretical treatment not only in terms of their spatial, but also in terms of their temporal, parameters. Conceptually this has wide-ranging implications for quantification of the preserved geologic record. Tectonic diversity is a function of time, and the longevity of a discernible imprint in the rock record is inversely proportional to the rate of recycling of a specific tectonic realm. The realms of the oceanic domain (basins of active margins to immature orogenic belts) should not be preserved in crustal segments older than ~100–300 Ma. This poor preservation potential, rather than any fundamental differences in the mode of coeval tectonic styles, may have been the major reason for the scarcity of, for example, glaucophane schists, paired metamorphic belts, and ophiolites in the Paleozoic and particularly the Precambian records (cf. Ernst 1983). Platforms, and the roots of former orogenic belts, should not usually survive beyond ~1300 Ma. In the crystalline continental basement, the bulk of the K/Ar ages should be obliterated by ~2.4 Ga.

We would like to emphasize that the recycling and evolutionary concepts are not mutually exclusive, but complementary. The preponderance of greenstone belts in the Archean crustal segments is an instructive illustration of this complementarity. Greenstone

B.

belts, regardless of t
tectonic analogue,
oceanic domain, as
contribution. They
oceanic rates prior t
ble continental crust
for the subsequent ≥
of survival to today
fore minimal. The
quency of Archean g
this recycling, sugge
sive original abundar
oceanic domain likely
tectonic regime on th

ACKNOWLEDGMENTS

nancial support of thi
Sciences and Enginee
of Canada, Universit
University, and North
Hearn and W. F. Sch
figures; J. Hayes for t
statistical data concer
ores; C. B. Gregor fo
with the data base; a
E. M. Cameron, A. L
Mackenzie, S. M. Mc
S. R. Taylor, and R. C
script review.

APPEN

GLOSSARY

t *time;*

A *geologic entity,* ments, area or v or continental cr of ores, etc. (in a area, or percenta

P *number of time in* sentation of the d

t *duration of* one *t* **PT** = total time;

n *growth model* ass given entity **A** (fi with **n** = 1/∞ = 0 situation, 0 ≤ **n** ≤ creasing, **n** ≥ 1 a ing, and **n** = 1 a

$\mathbf{t_0}$ *beginning* of the p recycling of the e

b *average recycling* ter (cf. fig. 1);

D the *recycled quant* present-day total ample, **D** = 50 fo that the recycled q

belts, regardless of their precise present-day tectonic analogue, were a product of the oceanic domain, as defined in the present contribution. They have been recycled at oceanic rates prior to incorporation into stable continental crust and at continental rates for the subsequent ≥2.2 Ga. Their chances of survival to today should have been therefore minimal. The present-day high frequency of Archean greenstone belts, despite this recycling, suggests therefore an excessive original abundance. It follows that the oceanic domain likely has been the dominant tectonic regime on the early Earth.

ACKNOWLEDGMENTS.—We acknowledge financial support of this work by the Natural Sciences and Engineering Research Council of Canada, University of Ottawa, Carleton University, and Northwestern University; E. Hearn and W. F. Schmiedel for drafting of figures; J. Hayes for typing; P. Laznicka for statistical data concerning age distribution of ores; C. B. Gregor for preprint of his paper with the data base; and R. L. Armstrong, E. M. Cameron, A. Lerman, Y. H. Li, F. T. Mackenzie, S. M. McLennan, N. H. Sleep, S. R. Taylor, and R. C. G. Walker for manuscript review.

APPENDIX 1: GLOSSARY OF TERMS

t *time;*

A *geologic entity*, such as mass of sediments, area or volume (mass) of oceanic or continental crust, reserves (tonnages) of ores, etc. (in arbitrary weight, volume, area, or percentage units);

P *number of time increments* utilized in presentation of the data and their simulation;

t *duration of* one *time increment* in years; **PT** = total time;

n *growth model* assumed for generation of a given entity **A** (fig. 2). A growth model with $n = 1/\infty = 0$ represents a steady-state situation, $0 \leq n \leq 1$ an exponentially decreasing, $n \geq 1$ an exponentially increasing, and $n = 1$ a linear growth model;

t_0 *beginning* of the process of generation and recycling of the entity **A** (fig. 2);

b *average recycling proportionality parameter* (cf. fig. 1);

D the *recycled quantity*, as compared to the present-day total of an entity **A**. For example, **D** = 50 for oceanic crust signifies that the recycled quantity was 50 times the mass of the presently existing oceanic crust;

τ_{50} *half-life* (half-mass, half-area) age or 50th percentile (fig. 1);

τ_{MAX} *oblivion age* or maximal life-span, here defined as 5th percentile;

The theoretical τ_Q for a steady state model ($n = 1/\infty$) can be calculated as

$$\tau_Q = T\left[\frac{\ln Q - \ln 100}{\ln (1 - bT)}\right],$$

where Q is the desired percentile. For accumulational models ($1/\infty \leq n \leq \infty$), $\tau_Q = (P - x)\,T$, where x is the root of the equation

$$\left(\frac{x}{P}\right)^n (1 - bT)^{P-x} - \frac{Q}{100} = 0$$

The root may be found by any algorithm such as bisection or Newton-Raphson method.

τ_{MEAN} *mean-age*, usually exceeds τ_{50} due to contribution of old ages from the tail. For $n = 1/\infty$ it is given by

$$\tau_{MEAN} = T\left[\frac{(1 - bT) - (1 - bT)^P}{bT} + \frac{(1 - bT)^P + 1}{2}\right].$$

For large **P**, τ_{MEAN} can be approximated by

$$\tau_{MEAN} = T\left[\frac{1 - bT}{bT} + \frac{1}{2}\right].$$

For the accumulation models it is:

$$\tau_{MEAN} = \frac{T}{2} = \frac{T}{P^n}\sum_{i=1}^{P-1} i^n (1 - bT)^{P-i}$$

b* *local recycling constant*. For steady-state model ($n = 1/\infty$) **b*** is related to **b** by

$$b^* = b\,(1 - b)^{m-1}$$

where **m** is the sought interval of duration **T** subsequent to the beginning of orogenesis.

t_T *time of transition* (cf. fig. 10). The formula for its derivation is:

$$t_T = \left[\frac{\ln (b_2/b_1)}{\ln (1 - b_1 T)} + 1\right]T,$$

where $b_1 > b_2$.

t_E *time of equality* (cf. fig. 10). The formula for its derivation is:

$$t_E = \left[\frac{\ln (b_1/b_2)}{\ln \left(\frac{1 - b_2 T}{1 - b_1 T} \right)} + 1 \right] T,$$

where $b_1 > b_2$.

Δ *age difference* between model Sm/Nd age and stratigraphic age of the same sediment.

For further details and specification of **t, A, P, T, n, t_0, b, D,** and Δ see Veizer and Jansen (1979).

REFERENCES CITED

ALLÈGRE, C. J., 1982, Chemical geodynamics: Tectonophysics, v. 81 p. 109–132.

——— and ROUSSEAU, D., 1984, The growth of the continents through geological time studied by Nd isotope analysis of shales: Earth Planet. Sci. Letters, v. 67, p. 19–34.

ARMSTRONG, R. L., 1968, A model for evolution of strontium and lead isotopes in a dynamic Earth: Rev. Geophys., v. 6, p. 175–199.

——— 1981, Radiogenic isotopes: the case for crustal recycling on a near-steady-state no-continental-growth Earth: Royal Soc. (London) Phil. Trans., v. A301, p. 443–472.

BERGER, W. H., and WINTERER, E. L., 1974, Plate stratigraphy and the fluctuating carbonate line: Spec. Publ. Int. Assoc. Sedimentol., v. 1, p. 11–48.

DACEY, M. F., and LERMAN, A., 1983, Sediment growth and aging as Markov chains: Jour. Geology, v. 91, p. 573–590.

DE PAOLO, D. J., 1983, The mean life of continents: estimates of continental recycling rates from Nd and Hf isotopic data and implications for mantle structure: Geophys. Res. Letters, v. 10, p. 705–708.

DEWEY, J. F., and WINDLEY, B. F., 1981, Growth and differentiation of the continental crust: Royal Soc. (London) Phil. Trans., v. A301, p. 189–206.

ERNST, W. G., 1983, A summary of Precambrian crustal evolution, *in* BOARDMAN, S. G., ed., Revolution in the Earth Sciences: Dubuque, IA, Kendall-Hunt, p. 36–55.

GARRELS, R. M., and MACKENZIE, F. T., 1971*a*, Gregor's denudation of the continents: Nature, v. 231, p. 382–383.

———, and ——— 1971*b*, The Evolution of Sedimentary Rocks: New York, Norton, 397 p.

GOLDSTEIN, S. D., and O'NIONS, R. K., 1982, Nd-isotopic study of river particulates, atmospheric dusts, and pelagic sediments: EOS, v. 68, p. 480.

———; ———; and HAMILTON, P. J., 1984, A Sm-Nd isotopic study of atmospheric dust and particulates from major river systems: Earth Planet. Sci. Letters, v. 70, p. 221–236.

GREGOR, C. B., 1970, Denudation of the continents: Nature, v. 228, p. 273–275.

——— 1980, Weathering rates of sedimentary and crystalline rocks: Proc. Koninklijke Nederlandse Akad. Wetenschappen, Ser. B, v. 83, p. 173–181.

——— 1985, The mass-age distribution of Phanerozoic sediments, *in* SNELLING, N. J., ed., The chronology of the geological record: Oxford, Blackwell, p. 284–289.

HAMILTON, P. J.; O'NIONS, R. K.; BRIDGWATER, D.; and NUTMAN, A., 1983, Sm-Nd studies of Archean metasediments and metavolcanics from west Greenland and their implications for the Earth's early history: Earth Planet. Sci. Letters, v. 62, p. 263–272.

HARRISON, T. M.; ARMSTRONG, R. L.; NAESER, C. W.; and HARASKAL, J. F., 1979, Geochronology and thermal history of the Coast Plutonic Complex near Prince Rupert, British Columbia: Can. Jour. Earth Sci., v. 16, p. 400–410.

HURLEY, P. M., and RAND, J. R., 1969, Pre-drift continental nuclei: Science, v. 164, p. 1229–1242.

JACOBSEN, S. B., and WASSERBURG, G. J., 1981, Transport models for crust and mantle evolution: Tectonophysics, v. 75, p. 163–179.

LAZNICKA, P., 1973, Development of non-ferrous metal deposits in geological time: Can. Jour. Earth Sci., v. 10, p. 18–25.

LAZNICKA, P., 1981, A computerized research file on global metallogeny—an experience with MANIFILE: Global. Tect. and Metall., v. 1, p. 224–245.

LI, Y. H., 1972, Geochemical mass balance among lithosphere, hydrosphere, and atmosphere: Am. Jour. Sci., v. 272, p. 119–137.

MCCULLOCH, M. T., and WASSERBURG, G. J., 1978, Sm-Nd and Rb-Sr chronology of continental crust formation: Science, v. 200, p. 1003–1011.

MICHARD, A.; GURRIET, P.; SOUDANT, M.; and ALBAREDE, F., 1985, Nd isotopes in French Phanerozoic shales: external vs. internal aspects of crustal evolution: Geochim. Cosmochim. Acta, v. 49, p. 601–610.

MOORE, T. C., and HEATH, G. R., 1977, Survival of deep sea sedimentary sections: Earth Planet. Sci. Letters, v. 37, p. 71–80.

O'NIONS, R. K.; HAMILTON, P. J.; and HOOKER, P. J., 1983, A Nd isotope investigation of sediments related to crustal development in the British Isles: Earth Planet. Sci. Letters, v. 63, p. 229–240.

PARSONS, B., 1981, The rates of plate consumption and creation: Geophys. Jour. Royal Astro. Soc., v. 67, p. 437–448.

——— 1982, Causes and consequences of the relation between area and age of the ocean floor: Jour. Geophys. Res., v. 87, p. 289–302.

PATCHETT, J., and CHAUVEL, C., 1984, The mean life of continents is currently not constrained by

Nd and Hf isotopes—commer
Letters, v. 11, p. 151–153.

REID, J., and JACKSON, H. R.
spreading rate and crustal
Geophys. Res., v. 5, p. 165–1

REYMER, A., and SCHUBERT, G.,
addition rates to the continenta
growth: Tectonics, v. 3, p. 63–

RONOV, A. B., 1976, Volcanism
cumulation, life: Geokhimija, v
1277 (in Russian).

——— 1980, The Sedimentary La
Moscow, Nauka, 131 p. (in Ru

———; KHAIN, V. E.; BALUKHO
SESLAVINSKIJ, K. B., 1980, Qua
of Phanerozoic sedimentation:
p. 311–325.

SCLATER, J. G.; JAUPART, C.; and C
The heat flow through oceanic
crust and the heat loss of
Geophys. Res., v. 81, p. 269–3

———; PARSONS, B.; and JAU
Oceans and continents: similar
ences in the mechanism of
Geophys. Res., v. 86, p. 11535–

SPRAGUE, D., and POLLACK, H. N.,
in the Mesozoic and Cenozoic: N
393–395.

TAYLOR, S. R., and MCLENNAN, S
Continental Crust: Its Composi
tion, Oxford, Blackwell, 312 p.

———; ———; and MCCULLOCH

Nd and Hf isotopes—comment: Geophys. Res. Letters, v. 11, p. 151–153.

REID, J., and JACKSON, H. R., 1981, Oceanic spreading rate and crustal thickness: Mar. Geophys. Res., v. 5, p. 165–172.

REYMER, A., and SCHUBERT, G., 1984, Phanerozoic addition rates to the continental crust and crustal growth: Tectonics, v. 3, p. 63–77.

RONOV, A. B., 1976, Volcanism, carbonate accumulation, life: Geokhimija, v. 1977/8, p. 1252–1277 (in Russian).

——— 1980, The Sedimentary Layer of the Earth: Moscow, Nauka, 131 p. (in Russian).

———; KHAIN, V. E.; BALUKHOVSKY, A. N.; and SESLAVINSKIJ, K. B., 1980, Quantitative analysis of Phanerozoic sedimentation: Sed. Geol., v. 25, p. 311–325.

SCLATER, J. G.; JAUPART, C.; and GALSON, D., 1980, The heat flow through oceanic and continental crust and the heat loss of the earth: Rev. Geophys. Res., v. 81, p. 269–311.

———; PARSONS, B.; and JAUPART, C., 1981, Oceans and continents: similarities and differences in the mechanism of heat loss: Jour. Geophys. Res., v. 86, p. 11535–11552.

SPRAGUE, D., and POLLACK, H. N., 1980, Heat flow in the Mesozoic and Cenozoic: Nature, v. 285, p. 393–395.

TAYLOR, S. R., and MCLENNAN, S. M., 1985, The Continental Crust: Its Composition and Evolution, Oxford, Blackwell, 312 p.

———; ———; and MCCULLOCH, M. T., 1983, Geochemistry of loess, continental crustal composition, and crustal model ages: Geochim. Cosmochim. Acta, v. 47, p. 1897–1905.

THOMPSON, R., 1984, A stochastic model of sedimentation: Jour. Int. Assoc. Math. Geol., v. 16, p. 753–778.

TURCOTTE, D. L., and SCHUBERT, G., 1982, Geodynamics: New York, Wiley, 450 p.

VAN BREEMEN, O., and DALLMEYER, R. D., 1984, The scale of Sr isotopic diffusion during post-metamorphic cooling of gneisses in the Inner Piedmont of Georgia, southern Appalachians: Earth Planet. Sci. Letters, v. 68, p. 141–150.

VEIZER, J., 1983, Geologic evolution of the Archean-Early Proterozoic Earth, *in* SCHOPF, J. W., ed., The Earth's Earliest Biosphere: Its Origin and Evolution, Princeton, Princeton Press, p. 240–259.

——— 1984, Recycling on the evolving Earth: geochemical record in sediments, *in* Proc. 27th Int. Geol. Congress, vol. 11: Utrecht, VNU Science Press, p. 325–345.

———, and JANSEN, S. L., 1979, Basement and sedimentary recycling and continental evolution: Jour. Geol., v. 87, p. 341–370.

WASSERBURG, G. J., 1961, Crustal history and the Precambrian time scale: Ann. New York Acad. Sci., v. 91, p. 583–594.

ZARTMAN, R. E., and DOE, B. R., 1981, Plumbotectonics—the model: Tectonophysics, v. 75, p. 135–162.